12-2010

The Removal of Wood Components from Hardwood by Hot Water

Rory Jara

THE REMOVAL OF WOOD COMPONENTS FROM HARDWOOD BY HOT WATER

By

Rory Jara

B.S. Universidad de Concepción, 1998

A DISSERTATION

Submitted in Partial Fulfillment of the

Requirements for the Degree of

Doctor of Philosophy

(in Chemical Engineering)

The Graduate School

The University of Maine

December, 2010

Advisory Committee:

Adriaan R.P. van Heiningen, Professor of Chemical Engineering, Advisor

Barbara J. W. Cole, Professor of Chemistry

David J. Neivandt, Associate Professor of Chemical Engineering

Douglas Ruthven, Professor of Chemical Engineering

Stephen M. Shaler, Professor of Wood Science and Technology

THE REMOVAL OF WOOD COMPONENTS FROM HARDWOOD BY HOT WATER

By Rory Jara

Thesis Advisor: Dr. Adriaan R.P. van Heiningen

An Abstract of Thesis Presented
in Partial Fulfillment of the Requirements for the
Degree of Doctor of Philosophy
(*in Chemical Engineering*)
December, 2010

Hot-water extraction of hemicelluloses from wood is a promising technology in the integrated biorefinery concept. A particular case is where the pulp industry makes co-products such as ethanol and acetic acid besides pulp thereby maximizing the value of biomass. Similarly, the oriented strand board (OSB) industry appears to be suitable for this technical approach as it is composed of large centralized facilities. Many studies have been carried out on the kinetics and mechanism of hot-water extraction of lignocellulosics. However, most of these studies were performed in batch reactors which are not best suited to determine intrinsic kinetics of hemicellulose dissolution because of further reaction of the hemicelluloses in solution.

As a first approach to study the extraction yield for hydrothermal treatments on red maple (*Acer rubrum*) strands, a batch reactor (ASE-100, Dionex) was used. A complete mass balance on extracted wood and wood extracts has been obtained by determining cellulose, hemicellulose, and lignin content on both solid and liquid phases

at different extraction temperatures and times, described by a combined parameter called the P-factor. In addition, a study was completed of the molecular weight distribution of dissolved polysaccharides in the liquid phase and of cellulose in the solid phase.

In the second part of this work a continuous mixed batch reactor was used to obtain the intrinsic kinetics of dissolution of hemicelluloses from hardwood (*Acer rubrum*) at three different temperatures (150°C, 160°C, and 170°C) and four constant pH values: 2, 3, 4 and 5. Wood-meal and a high flow rate (100 mL/min) were used to avoid mass transfer limitations during dissolution of the hemicelluloses. An improved mechanism for xylan dissolution is proposed which is in agreement with recent knowledge of the topochemistry of hardwood fibre cell walls. Finally, it is shown that a modified P_H-factor can describe the effect of pH and time and temperature on xylan dissolution during pH-controlled hot water extraction of red maple wood.

ACKNOWLEDGMENTS

It is a pleasure to thank the many people who made this thesis possible.

I am heartily thankful to my supervisor, Dr. Adriaan van Heiningen, whose encouragement, guidance, support, freedom for initiative, and efforts to provide a friendly work environment from the initial to the final level, enabled me to enjoy my research and develop both an understanding and enthusiasm for the subject.

Besides my advisor, I would like to thank the rest of my thesis committee: Prof. Stephen Shaler, Prof. David Neivandt, Prof. Douglas Ruthven, and Prof. Barbara Cole for their encouragement, insightful comments, and always willing disposition to help.

I would like to thank the wonderful people who helped me in many ways at the beginning of this path: Sarah and Mireille from the OIP, Prof. Barry Goodell, Dr. Habib Dagher, and Prof. Stephen Shaler. Thank you all for your will to help me out.

Special thanks to Dr. Martin Lawoko, for his friendship and for all the interesting discussions and contributions about many issues related to wood chemistry during my thesis work.

In my daily work I have been blessed with a friendly and cheerful group of friends and fellow students, I will miss our coffee breaks: Yang, Mohit, Sefik, and Martin. Also thanks to all Ober group graduate students for their great help along this work: Yun, Sefik, Sarah, and Xiaowen.

I wish to thank all the staff in the Chemical Engineering Department, especially Nick Hill and Amos Cline, and secretaries Angel and Cathy. I also appreciate all the help

and assistance provided by the staff of the Process Development Center: Keith Hodgins, Seong Park, Haixuan Zou, and Heok Kwon.

I am grateful to the staff of the AEWC Center specially Russell Edgar and John Hill for their valuable help and assistance during the wood sample preparation activities.

For their support, friendship, and many good times gathering around a barbeque thanks to Stefano and Sandra, Russell and Cynthia, Jacques and Anita, Juan and Bernardita, and Felipe and Daniela. My deepest gratitude for all the support and friendship during my time in Maine to the Reyes Family: Roberto, Cathie, Kristi, and Kassi.

I would like to express my sincere gratitude and appreciation for all the support and help to Bill Desisto and the Hwalek Family, John and Ginger, during the difficult last months of my work in Maine. I will miss the wonderful evenings with nice food and a glass of good red wine.

Last but not the least, I would like to thank my family: my mother Chilia Moreno and my brother Alvaro Jara, for their unconditional love and spiritual support throughout my life. My genuine, warm recognition to my beloved wife Gloria, for her support, encourage, and unconditional love; without her I wouldn't have reached this degree. Also thanks to my beloved children Isabel and Diego for their laughs and warm love.

TABLE OF CONTENTS

ACKNOWLEDGMENTS iv

LIST OF TABLES x

LIST OF FIGURES xii

CHAPTER

1 INTRODUCTION 1

2 LITERATURE REVIEW 4

2.1 Chemical composition of wood 4

2.1.1 Cellulose 4

2.1.2 Hardwood hemicellulose 5

2.1.3 Lignin 7

2.2 Ultrastructure arrangement of the fibre wall 11

2.3 Pre-extraction of hemicellulose with steam/hot water 12

2.4 Hemicellulose hydrolysis and degradation in acidic medium 17

2.4.1 Mechanism of acidic hydrolysis 17

2.4.2 Mechanism of sugar degradation 18

2.5 Kinetic models 20

3 OBJECTIVES AND EXPERIMENTAL SETUP 24

3.1 Objectives 24

3.2 Experimental setup and chemical analysis 25
3.2.1 Materials 25
3.2.2 Reactor Setup 26
3.2.3 Chemical analysis 33
4 DATA COLLECTION AND VALIDATION OF CONTINUOUS MIXED BATCH REACTOR 45
4.1 Determination of the residence time distribution of the reaction system 45
4.2 UV-VIS Absorption Calibration 45
4.3 Data Reduction Procedure 47
4.3.1 Lignin Removal Rate 47
4.3.2 Smoothing the Monosaccharide Concentration Data 50
4.3.3 Xylan Removal Rate 52
4.4 Validation of Continuous Mixed Batch Reactor Operation 53
4.4.1 Mass balance study 53
4.4.2 Data Repeatability 55
4.4.3 Effect of Different Flow Rates 57
4.4.4 The effect of wood particle size on xylan and lignin removal rate 58
4.4.5 Conclusions 64
5 RESULTS AND DISCUSSIONS 65
5.1 Removal of wood components from OSB strands by hot water in a batch reactor 65
5.1.1 Introduction 65

5.1.2 Hydrothermal dissolution of wood components from OSB strands. The effect of P-factor on the extraction yield. 66

5.1.3 Hydrothermal dissolution of wood components from OSB strands. The effect of P-factor on the residual concentration of wood components 76

5.1.4 Hydrothermal dissolution of wood components from OSB strands. The effect of P-factor on the molecular weight distribution of wood extracts 83

5.1.5 Effect of P-factor on degree of polymerization of cellulose in pulp 88

5.1.6 Conclusions 93

5.2 Intrinsic kinetics on the removal of wood components from hardwood by hot water extraction in a continuous mixed batch reactor 96

5.2.1 Introduction 96

5.2.2 Effect of temperature 97

5.2.3 Effect of pH 107

5.2.4 Conclusions 118

5.3 Chemical mechanism and rate determining step(s) in hemicellulose removal and kinetics study 121

5.3.1 Introduction 121

5.3.2 Molecular weight distribution in hemicellulose extracts 123

5.3.3 Solubility of hemicellulose extracts 129

5.3.4 Possible chemical mechanism and rate determining step(s) in hemicellulose removal using DI-water 133
5.3.5 Modeling xylan dissolution from hardwood by DI-water 143
5.3.6 Conclusions 150
6 SUMMARY OF CONCLUSIONS AND RECOMMENDATIONS FOR FUTURE WORK 153
6.1 Conclusions 153
6.1.1 Removal of wood components from OSB strands by hot water in a batch reactor 153
6.1.2 Intrinsic kinetics of removal of wood components from hardwood by hot water extraction in a continuous mixed batch reactor 155
6.1.3 Chemical mechanism, rate determining step(s) and kinetics of wood polymer removal during hot water treatment of hardwood 157
6.2 Recommendation for future work 159
REFERENCES 161
APPENDIX: HYDROLYSIS OF XYLAN MODEL COMPOUND (BIRCH XYLAN) IN SULFUR DIOXIDE AQUEOUS SOLUTIONS 166
BIOGRAPHY OF THE AUTHOR 186

LIST OF TABLES

Table 2.1. Major components of wood 5

Table 2.2. Proportion of different types of linkages connecting the phenylpropane units in lignin 8

Table 2.3. Kinetic parameters for pentosan hydrolysis. 21

Table 3.1. Chemical composition of red maple 26

Table 3.2. Extraction conditions. 43

Table 3.3. Alkaline cooking conditions. 44

Table 4.1. Klason and acid soluble lignin for original and extracted wood 47

Table 4.2. Average extinction coefficient for removed lignin. 47

Table 4.3. Mass balance for liquid and solid phase 54

Table 4.4. Weisz modulus for different wood samples. 62

Table 5.1. Residual molar ratio of acetyl and 4OMeGUA side groups per 10 anhydrous xylose units in original and extracted wood. 80

Table 5.2. Mass balance comparison between the liquid and solid phases at different P-factor values. 82

Table 5.3. Average molecular weight and degree of polymerization for wood extracts at different extraction conditions. 87

Table 5.4. Calculation of cellulose and hemicellulose content of pulp. 88

Table 5.5. Remaining wood mass fraction after hot water extraction 89

Table 5.6. Chemical composition of original wood 98

Table 5.7. Intrinsic viscosity, degree of polymerization and scission number for described solid samples. 103

Table 5.8. Intrinsic viscosity, degree of polymerization and scission number for described solid samples. 112

Table 5.9. Mass balance for acetyl groups and final acetyl group/10 xylose ratio in extracted wood. 114

Table 5.10. Chemical concentration of wood extract fractions. 124

Table 5.11. Chemical composition of wood extract fractions based on original dry wood 125

Table 5.12. Molar Mass of studied samples 127

Table 5.13. Initial concentration and turbidity for xylan and lignin in extract fractions. 130

Table 5.14. Estimated saturation point values. 132

Table 5.15. Comparison of results for the removal of xylan an lignin on two different systems 141

Table A.1. Composition of simulated extracts 169

Table A.2. Experiment description for SO_2 releasing 180

LIST OF FIGURES

Figure 2.1. Structure of cellulose. 5

Figure 2.2. Cellulose fibrils 5

Figure 2.3. Structure of major hardwood hemicelluloses 6

Figure 2.4. Structure of lignin precursors phenyl propanoid units 7

Figure 2.5. A model for softwood lignin 9

Figure 2.6. Proposed structures for lignin carbohydrate complexes 10

Figure 2.7. Cell wall model with the fibrillar structure of the cell wall layers 11

Figure 2.8. Model for the arrangement of cellulose, xylan, and lignin in the secondary cell walls of aspen wood 12

Figure 2.9. Mechanism of the acid-catalyzed hydrolysis of the glycosidic bond via the cyclic carbonium-oxionium ion 19

Figure 2.10. Formation of furfural, hydroxymethyl-furfural, levulinic acid and formic acid from monosaccharides in acidic medium 19

Figure 3.1. Extraction of hemicellulose using a modified version of Dionex ASE-100. 26

Figure 3.2. Continuous mixed batch reactor design scheme 29

Figure 3.3. Berty stationary basket inside the reactor 29

Figure 3.4. Reactor setup and Berty stationary basket 30

Figure 3.5. Temperature and pressure profiles of the reactor during water extraction. 32

Figure 3.6. pH profile during extraction of hemicelluloses from wood meal with an acetic acid solution of 1 g/L concentration. 32

Figure 3.7. Experimental design for extraction of hemicelluloses from hardwood. 33

Figure 3.3.8. Calibration curve applying Pullulan standards 41

Figure 4.1. Concentration and removal rate of lignin 49

Figure 4.2. Removal rate vs. residual lignin 50

Figure 4.3. Concentration of monosaccharides in extract samples. 51

Figure 4.4. Concentration of monosaccharides after smoothing. 51

Figure 4.5. Removal rate of xylan with time and residual concentration 52

Figure 4.6. Concentration of xylan and lignin with time for three different experiments. 55

Figure 4.7. Distribution of mean concentration with standard error bars for xylan and lignin 56

Figure 4.8. Concentrations of xylan and lignin at two different flow rates. 57

Figure 4.9. Removal rates of xylan and lignin at two different flow rates. 58

Figure 4.10. Concentration of xylan and lignin with time for two different wood meal particle sizes. 59

Figure 4.11. Xylan and lignin removal rates versus their residual concentration in wood. 61

Figure 4.12. Comparison of xylan kinetics for two different rotational speeds in the Berty reactor during the extraction 63

Figure 5.1. Extraction yield of red maple wood strands with DI-water 67

Figure 5.2. Extraction yield based on solid phase versus P-factor. 67

Figure 5.3. Total lignin in liquid extracts calculated as the sum of Klason lignin, acid soluble lignin, and lignin precipitate 69

Figure 5.4. Free acetic and formic acids in extracts and its effect on the pH and extraction yield 70

Figure 5.5. Solid weight lost, total, main, and minor wood components yield at different P-factor values in liquid phase 72

Figure 5.6. Oligomeric and monomeric xylan versus P-factor 74

Figure 5.7. Molar ratio of acetyl and MeGUA side groups to 10 xylose units in wood extracts 74

Figure 5.8. Molar ratio of glucan:mannan in wood extracts. 76

Figure 5.9. Residual concentration for main and minor wood components as a function of P-factor 77

Figure 5.10. Residual uronic acids with two different analytical techniques 78

Figure 5.11. Residual galacturonic and 4-O-methyl glucuronic acids in original and extracted wood at different P-factor values. 79

Figure 5.12. Gel permeation chromatography analysis of wood extracts at different extraction conditions. 85

Figure 5.13. Molecular weight distribution for wood extracts at different extraction conditions. 87

Figure 5.14. Effect of severity of the pre-extraction on the kappa number and pulp yield 90

Figure 5.15. The effect of the extraction severity on the cellulose and xylan pulp mass fractions. 92

Figure 5.16. The effect of the extraction severity on the DP of cellulose. 92

Figure 5.17. Concentration versus time for lignin and polysaccharides at three temperature conditions during the hot water extraction 99

Figure 5.18. Concentration versus time for minor polysaccharides at three temperature conditions during the hot water extraction 100

Figure 5.19. Extraction yield for lignin, xylan, and the overall process at different temperatures. 101

Figure 5.20. Extraction yield for minor polysaccharides at different temperatures. 102

Figure 5.21. Removal rates for xylan and lignin at all three temperature conditions 105

Figure 5.22. Xylan and lignin removal rates versus their residual concentration in wood at different temperature conditions. 106

Figure 5.23. Concentration curves of lignin and polysaccharides for all four pH conditions along the extraction process. 109

Figure 5.24. Extraction yield for lignin, xylan, and the overall process at different pH conditions. 110

Figure 5.25. Extraction yield for minor polysaccharides at different pH conditions..... 111
Figure 5.26. Molar ratio for glucan and mannan at different pH conditions..... 111
Figure 5.27. Concentration of acetyl groups along the extraction process at four different pH conditions. 113
Figure 5.28. Amount of units acetyl groups per every 10 units of dehydrated xylose at four different pH conditions. 113
Figure 5.29. Removal rates for xylan and lignin at all four pH conditions..... 116
Figure 5.30. Xylan and lignin removal rates versus their residual concentration in wood..... 117
Figure 5.31. Size exclusion chromatography analysis for Sample 1. 126
Figure 5.32. Size exclusion chromatography analysis for Sample 2. 126
Figure 5.33. Molar Mass Distributions of the samples relative to pullulan standards..... 127
Figure 5.34. Total and monomeric concentration for xylan, glucan, and mannan during water extraction 128
Figure 5.35. Effect of total wood polymers concentration on wood extracts turbidity. 131
Figure 5.36. Effect of xylan concentration on wood extracts turbidity..... 131
Figure 5.37. Effect of lignin concentration on wood extracts turbidity 131
Figure 5.38. Xylan removal rate at different temperatures. 135

Figure 5.39. Model for the arrangement of cellulose, xylan, and lignin in the secondary cell walls of aspen wood 138

Figure 5.40. Xylan removal rate at different temperatures versus its residual concentration in wood. 145

Figure 5.41. Determination of the activation energy for the cleavage of gycosidic bonds in xylan 146

Figure 5.42. Determination of the reaction order with respect to the proton concentration 147

Figure 5.43. Xylan yield versus P-factor for the temperature and pH effect 148

Figure 5.44. Xylan yield versus the modified P_H-factor for the temperature and pH effect 149

Figure 5.45. Xylan yield versus P_H-factor for the temperature and pH effect 149

Figure A.1. Multireactor-system for the kinetic study of hydrolysis of xylo-oligomers. 168

Figure A.2. Dissolution of SO_2 into simulated extracts. 169

Figure A.3. Analytical procedure for the hydrolisate after the catalytic hydrolysis with SO_2. 170

Figure A.4. Pressure study set up showing the wireless pressure sensor. 171

Figure A.5. Effect of SO_2 concentration, temperature and time on xylose yield for the simulated hot water hemicellulose extract 173

Figure A.6. Effect of SO_2 concentration, temperature and time on the xylose yield for the simulated hot water hemicellulose extract 174

Figure A.7. Effect of SO_2 concentration of pH at 25°C. 174

Figure A.8. Relative molar percentage of SO_2·H2O, hydrogen sulfite, and sulfite ions as a function of pH at 25°C. 174

Figure A.9. Effect of SO_2 concentration, temperature and time on the xylose yield for the simulated near neutral hemicellulose extract 175

Figure A.10. Effect of SO_2 concentration, temperature and time on the xylose yield for the simulated near neutral hemicellulose extract 176

Figure A.11. Effect of severity on the xylose yield for the hydrolysis of the simulated hot water extract. 178

Figure A.12. Effect of severity on the xylose yield for the hydrolysis of the simulated hot water extract. 178

Figure A.13. Effect of severity on the xylose yield for the hydrolysis of the simulated near-neutral extract. 179

Figure A.14. Effect of SO_2 concentration on the hydrogen ion concentration at 25°C. 180

Figure A.15. Set up scheme for the recovery of SO_2 from the hidrolisate. 181

Figure A.16. Recovery of SO_2 from simulated hot water hydrolisate 181

Figure A.17. Reproducibility of pressure measurements. 182

Figure A.18. Absolute vapor pressure for pure water and effect of air at different temperatures. 183

Figure A.19. Effect of SO_2 concentration and temperature on the total pressure. 184

Figure A.20. Effect of SO_2 concentration and temperature on the partial pressure of SO_2. 184

CHAPTER

1 INTRODUCTION

Climate change and energy sustainability are presently the most pressing global problems. The latter is shown in a recent study (Nashawi et al., 2010) of the world oil production using a multicyclic Hubbert model for the 47 major oil producing countries. This study estimates that the world production will peak in 2014 at a rate of 79 MMSTB/D. Combustion of fossil fuels is also considered the major factor responsible for global warming by releasing 7.0 billion tons of carbon/year into the atmosphere, equaling 82% of net green house gas emissions (Zhang, 2008). Therefore considerable funds and efforts have been invested in alternative energy resources such as biomass, wind, geothermal and solar energy in order to meet the developmental and environmental requirements. Among these resources, plant biomass is considered to be the only sustainable and carbon-neutral source for liquid fuels (Huber et al., 2006). Also, biomass has the potential to be an important source for biobased chemicals and polymers (Carole et al., 2004) replacing oil based products. Among lignocellulosics, woody biomass is most abundant and uniformly distributed around the world. In addition, woody biomass collection and processing has significant advantages over annual agricultural lignocellulosics due to its 3-4 times higher bulk density and one order of magnitude lower ash content.

One of the biggest challenges of converting woody biomass into biofuels and chemicals is overcoming the difficulty to cleanly fractionate lignocellulosics into the individual polymers: cellulose, hemicellulose and lignin (Bozell, 2010). One of the promising methods is autohydrolysis whereby hemicellulose is dissolved using water/steam as the only solvent. Also, autohydrolysis is cheap and environmentally friendly because it results in simpler downstream processes compared to dilute acid and alkaline pre-hydrolysis. Autohydrolysis may also be used in combination with kraft pulping to produce co-products such as ethanol and acetic acid (Mao et al., 2008) besides pulp (Mendes et al., 2009; San Martín et al., 1995). Similarly, the oriented strand board (OSB) industry appears to be suitable for this technical approach as it is composed of large centralized facilities. During autohydrolysis, acetic acid is released from O-acetyl groups in the polysaccharides, which lowers the pH of the extract to 3~4 (Brasch and Free, 1965). The hemicelluloses are then dissolved as oligomers after acid hydrolysis of the polymeric structures. Subsequently the hemicellulose oligomers in solution are partially further hydrolyzed to mono sugars and sugar degradation products. Sugar degradation products include hydroxyfurfural (HMF) formed from hexose sugars and furfural generated from pentoses and carbon dioxide by decarboxylation of uronic acids (Leschinsky et al., 2009).

To date the kinetics and mechanism of hemicellulose dissolution from wood using hot water is not well understood. Previous research for autohydrolysis was mostly carried out in batch reactors (Garrote et al., 1999; Jacobsen and Wyman, 2002; Mittal et al., 2009; Conner and Lorenz, 1986; Conner, 1983; Garrote et al., 2004; Nabarlatz et al.,

2005). Unfortunately batch reactors are not best suited to study the intrinsic kinetics of xylan dissolution because the dissolved hemicelluloses are further degraded in solution. On the other hand, the use of flow-through systems has shown that xylan removal increases with flow rate which is inconsistent with intrinsic homogeneous kinetics (Liu and Wyman, 2003). In addition, studies on the degree of polymerization of xylan using the flow-through system suggest that lignin-xylan oligomers and their solubility could have a large effect on the rates of removal and yields of lignocellulosic biomass pretreatment (Yang and Wyman, 2008). More recently, a continuous mixed batch reactor (CMBR) was used to study the kinetics of removal of hemicelluloses and lignin from mixed southern hardwood (SHM) chips with hot water. The system was shown to be suitable to study the intrinsic kinetics of the autohydrolysis process because the wood component dissolution rates were independent of flow rate and wood-to-liquid mass ratio (Chen et al., 2010). However, the rates were still affected by diffusional transport of the components out of the wood chips. Also the pH was not well controlled in the acid region. Therefore the same continuous mixed batch reactor was used in the present work but now wood-meal was used to study the kinetics of the removal of hemicellulose from hardwood (*Acer rubrum*) at carefully controlled temperature (150, 160, and170°C) and pH (2, 3, 4, and 5) conditions.

CHAPTER

2 LITERATURE REVIEW

2.1 Chemical composition of wood

The main structural components of the wood cell are cellulose, hemicelluloses and lignin. In addition there are also small amounts of pectic substances (Fengel and Wegener, 1983). Typical compositions for softwood and hardwoods are shown in Table 2.1. Generally polysaccharides represent the major part of the wood mass.

2.1.1 Cellulose

Cellulose is the main polysaccharide of wood. It is a linear polymer of anhydro D-glucopyranose units connected by β-1,4-glycosidic bonds (Figure 2.1). Because of its linear structure and intramolecular hydrogen bonding this polymer forms a very organized structure in the wood fibers (Sjöström, 1993). Cellulose fibrils contain alternating crystalline and amorphous regions. The fibrils are highly ordered in the crystalline region, whereas they are less ordered in the amorphous regions (Figure 2.2). This is an important property since cellulose is much more susceptible to react in its amorphous regions rather than the crystalline regions due to the accessibility of the reagents. Molecular weight measurements have shown that the degree of polymerization (DP) of cellulose is in the range of 10,000 to 15,000 depending on the source.

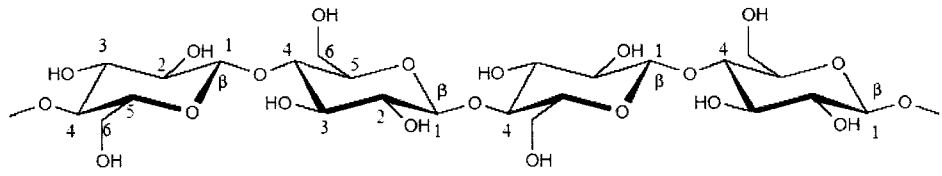

Figure 2.1. Structure of cellulose.

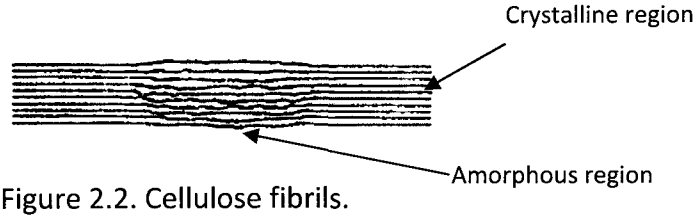

Figure 2.2. Cellulose fibrils.

Table 2.1. Major components of wood (weight % of dry wood). Adapted from Sjöström (1993).

	Cellulose	Glucomannan	Xylan	Other polysaccharides	Lignin
Softwood	33-42	14-20	5-11	3-9	27-32
Hardwood	38-51	1-4	14-30	2-4	21-31

2.1.2 Hardwood hemicellulose

Unlike cellulose, hemicelluloses are a group of branched heteropolysaccharides. The hemicelluloses in softwoods differ in structure from those in hardwoods. Galactoglucomannans are the principal hemicelluloses in softwood, whereas glucuronoxylan is the main hemicellulose in hardwood species.

The backbone of O-acetyl-4-O-methylglucurono-ß-D-xylan (Figure 2.3) consists of β-1,4-linked xylopyranose units. Most of the hydroxyl groups at the C2 and/or C3 of the xylose units are substituted with acetyl groups with about seven acetyl residues per ten xylose units. In addition, xylose units are substituted with α-1,2-linked 4-O-

methylglucuronic acid residues in most hardwood xylans on average at every 10th xylose unit. Unlike softwood xylan, hardwood xylan does not contain arabinose side chains. The average degree of polymerization of xylan is approximately 100. Hardwood also contains glucomannan with a backbone of β-1,4-linked D-mannopyranose and D-glucopyranose units (Fengel and Wegener, 1983; Sjöström, 1993). The ratio of mannose to glucose units is between 1:1 and 2.3:1.

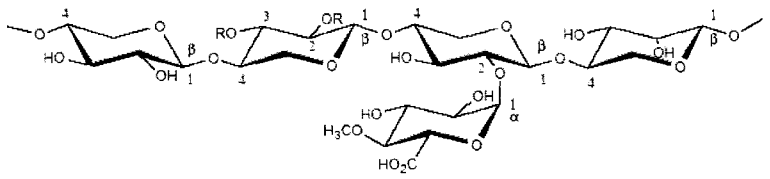

Figure 2.3. Structure of major hardwood hemicelluloses.

Hardwood also contains glucomannan with a backbone of β-1,4-linked D-mannopyranose and D-glucopyranose units. The ratio of mannose to glucose units is between 2.3:1 and 1:1 (Sjöström, 1993).

There are other minor polysaccharides in wood. Starch, which is made of glucan oligomers can be found in parenchyma cells of wood tissue. Pectins comprise galacturans, galactans and arabinans. In particular, rhamnogalacturan has a backbone of α-(1-4)-linked galacturonic acid units which contains a rhamnose unit at regular intervals of about 8 units; about half of them carry a galactan side chain (Fengel and Wegener, 1983).

2.1.3 Lignin

Lignin is a natural polymer of modified phenylpropane units (Sjöström, 1993). The main precursor of lignin in softwoods is trans-coniferyl alcohol (1) (Figure 2.4). In hardwoods, trans-sinapyl alcohol (2) and trans -p-coumaryl alcohol (3) are also lignin precursors. The precursors are polymerized during lignin biosynthesis.

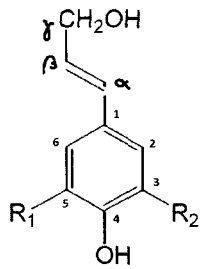

(1) R_1 = H, R_2 = OCH_3
(2) R_1 = R_2 = OCH_3
(3) R_1 = R_2 = H

Figure 2.4. Structure of lignin precursors phenyl propanoid units.

The phenylpropane units are joined together both with C-O-C (ether) and C-C linkages. The ether linkages dominate; approximately two thirds or more are of this type, and the rest are of the carbon-to-carbon type. These structural elements are not linked to each other in any particular order, although some of the linkage types seem to be more thermodynamically favoured (Table 2.2). The polymerization results in a highly branched three-dimensional crosslinked polymer of unknown molecular mass (Figure 2.5).

Table 2.2. Proportion of different types of linkages connecting the phenylpropane units in lignin[a].

Linkage type	Dimer structure	Percent of the total linkages
β-O-4	Arylglycerol-β-aryl ether	60[b]
α-O-4	Noncyclic benzyl aryl ether	7
β-5	Phenylcoumaran	6
5-5	Biphenyl	5
4-O-5	Diaryl ether	7
β-1	1,2-Diaryl propane	7
β-β	Linked through side chains	3

[a] Adapted from Sjöström (1993)

[b] Of these structures about 40% are of guaiacyl type and 60% of syringyl type.

Lignin-carbohydrate bonds

The existence of covalent bonds between lignin and polysaccharides has been a subject of intensive studies in the past and of great interest today. Because of other association forces of a physical nature between lignin and carbohydrates, it is difficult to verify the existence of such bonds. Lately Lawoko and coworkers have developed a new method for quantitative isolation of lignin-carbohydrate complexes (LCC) from softwood pulp (Lawoko et al., 2003). By using this method it has been proposed that all lignin is chemically linked to polysaccharides in softwood (Lawoko, 2005). The presence of LCC has been reported for hardwoods where lignin was found to be bound to xylan and cellulose. The existence of carbohydrate-free lignin was also reported (Lawoko and van Heiningen, 2010). The linkages between lignin and carbohydrates can be either of ether, ester, or glycosidic type (Figure 2.6).

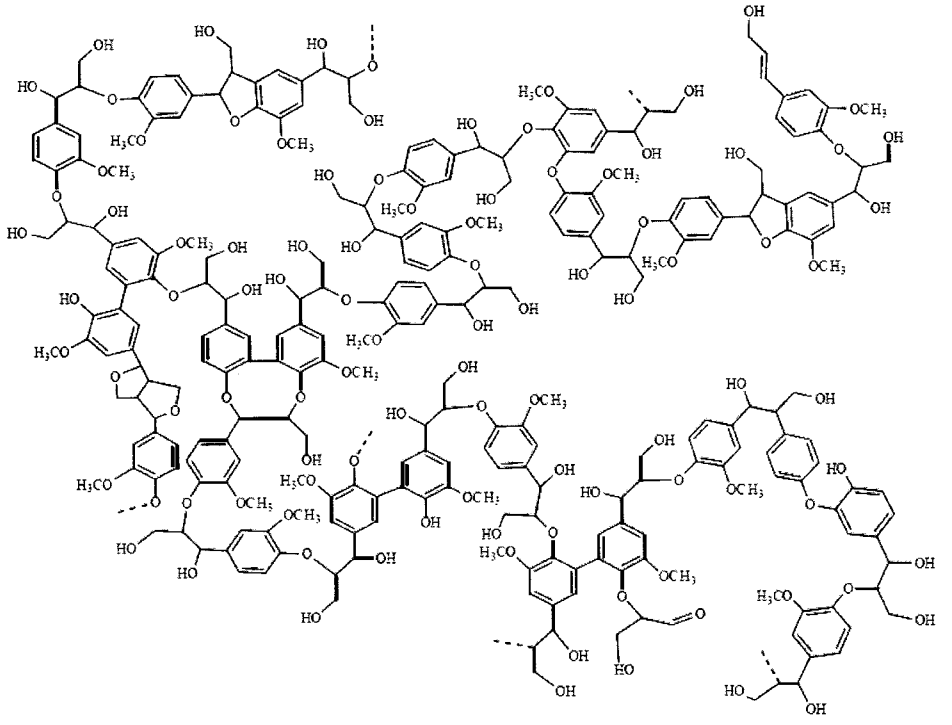

Figure 2.5. A model for softwood lignin (Henriksson, 2009).

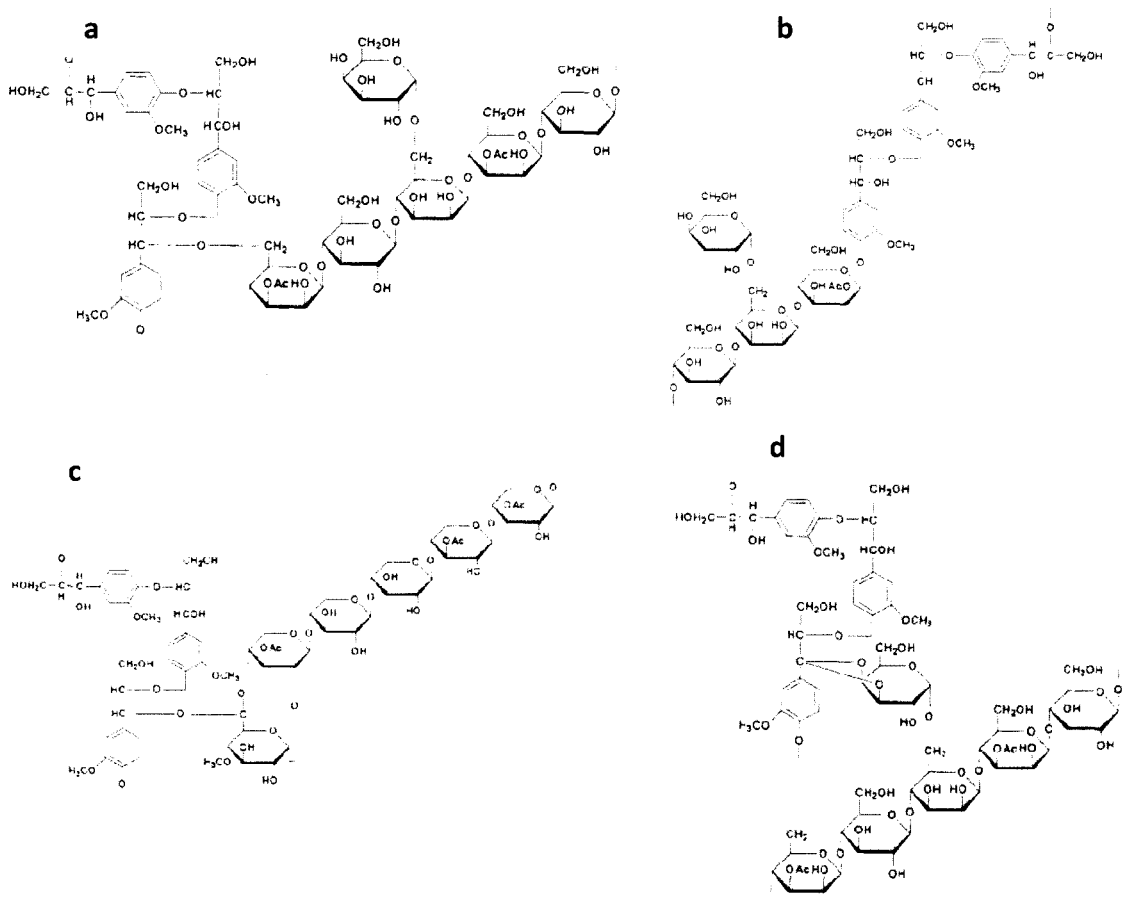

Figure 2.6. Proposed structures for lignin carbohydrate complexes: a) benzyl ether bond, b) glycoside bond, c) benzyl ester bond, d) acetal bond (Watonabe, 2003).

2.2 Ultrastructúre arrangement of the fibre wall

The wood fibre cell walls are composed of the three groups of structural wood polymers; cellulose, hemicelluloses, and lignin. These three components make up the different layers of the cell wall which consists of the middle lamella (ML), primary wall (P), and the secondary wall. The latter consists of a thin outer layer (S_1), a thick middle layer (S_2) and a thin inner layer (S_3). These layers differ in their fibrillar orientation and distribution, and in structure and chemical composition. Figure 2.7 show a simplified structure model of a woody fiber (Sjöström, 1993).

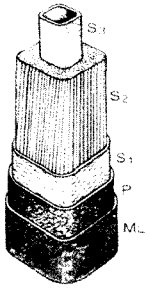

Figure 2.7. Cell wall model with the fibrillar structure of the cell wall layers. ML = Middle lamella; P = Primary wall; S = Secondary wall (S_1, S_2, S_3).

The type of association of the wood components in the cell wall strongly affects the mechanical properties and the performance of the material. It is also a key factor for the interpretation of the kinetics and mechanism of wood fractionation with hot water. Recent studies on the ultrastructure of the cell wall have generated new understanding of the associations between xylan, cellulose, and lignin. In a recent work Dammström et al. (2009) conclude that there is one fraction of xylan that is strongly associated with cellulose. In their model they identify three types of xylan: glucuronoxylan (GX) tightly

coated to the surface of cellulose microfibrils, free xylan, and xylan attached to lignin by LCC bonds (Figure 2.8). In an earlier study Reis and Vian (2004) investigated the role of glucuronoxylan during the early assembly of the helicoidal cell walls in the wood fibre. They concluded that cellulose and xylan associate with each other forming a cellulose/GX composite, which is charged and highly anisotropic as a consequence of the carboxylic groups of the glucuronoxylans. The cellulose/GX composite structures are arranged in a face to face manner, forming a sort of 'host structure' for lignin precursors during lignin polymerization.

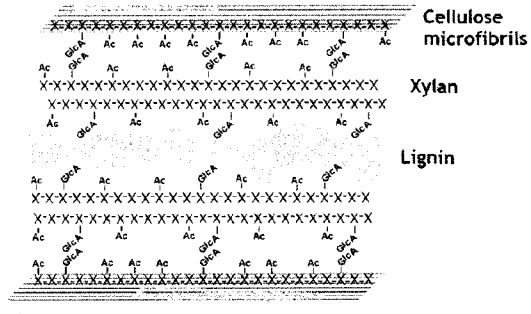

Figure 2.8. Model for the arrangement of cellulose, xylan, and lignin in the secondary cell walls of aspen wood (Dammström et al., 2009).

2.3 Pre-extraction of hemicellulose with steam/hot water

Pre-extraction processes on lignocellulosics have been widely studied during the last decades. There are at least three applications identified of this biomass process: pre-extraction/kraft cooking of wood chips for further production of dissolving pulp and specialty cellulose, and lately for the simultaneous production of ethanol and conventional kraft quality pulp; as a pre-treatment of biomass required to alter its ultrastructure making cellulose more accessible for enzymatic hydrolysis; and pre-

extraction of hemicelluloses from lignocellulosics as a source for further production of chemicals and fuels.

The concept of pre-hydrolyzing wood chips before conventional pulping is not new. Literature has focused on pretreatment of wood chips before Kraft pulping using various acids, sulfite liquor, or autohydrolysis with hot water (Rydholm, 1965). Generally, these studies were intended for the production of low-hemicellulose-content dissolving pulps. Casebier et al. (1969, 1973) investigated the chemistry and mechanism of water prehydrolysis on both softwood and hardwood. However, until now, water prehydrolysis and thus the recovery of the dissolved material are not practiced mainly because of the formation of uncontrollable (sticky) lignin-derived precipitates (Leschinsky et al., 2007).

It has been proposed to transform pulp mills into an integrated forest biorefineries (IFBRs) due to global competition and local concerns about employment and sustainability (van Heiningen, 2006). This same approach has been proposed for the OSB industry (Paredes et al., 2008).The aim of this new concept is the removal and commercialization of material, such as hemicelluloses, that do not contribute to the final product properties. However, as a result of the removal process, the remaining cellulose should not undergo significant degradation. The pre-extraction of softwood (Loblolly pine) with hot water followed by kraft cooking has been investigated. A maximum of about 12% of the wood mass was extracted as wood sugars at an H-factor of about 1,500 hours. The delignification rate constants for kraft cooking of water pre-extracted chips were 40 to 60% higher than corresponding kraft control cooks.

Unfortunately, the total pulp yield based on the original wood was much lower than the control (Yoon et al., 2006). Mao et al. (2008) modeled a near-neutral pre-extraction process, which involves the extraction of wood hemicellulose using green liquor prior to conventional Kraft pulping, using WinGEMS and ASPEN Plus software. The rate of return on investment was found to vary between 10 and 14 percent depending upon the size of the pulp mill (750 to 1,500 tonne per day pulp production rate) for the case where the extraction vessel is available and the utilities and waste treatment facilities are sufficiently large to handle the additional requirements for the process.

Pretreatment of lignocellulosic material is used to make cellulose more accessible for enzymatic hydrolysis. These pretreatments remove hemicelluloses together with lignin, and lead to cellulose degradation. There are numerous reviews in the literature summarizing these treatments (McMillan, 1994; Sun and Cheng, 2002; Mosier et al. 2005). The most studied treatments are catalyzed and uncatalyzed steam explosion, dilute-acid hydrolysis and liquid hot water extraction.

Steam explosion refers to a pretreatment technique in which lignocellulosic biomass is heated rapidly by high-pressure steam. The biomass/steam mixture is held for a period of time to promote hemicellulose hydrolysis, and terminated by an explosive decompression. Steam explosion is typically initiated at a temperature of 160-260°C for several seconds to a few minutes before the material is exposed to atmospheric pressure (Sun and Cheng, 2002). Steam explosion (and hot water) involves chemical effects where acetic acid is generated from hydrolysis of acetyl groups associated with the hemicellulose which then further catalyze hydrolysis but also xylose

or glucose degradation (Mosier et al., 2005). These compounds, principally furfural from pentoses and 5-hydroxymethyl furfural from hexoses, are inhibitory to microbial fermentation (Palmqvist and Hahn-Hagerdal, 2000). The process can also cause lignin condensation due to high temperature and acidity. In many respects, the effects of the process on the lignin fraction are similar to those obtained with acidolysis and ethanolysis. Depolymerization and condensation reactions of lignin have been found to occur during the steaming process of wood (Chua et al., 1979).

Addition of H_2SO_4, SO_2 or CO_2 in steam explosion can improve enzymatic hydrolysis, decrease the production of inhibitory compounds, and lead to more complete removal of hemicelluloses (Wayman et al., 1986; Morjanoff and Gray, 1987; Wayman et al., 1988; McMillan, 1994). Wayman et al. (1986) reported removal of up to 89% of the hemicelluloses in wood using up to 2.6% SO_2 on wood as catalyst, and also found that nearly all of the removed sugars were present as monomers. Puri and Mamers (1983) investigated lignocellulosic material subjected to the action of steam and high-pressure carbon dioxide. Examination of the exploded furnishes indicated the pretreatment had substantially solubilized the hemicellulose fraction of *Eucalyptus regnans*, giving a liquor rich in xylan with close to 70% in the form of monomers.

Water pretreatments use pressure to maintain the water in the liquid state at elevated temperatures. This type of pretreatment has been termed hydrothermolysis, aqueous or steam/aqueous fractionation, uncatalyzed solvolysis, and aquasolv (Mosier et al., 2005). Up to 60% of biomass under hot water pretreatment at temperatures

between 200-230°C for up to 15 min can be dissolved. At these conditions all of the hemicellulose, 4-22% of the cellulose, and 35-60% of the lignin can be removed.

Fractionation of lignocellulosic materials using autohydrolysis has been investigated for the production of xylo-oligosaccharides from different lignocellulosics using batch reactor systems (hardwood, corncobs, husks, almond shells) (Garrote et al., 2003; Garrote et al., 2004; Nabarlatz et al., 2005). Complete chemical characterization, kinetic models and optimal operational conditions have been established. Autohydrolysis of *Eucalyptus globulus* wood chips has been investigated to study the kinetics of hemicellulose degradation and the effects on cellulose and lignin (Garrote et al., 1999; Garrote and Parajó, 2002). It was reported that 90.4% of the initial xylan was removed, which also caused some delignification (up to 13.8% of the initial lignin was removed), whereas cellulose was almost quantitatively retained in the solid phase. On the other hand, the use of flowthrough systems has shown that xylan removal increases with flow rate which is inconsistent with intrinsic homogeneous kinetics (Liu and Wyman, 2003). In addition, studies on the degree of polymerization of xylan using the flowthrough system suggest that lignin-xylan oligomers and their solubility could have a large effect on the rates of removal and yields of lignocellulosic biomass pretreatment (Yang and Wyman, 2008).

Dilute acid hydrolysis has been successfully developed for pretreatment of lignocellulosic materials. This process can achieve high reaction rates and significantly improve cellulose hydrolysis. (Esteghlalian, 1997). Acid hydrolysis releases oligomers and monosacharides and has been modeled in the past as a homogeneous reaction in

which acid catalyzes breakdown of cellulose/xylan to glucose/xylose followed by breakdown of the glucose/xylose released to form hydroxymethyl furfural (HMF)/furfural (F) and other degradation products. This reflects the approximately equal reactivity of glycosidic bonds in these polymers with respect to hydrolysis (Mosier et al., 2005). At moderate temperatures, direct saccharification suffers from low yields because of sugar decomposition. High temperature dilute treatment is favorable for cellulose hydrolysis (McMillan, 1994). Although dilute acid pretreatment can significantly improve the cellulose hydrolysis, its cost is usually higher than some physical-chemical pretreatment processes such as steam explosion. Neutralization is necessary for the downstream enzymatic hydrolysis or fermentation processes. Recently developed dilute acid hydrolysis processes use less severe conditions and achieve high xylan to xylose conversion yields using several lignocellulosic materials (Martínez et al., 1995; Kim et al., 2001; Neureiter et al., 2002; Sanchez et al., 2004; Yang et al., 2006; Sun and Cheng, 2002).

2.4 Hemicellulose hydrolysis and degradation in acidic medium

2.4.1 Mechanism of acidic hydrolysis

The mechanism which is most widely accepted for the acid catalyzed hydrolysis of wood chemical species containing glycosidic bonds (e.g., polyoses) is based on the protonation of the glycosidic oxygen (Abatzoglou and Chornet, 1998; Fengel and Wegener, 1983; Sjöström 1993). In this mechanism shown in Figure 2.9, protonation is

followed by breaking of the glycosidic bond and simultaneous formation of a lower molecular weight polyosic chain and a relatively unstable carbocation which reacts with water to give birth to another smaller polyosic chain. The carbocation is the one which produces, with water addition, the reducing hemiacetalic hydroxyl.

It is also indicated that furanosidic ring structures are hydrolyzed more rapidly than pyranosidic rings, due to higher structural angle strains in the conformation of furanosidic sugar units as compared to the strain-free pyranose ring (Fengel and Wegener, 1983).

2.4.2 Mechanism of sugar degradation

In addition to hydrolysis, a large number of side reactions occur, among which dehydration reactions are considered most important (Abatzoglou and Chornet, 1998). Acid-catalyzed dehydration under mild conditions leads to the formation of anhydro sugars with intramolecular glycosidic linkages, resulting from the elimination of a water molecule from two hydroxyl groups. The most important degradation products with regards to yield and potential utilization are the cyclic furfurals formed from pentoses and uronic acids, and hydroxymethylfurfural (HMF) from hexose sugars, mainly glucose. High yield of these compounds are only obtained in concentrated acids at elevated temperatures (Fengel and Wegener, 1983).

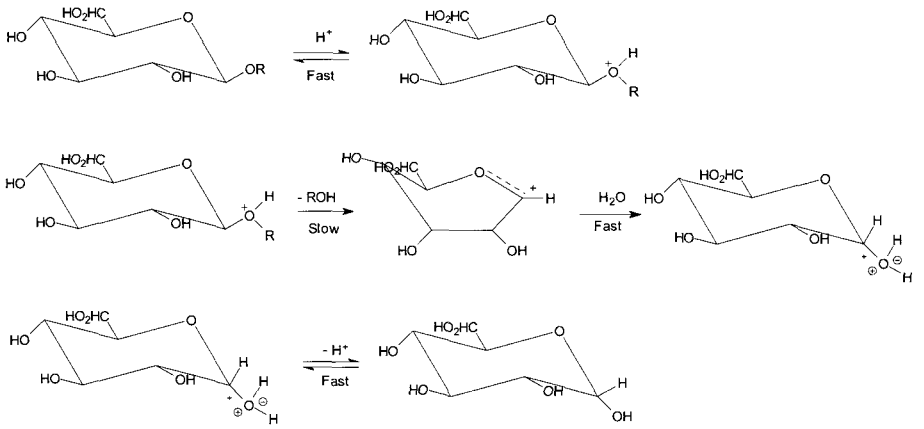

Figure 2.9. Mechanism of the acid-catalyzed hydrolysis of the glycosidic bond via the cyclic carbonium-oxionium ion.

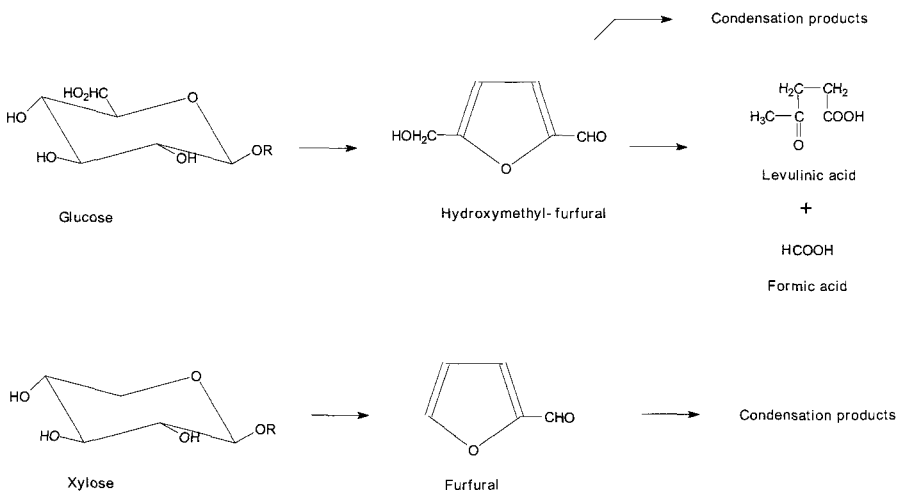

Figure 2.10. Formation of furfural, hydroxymethyl-furfural, levulinic acid and formic acid from monosaccharides in acidic medium.

2.5 Kinetic models

The description of hemicellulose hydrolysis has been mainly through the use of pseudokinetic models, because of the nonuniform polymeric nature of the hemicelluloses and the presence of an important number of still unknown side reactions referred in the literature as degradation and condensation reactions (Abatzoglou and Chornet, 1998). Abatzouglou et al. (1990) propose a model with the following reaction path:

$$X_y \overset{k_3}{\rightarrow} X \overset{k_4}{\rightarrow} F \overset{k_6}{\rightarrow} DP \qquad \text{Equation 2.1}$$
$$\downarrow k_8$$
$$CP$$

where,

X_y : xylan

X : xylose,

F : furfural,

DP : degradation products,

CP : condensation products,

and k_i the rate constant equal to $k_{0i} C_A^{n_i} \exp\left(-\frac{E_i}{RT}\right)$, where C_A is the concentration of acid.

This model was developed for the case of a plug flow reactor giving the results shown in Table 2.3.

Table 2.3. Kinetic parameters for pentosan hydrolysis.

Reaction	k_i (min^{-1})	n_i	E_i (kJ/kmol)
3	6.2×10^{13}	1.17	122,475
4	2.3×10^{12}	0.69	113,407
6	5.6×10^{5}	0.58	75,240
8	4.1×10^{11}	0.52	122,622

Another approach to model the hemicellulose solubilization is to consider the pentosans and hemicellulosic hexosans as part of the solids and explore their solubilization patterns. This approach of kinetic modeling is phenomenological. For very complex systems, such as lignocellulosic biomass, reactions can be modeled through the use of severity factors which try to combine the effects of different operational variables into a single parameter

A simple severity factor was proposed by Overend and Chornet (1987) combining treatment temperature and time in a single severity parameter R_O for hemicellulose depolymerization by steam or aqueous pretreatments without acid addition (Equation 2.2) in which the time t is usually expressed in minutes and T is the temperature in °C.

$$R_o = t \cdot e^{\left(\frac{T-100}{14.75}\right)} \qquad \text{Equation 2.2}$$

The severity parameter was subsequently extended to include the effect of acid addition on hemicellulose solubilization and sugar recovery in a combined severity parameter for dilute acid hydrolysis defined as:

$$C_o = B \cdot t \cdot e^{\left(\frac{T-100}{14.75}\right)} \qquad \text{Equation 2.3}$$

where, B = proton concentration (mole/L) (Abatzouglou et al., 1986)

= n·A (Lloyd et al., 2003)

n : proportionality constant

A : acid concentration in weight percent

Abatzoglou et al. (1992) generalized the severity factor which includes the effect of temperature, time and acid catalyst loading for isothermal conditions as follows:

$$R_{oH} = exp\left(\frac{x-x_{ref}}{\lambda x_{ref}}\right) \cdot exp\left(\frac{T-T_{ref}}{\omega'}\right)\frac{t_R^{\gamma}}{\gamma} \qquad \text{Equation 2.4}$$

with $\omega' = \frac{RT_{ref}^2}{E_i - nx_{ref}}$, $\lambda = \left[mx_{ref} - \frac{nx_{ref}}{T_{ref}}\right]^{-1}$, and $0 < \gamma \leq 1$

where,

E_i : activation energy of uncatalysed system

T_{ref} : reference (or base) temperature (°C)

t_R : reaction time, min

x : acid loading, g of acid/g of dry biomass

x_{ref} : reference (or base) acid loading, g of acid/g of dry biomass

R : universal gas constant

n, m : parameters expressing catalyst effect in activation energy and entropy

The P-factor has been applied to pre-hydrolysis of wood chips prior to kraft pulping. This factor expresses the pre-hydrolysis time and temperature also as a single variable and is defined as (Sixta, 2006):

$$P = \int_{t_0}^{t} k_{rel} \cdot dt \qquad \text{Equation 2.5}$$

in which k_{rel} is the rate of acid-catalyzed hydrolysis of glycosidic bonds relative to that at 100°C. An Arrhenius-type equation is used to express the temperature dependence on the relative reaction rate, and an activation energy value of 125.6 kJ mol^{-1} is used to give a final expression for this factor as follows:

$$P = \int_{t_0}^{t} Exp(40.78 - \frac{15106}{T}) \cdot dt \qquad \text{Equation 2.6}$$

where t is in hours and T in Kelvin.

CHAPTER

3 OBJECTIVES AND EXPERIMENTAL SETUP

3.1 Objectives

To date the kinetics and mechanism of hemicellulose dissolution with hot water from wood is not fully understood. The aim of this thesis is to understand the intrinsic kinetics of the removal of components with hot water from hardwood (*Acer rubrum*) with particular emphasis on the removal of hemicelluloses. In order to accomplish this, the following specific objectives have been identified:

i. To investigate the influence of operating conditions, namely temperature and time, on the total extraction yield of hardwood with hot water.

ii. To investigate the chemical composition of hemicellulose extracts as a function of the severity of the water extraction.

iii. To study the degree of polymerization (DP) of cellulose in the extracted wood as a function of the severity of the extraction.

iv. To investigate the kinetics of hemicellulose and lignin removal from hardwood by studying the effect of temperature, pH, and particle size.

v. To investigate the mechanism of hemicellulose removal from hardwood by hot water extraction.

3.2 Experimental setup and chemical analysis

3.2.1 Materials

Red maple (*Acer rubrum*) trees were felled and cut into three logs. Logs were debarked mechanically with a chain saw rigged with a debarking head. Strands were produced using a Carmanah 12/48 ring strander. Strands with thickness of 0.75 mm, 10 cm length, and varying width were used for the batch system described in the next section. The chemical composition of red maple wood was determined and is shown in Table 3.1. A different tree was later felled and cut into four logs. Two logs were selected and cut in half longitudinally. One half was stranded and wood chips were produced manually from the other. Strand thickness was determined with a Mitutoyo digital caliper with precision of 0.0025 mm. Strands were dried in a dry kiln (38°C) for 24 hours and then stored in double plastic bags. Wood meal was produced from strands as needed with a Wiley mill under 1 mm hole size mesh and then sieved to 40 and 70 mesh particle size (420 and 210 μm, respectively). This last fraction was used in the Continuous Mixed Batch Reactor system described in the next section.

Table 3.1. Chemical composition of red maple. Values in mg/g of dry wood.

Chemical Component	Amount	Chemical Component	Amount
Arabinan	6.3 ± 0.2	Acetyl	26 ± 2
Galactan	6.1 ± 0.1	Uronic Acid	24 ± 2
Rhamnan	4.1 ± 0.1	Total lignin	243 ± 3
Glucan	455 ± 4	Ash	3.5 ± 0.3
Xylan	182 ± 4		
Mannan	30.4 ± 0.4		

3.2.2 Reactor Setup

Batch reactor

Extractions were performed in a batch system using a modified ASE-100 extractor (Tunc, 2008) operating at pressures of 100-150 atm. The steps are summarized in Figure 3.1. Approximately 30 grams of dry wood were used for each extraction. Deionized water was used as extraction solvent.

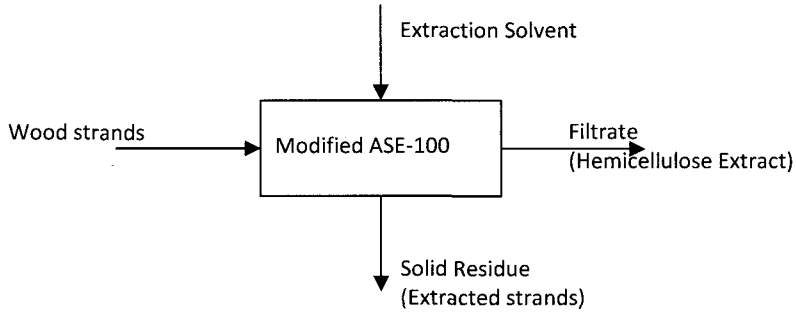

Figure 3.1. Extraction of hemicellulose using a modified version of Dionex ASE-100.

The moisture content of the wood particles was determined before they were loaded into the extraction cell. Filters are present at the inlet and outlet of the extraction cell. At the end of the extraction process the liquid phase in the extraction cell was flushed into a collection bottle using fresh water, 1.5 times the volume of the extraction cell (i.e. 150 ml). The wood remaining in the extraction cell was removed after the flushing process.

The modified ASE-100 was programmed for the desired extraction temperature and time. The liquid to wood ratio (L/W) of the extraction cell depends on the density (δ_w) and weight (m_w) of the wood sample and the volume of the extraction cell (V_c), as given in Equation 3.1.

$$\frac{L}{W} = \frac{V_c - \left(\frac{m_w}{\rho_w} + \frac{P_a}{P_b} \left\{ V_c - \frac{m_w}{\rho_w} \right\} \right)}{m_w} \qquad \text{Equation 3.1}$$

where, P_a (14.7 psig) and P_b (1700 psig) are the pressures inside the extraction cell before and during the extraction operation, respectively.

The liquid and solid phases are treated separately. The weight and pH of the liquid phase are recorded. Two samples of approximately 25 mL are taken, centrifuged to remove fine particles, and then freeze dried for solid content determination. Both the freeze dried solids and the remaining liquid phase are stored at 4°C for future analysis. The remaining wood material in the extraction cell was oven dried overnight at 100 °C (±5) and its weight determined.

Continuous mixed batch reactor

The design of the continuous mixed batch reactor (CMBR) system is shown in Figure 3.2. The extraction solution is first degassed (air) by vacuum and then pressurized by helium at 170 psi in a 5-gallon stainless high pressure vessel (R-1). It is delivered at this pressure to a one liter stainless steel high pressure vessel (R-2) kept at the desired temperature by external band heaters. The valve (V-1) in the downstream of vessel R-2 remains closed until the actual reactor vessel (R-3) is preheated to 130°C. This 280 mL reactor vessel is a so-called Berty reactor manufactured by Autoclave Engineers with a 100 mL stationary basket which holds the wood meal in a packed bed (Figure 3.4). A rotor underneath the basket induces a rapid circulating flow through the wood bed within the Berty reactor (Figure 3.3).

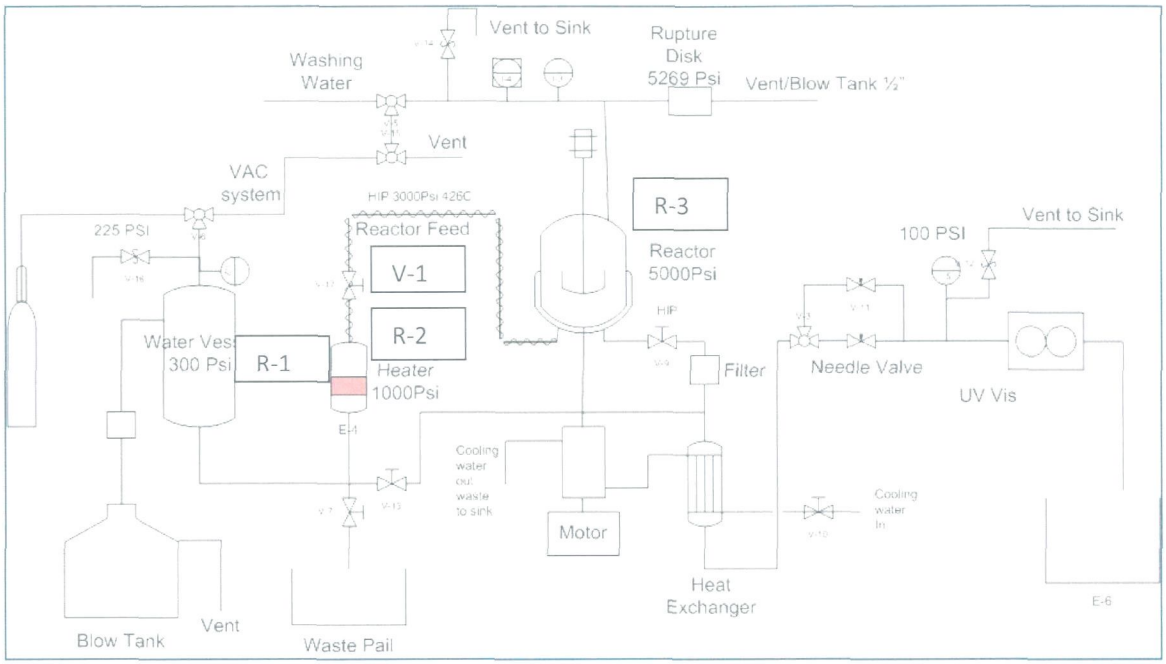

Figure 3.2. Continuous mixed batch reactor design scheme

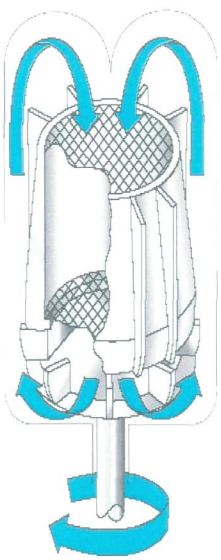

Figure 3.3. Berty stationary basket inside the reactor

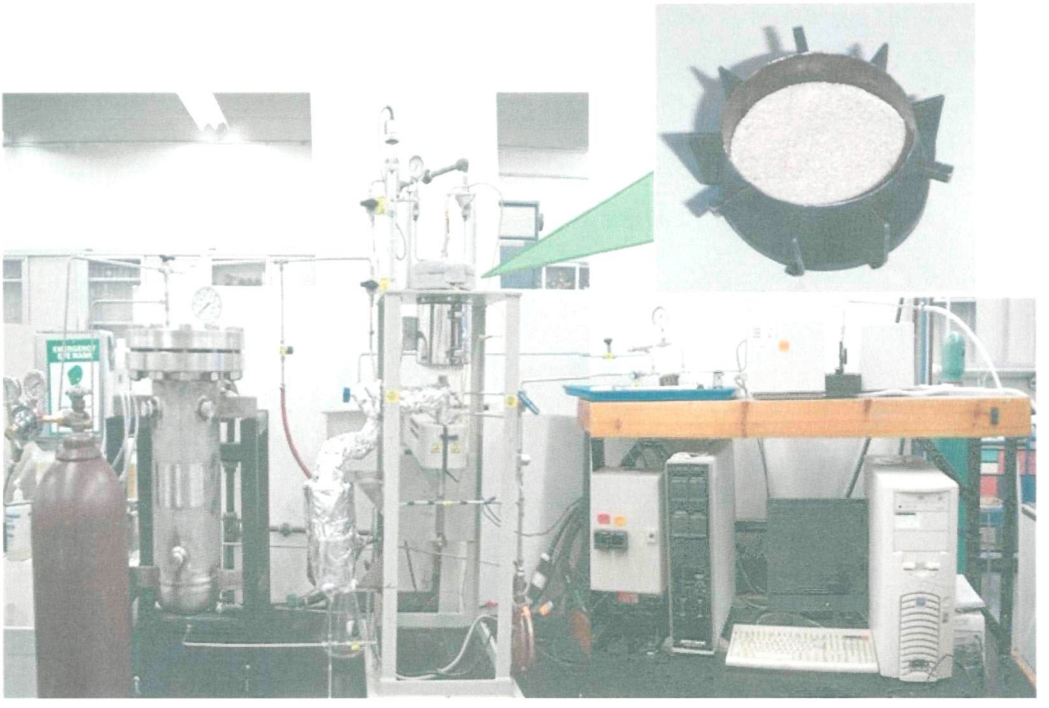

Figure 3.4. Reactor setup and Berty stationary basket

Before preheating the Berty reactor, approximately 20 mL of DI-water is added in the bottom of the reactor and air is removed by a vacuum pump. The presence of water in the reactor generates low-temperature saturated steam (130°C) during preheating which increases the accessibility of the feed solution into the wood sample because it removes part of the air trapped inside the particles. The temperature and pressure of the steam are monitored with a thermocouple and pressure transducer, respectively.

As soon as the temperature of the steam reaches the desired temperature, valve V-1 is opened so that the extraction solution enters and completely fills the reactor (R-3). The hot feed stream and external heating raises the whole reactor content to the

desired temperature in approximately 10 minutes (Figure 3.5). The outflow stream is cooled using a heat exchanger before it enters to an on-line spectrophotometer (UV-VIS) flow cell where UV adsorption data are collected every 30 seconds. The UV data are then converted into dissolved lignin concentrations using an extinction coefficient of 17 L/g·cm determined by calibration.

Liquid samples are collected at 2, 4, 6, 10, 20, 30, 40, 50, 60, 80, and 90 minutes for sugar and acetate analysis. The total amount of liquor is also collected to verify the total mass balance.

The extraction is terminated by flushing the reactor with cold water. The temperature inside the reactor is cooled down to 40°C in less than five minutes. The solid wood residue is then removed from the basket for yield, sugar and lignin measurements.

Extractions on wood chips performed with de-ionized water have shown that the pH changes during the extraction (Chen et al., 2010). Chen also found that by using 1 g/L of acetic acid solution as extraction solvent the pH can be kept almost constant at a pH of 3.2. Based on these findings a solution of 1 g/L acetic acid is also selected for the present extraction of red maple (Figure 3.6). The higher initial effluent pH is principally due to an ion- exchange reaction between the inorganic cations bound to acid groups in the wood and the hydronium ions in the applied solution (Springer and Harris, 1985). However, for the investigation of the pH effect on the extraction kinetics, different concentrations of formic acid (HFA) and sodium formate (NaFA) are prepared to achieve the following pH targets: pH 2, 3, 4, and 5. The solutions are prepared as follows: 6.67

g/L HFA (pH 2.1 ±0.1), 1.00 g/L HFA + 0.33 g/L NaFA (pH 3.0 ±0.1), 1.00 g/L NaFA + 0.19 g/L HFA (pH 4.0 ±0.1), and 2.0 g/L NaFA + 3.7 mg/L HFA (pH 5.0 ±0.1).

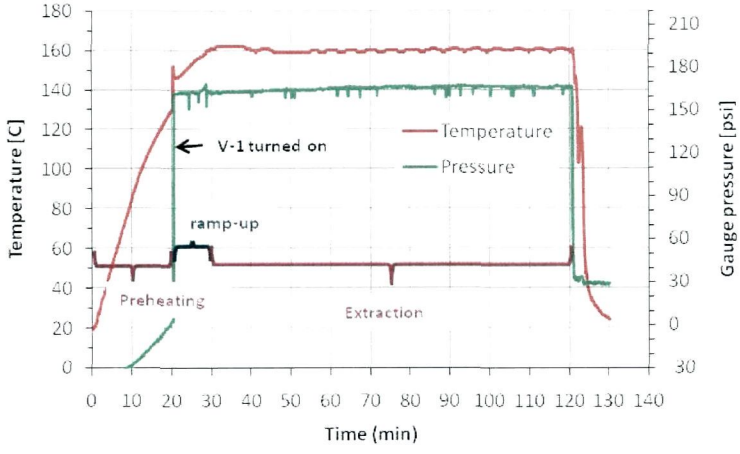

Figure 3.5. Temperature and pressure profiles of the reactor during water extraction.

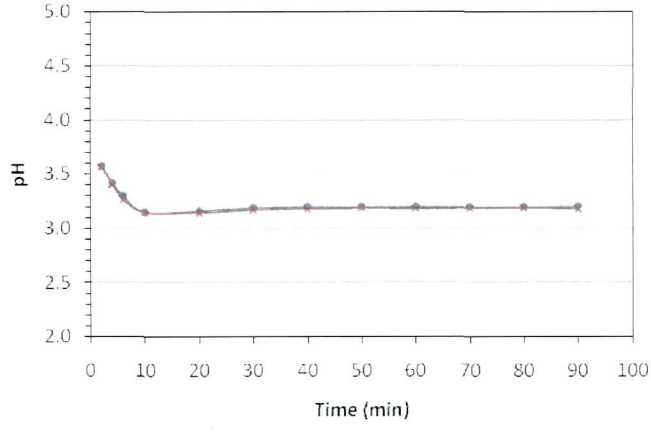

Figure 3.6. pH profile during extraction of hemicelluloses from wood meal with an acetic acid solution of 1 g/L concentration.

3.2.3 Chemical analysis

The experimental analysis scheme for the extraction of wood components from hardwood is summarized in Figure 3.7. The solid phase is analyzed for carbohydrate (cellulose and hemicellulose) and lignin content. The liquid phase is analyzed for carbohydrate, lignin, furfural, hydroxymethylfurfural, and acetyl groups.

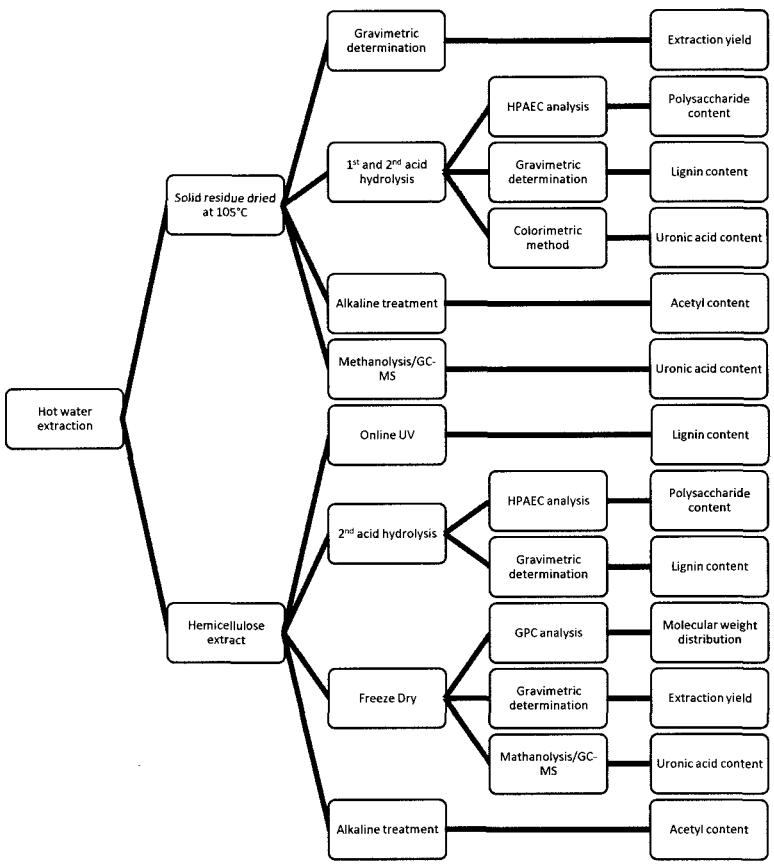

Figure 3.7. Experimental design for extraction of hemicelluloses from hardwood.

Total yield

The extraction yield was calculated by comparing the amount of oven dry wood in the extraction cell before and after water extraction as:

$$Yield^{SPh}(\%) = (1 - \frac{solid\ residue\ (o.d.) after\ extraction}{wood\ (o.d.) before\ extraction}) \times 100 \qquad \text{Equation 3.2}$$

In the same way, the extraction yield obtained from the liquid phase was calculated based on a determination of its solid content (SC, w/w) using the following expression. SC was determined in duplicate by freeze drying two liquid samples of the extract.

$$Yield^{LPh}(\%) = \frac{SC \times total\ weight\ extract}{wood\ (o.d.) before\ extraction} \times 100 \qquad \text{Equation 3.3}$$

Monosugar and polysaccharide determination

Liquid samples:

Liquid samples (8.4 mL) were mixed with 0.3 mL of sulfuric acid (72% w/w) for a final concentration of 4% w/w of sulfuric acid. A set of six monosaccharide standards (arabinose, galactose, rhamnose, glucose, xylose, and mannose) were dissolved in 4% w/w sulfuric acid for calibration with final concentrations of 0.1-1.0 g/L. Samples were placed in an autoclave set at 121°C for one hour for acid hydrolysis to monomers. Standards were also autoclaved together with samples in order to correct for acid degradation of monomers to furfural/hydroxymethylfurfural during acid hydrolysis. After autoclaving 0.2 mL of fucose 50 mg/mL was added to all samples and standards.

The total monosugar content was then determined by High Performance Anion Exchange Chromatography with Pulse Amperometric Detection (HPAEC-PAD, Dionex) analysis as described by Davis (1998). Samples and standards were diluted 10 times before injection into the HPAEC-PAD instrument for monosugar determination.

The monosugar content in the extract sample was measured by directly injecting the extract solution in the HPAEC-PAD instrument. In this case the set of monosaccharide standards sugars were not autoclaved. Results were an average from three injections in the HPAEC.

Solid samples:

Close to 100 mg of wood sample was subjected to a standard sequential double acid hydrolysis at 72% and 4% sulfuric acid (H_2SO_4) concentration for monosaccharide determination as described by Davis (1998). The final volume of the autoclaved 4% sulfuric acid solution is 44.5 mL. The same set of six monosaccharide standards as for liquid samples were dissolved in 4% w/w sulfuric acid for calibration with final concentrations of 0.1-7.0 g/L. Standards were placed in an autoclave set at 121°C for one hour together with wood samples. After autoclaving 1 mL of fucose 50 mg/mL was added to all samples and standards and diluted 10 times before injecting them into the HPAEC-PAD instrument for monosugar determination. Results were an average from two sample replicates and three injections in the HPAEC.

Lignin

Solid samples:

The acid insoluble lignin or Klason lignin in the original/extracted wood was determined according to Effland (1977), while the acid soluble lignin (ASL) concentration was determined according to Tappi Method 250.

Liquid samples:

The total lignin content in liquid samples was determined as the sum of the precipitate after the second hydrolysis step for monosaccharide determination sample preparation (Klason lignin) and of ASL in the filtrate. For online determination in the CMBR system the extinction coefficient of hardwood lignin dissolved in aqueous media was determined separately in order to convert the absorbance readings from the online UV-VIS spectrophotometer into a concentration of lignin in grams per liter as described in section 4.2.

Acetate

The total acetyl group content was determined from the acetic acid content in the hydrolysate produced after the second hydrolysis step during sample preparation for monosaccharide determination in wood and extracts.

Sample preparation for liquid samples: The pH of 5 mL of extract sample was adjusted to a value of 12 with a 2M NaOH solution. Then, the sample was heated at 70°C in a water bath for 1 hour for complete deacetylation (Song et al., 2008).

Sample preparation for solid samples: 100 mg of extracted wood sample was hydrolyzed with 5 mL of 1 M NaOH solution and heated at 70°C in a water bath for 1 hour for complete deacetylation. The original wood sample was hydrolyzed in acidic media with 4% sulfuric acid solution at 121°C for one hour. In this case the hydrolyzed sample was neutralized before using the kit for acetyl group determination.

The acetic acid content was determined by high performance liquid chromatography (HPLC) using a refractive index detector and BIO-RAD Aminex HPX-87H column. The mobile phase used was 5 mM H_2SO_4 with a flow rate of 0.6 mL/min and the oven temperature was 60°C. The determination was based on a calibration curve for acetic acid.

The total acetyl group concentration in liquid and solid samples was also determined by using the Megazyme Acetic Acid kit (K-ACET).

Uronic anhydride

The uronic anhydride content of original/extracted wood was determined using the chromophoric group analysis after a two-step acid hydrolysis treatment developed by Scott (1979). Dimethylphenol was used as standard, and the content of uronic anhydride was calculated from the difference in UV absorption at 400 and 450 nm.

In wood there are different sources for uronic acids. They can be found in pectin (galacturonic acid, GalUA), other minor sugars (glucuronic acids), and as a branch on xylans (Sjöström, 1993). Methanolysis coupled with gas chromatography has shown to

be a method able to identify and quantify all different uronic acids in wood. Methanolysis was performed according to Li et al. (2007) on selected solid and liquid samples. Liquid samples were freeze dried and 5-10 µg were weight for the analysis. Solid samples were ground below 40 mesh. A sample close to 5 mg was placed in a 10 mL flask and dried in a rotary evaporator with vacuum at 50°C adding 1 drop of methanol.

After methanolysis samples were acetylated adding 300 µL of pyridine and acetyl anhydride (1/1 volume) and samples were kept at room temperature for 30 minutes. Then, samples were dissolved in ethyl-acetate and analyzed by gas chromatography with mass spectrometry detector (GC-MS) (SHIMADZU model GC2010 with detector QP2010S). The instrument used a capillary column type RTX 225 (length 30 m, internal diameter 0.25 mm, film thickness 0.25 µm). Sorbitol was used as an internal standard. The GC-MS conditions were: 1 µL of sample was injected in the GC operating in split ratio mode of 1:20. The injection temperature was maintained at 250 °C and the detector temperature at 260 °C. The oven temperature program was as follows: from 120 °C to 200 °C at a rate of 5 °C/min and held at 200 °C for 5 minutes, then from 200 °C to 280 °C at a rate of 4 °C/min and held at 280 °C for 10 minutes. The total flow was maintained at 25 ml/min.

Molecular weight distribution of extracts

The dimethylacetamide system:

A 0.8% solution of lithium chloride in dimethylacetamide (0.8% LiCl/DMAc) was prepared. This solvent system for cellulosic material was first described by McCormick (1981). Liquid samples were freeze-dried and 100 mg of the freeze dried material was placed in small 30 mL volume glass vials equipped with teflon coated screw locks, and 10mL of 0.8% LiCl/DMAc was added and the vials capped. The mixture was stirred with a metallic teflon coated bar on a magnetic/electric heater set at 80°C for 10 minutes. Complete dissolution of the solid material was obtained. Then, 2ml of samples were transferred to small GPC vials for the Gel Permeation Chromatography (GPC) or Size Exclusion Chromatography (SEC) analysis.

The GPC instrument used was a Viscotek system equipped with spectrophotometric (UV-Vis), refractive index (RI), and intrinsic viscosity differential pressure (IV-DP) detectors. The RI detector is run at ambient temperature. The UV detector is set at 295nm to offset any interference from the solvent absorbance. The system also consisted of three PLgel columns coupled in series, and incubated at 80°C. The solvent system applied is 0.8% LiCl/DMAc at a flow rate of 0.7mL/min.

For calibration, the universal calibration method is applied. Pullullan standards are used. Known Mark Houwink constants of the standards and for cellulose as reported in literature (Bikova and Treimanis, 2002) are used to convert retention volumes into molar mass distributions from the relationship in Equation 4.4.

$$K_{Std}^{a1} \cdot M_{Std} = K_S^{a2} \cdot M_S \qquad \text{Equation 4.4}$$

where,

K_{Std}^{a1}, K_S^{a2} : Mark Houwink constants for standards and cellulose, respectively.

M_{Std}, M_S : molar masses for standards and hemicelluloses at any given elution volume.

Once M_S is calculated relative to pullullan, a plot of Logarithm of M versus detector response is generated. From this plot, it is possible to calculate the average molar mass by applying equation 4.5.

$$M_V = \left[\frac{\sum_i A_i M_i^a}{\sum_i A_i}\right]^{1/a} \qquad \text{Equation 4.5}$$

where,

M_V, M_i : viscosity average molecular weight and molecular weight at each retention volume respectively.

Ai : area under the chromatogram between each retention volume interval.

a : Mark Houwink coefficient.

The alkaline (NaOH) system:

The GPC instrument used for this system was the Viscotek system described above.

Calibration Standards: Pullulan standards were applied (Mw = 342, 1320, 5900, 11800, 22800, 47,300). All standards were completely dissolved in 0.4M NaOH. Concentrations used were 5 mg/mL.

Sample preparation: Liquid samples were concentrated using a rotary evaporator to the desire concentration. The concentrated samples were dissolved completely by adding 1 volume of 0.4M NaOH to 2 volumes of sample. The resulting dissolved wood polymer concentration was between 10-15 mg/mL. Since the UV signal is far more sensitive than the other detectors, such concentrations resulted in a UV-overshoot signal. Thus another run is performed at concentrations as low as 0.2mg/mL to get a proper UV response.

Calibration Method: Direct calibration method was performed using Pullullan standards. Figure 3.8 shows the calibration curve.

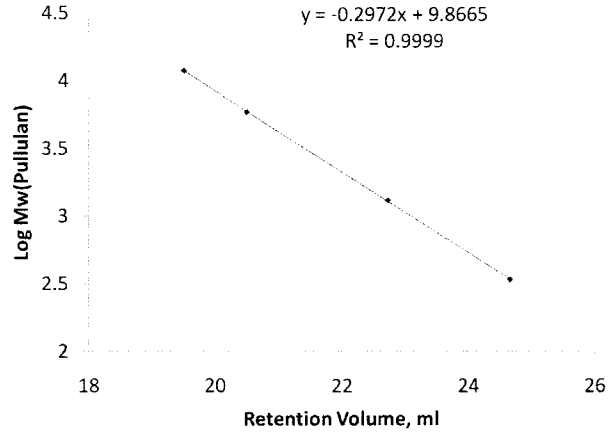

Figure 3.8. Calibration curve applying Pullulan standards

Intrinsic viscosity

The intrinsic viscosity of extracted/original wood was determined after partial chlorite delignification. The final lignin content was determined as the sum of Klason and ASL. The intrinsic viscosity is a measure of the degree of polymerization of the

cellulose chains in wood/pulp and it was measured according to ASTM standard D 1795-62.

Chlorite delignification

Chlorite delignification was performed according to a previously described method (TAPPI test T211 om-85, 1985). 5 gram of original/extracted wood was mixed with 200 mL of water at 70°C. At temperature 2.0 mL glacial acetic acid and 5 gram of sodium chlorite were added. The mixture was held at 70°C for 3 hours while shaking. Samples were then washed and put under suction on filter paper and rinsed with acetone.

Kappa number

The kappa number is defined as the number of milliliters of 0.1 N $KMnO_4$ solution consumed per gram of moisture free pulp under standardized conditions. It is a measure of the lignin content of pulp. The kappa number of pulp was measured by using TAPPI standard method T236 cm-76.

Alkaline cooks on original and extracted wood

Materials and equipment:

Red maple (*Acer rubrum*) wood strands were produced using a Carmanah 12/48 ring strander. Strands with thickness of 0.035 inches, 4-inch length, and varying width were used for extraction with DI-water. Extractions and cooks were performed in an Oil

Bath Laboratory Multi-digester (OBLMD) system. The OBLMD system consists of eight high-pressure bombs (220 mL volume) which can rock back and forward in a hot oil bath. The system is designed to operate at high temperatures and employs polyethylene-glycol (PEG 400, BAKER) as a heat transfer fluid that is temperature controlled through an Isotemp 2150 controller (Fisher Scientific).

Extractions:

The extractions were performed using DI-water as solvent. The extraction conditions are shown in Table 3.2. In each reactor 40 grams of dry wood strands were placed. The experiment was stopped by placing the reactors in an ice bath for approximately 10 minutes. Then, the reactors were opened and the extracted wood was washed with 200 mL DI-water. The washed extracted wood was then placed in a tray and air dried for one week. Dried wood was then stored at room temperature for further pulp production.

Table 3.2. Extraction conditions.

Extraction	Temperature (°C)	Time (min)
1	140	45
2	150	45
3	160	45
4	160	90

Alkaline cooks:

The moisture content of the original and the air dried extracted wood strands was carefully determined using a representative sample before cooking. A known weight of strands (30 g o.d.) was cooked in each of the 8 reactors on the OBLMD system at a liquid to wood ratio of 4.0 L/kg. The cooking temperature was kept at 170°C and the time adjusted for a final H-factor of 1000 while the alkali charge and sulfidity were varied. Alkaline cooks were performed at conditions indicated in Table 3.3. Cooks for original wood were done in quadruples for each cooking condition. For extracted wood strands, cooks were done in duplicate.

The cooked wood strands were disintegrated and washed manually using a cloth bag. There was no rejects (wood material not fully cooked) probably because of the use of thin strands instead of wood chips. The pulp was placed on a tray and then air dried for a week. The air dry pulp was carefully weighed and the moisture content was determined using a representative sample. The total yield was calculated based on the dryness of pulp, the total air dry pulp weight, and the dry weight of the wood strands added to the cook.

Table 3.3. Alkaline cooking conditions.

Condition	EA (% b.w)	Sulfidity (%)
1	13	30
2	15	30
3	17	30
4	19	0
H-factor	1000 hr	

CHAPTER

4 DATA COLLECTION AND VALIDATION OF CONTINUOUS MIXED BATCH REACTOR (CMBR)

4.1 Determination of the residence time distribution of the reaction system

The Residence Time Distribution (RTD) and dead volume of the CMBR setup were determined by Ji (2007). The reactor volume is specified as 280 ml by the manufacturer, while the stainless steel basket and wood samples (about 10g) take up about 15 cm^3. So the available reactor volume is 265 mL. The piping volume between the reactor and the UV detector in the current system is the same as that of Ji's system. Just as in Ji's case this volume will be treated as 96 mL of plug flow volume.

4.2 UV-VIS Absorption Calibration

The extinction coefficient of hardwood lignin dissolved in aqueous media had to be determined in order to convert the absorbance readings from the online UV-VIS spectrophotometer in the CMBR system to a concentration of lignin in grams per liter. A set of three experiments was performed at the following extraction conditions: temperature at 160°C; flow rate of 100 mL/min; acetic acid solution of 1 g/L as extraction solvent with a final pH value of 3.2; and three different extraction times: 10, 40, and 90 minutes. The total extraction volume was collected and weighed for each of

the three experiments. A homogeneous sample of 5 mL from each extract was mixed with 90 µL of a 2M sodium hydroxide (NaOH) solution to a final pH value of 12. The sample was then placed in a bench UV-VIS spectrophotometer and absorbance was read at a wavelength of 280 nm (Table 4.2). The extracted wood samples were washed with cold water after extraction and then placed in an oven at 105°C overnight for weight loss determination. Klason and ASL were determined in the original and extracted woods meals (Table 4.1). The total lignin is the sum of those two determinations. The removed lignin is calculated as the difference between the amount in the original wood and that in the extracted wood. The concentration is then calculated by dividing by the total final extract volume. Then, the extinction coefficient is calculated with equation 4.1.

$$\varepsilon = \frac{A}{C \cdot F \cdot d} \qquad \text{Equation 4.1}$$

where,

ε is the extinction coefficient,

A is the absorbance at 280 nm,

C is the lignin concentration in g/L,

F is the dilution factor, and

d is the light path (1 cm).

Results are shown in Table 4.2. An average value of 17.0 (L/g·cm) is obtained. This value is higher than the extinction coefficient of milled wood lignin (MWL) for beech and maple hardwoods found in literature of about 13-14 (L/g·cm) (Fengel & Wegener, 1983).

This difference could be caused by structural modifications of lignin during the extraction process (Chua & Wayman, 1979) since lignin needs to be degraded before it can be dissolved.

Table 4.1. Klason and acid soluble lignin for original and extracted wood.

	Klason lignin (mg/g odw)	ASL (mg/g odw)	Total lignin (mg/g odw)
Original wood	232.4±0.4	33.6 ± 0.5	266 ± 0.5
Extraction time			
10 min	166.8 ± 0.6	21.1 ± 0.5	187.9 ± 1.1
40min	106.6 ± 0.4	8.4 ± 0.1	115.0 ± 0.1
90min	98.0 ± 4.6	4.5 ± 0.6	102.5 ± 5.2

Table 4.2. Average extinction coefficient for removed lignin.

Extraction time	Concentration (g/L)	Absorbance (280 nm)	Dilution factor	Extinction coefficient (L/g·cm)
10 min	0.74	0.625	20	16.8
40min	0.39	0.630	10	16.3
90min	0.17	0.299	10	17.9
		Average		17.0
		Standard deviation		*0.8*

4.3 Data Reduction Procedure

4.3.1 Lignin Removal Rate

The dissolved lignin mass balance for the well mixed reactor during time interval, dt, is:

Inflow - Outflow + Dissolved by Reaction = Accumulated in Reactor

which can be expressed as:

$$0 - \phi_v C(t)dt + r(t)m_p dt = V_r dC(t) \qquad \text{Equation 4.2}$$

by reorganizing Equation 4.2, one gets

$$r(t) = \left[\phi_v C(t) + V_r \frac{dC(t)}{dt}\right]\frac{1}{m_p} \qquad \text{Equation 4.3}$$

where $r(t)$ is the rate of delignification ([mg lignin/min]/g of wood)

ϕ_v is the liquid flow rate (mL/min)

$C(t)$ is the dissolved lignin concentration (g/L)

V_r is the reactor volume (mL)

m_p is the wood weight (g o.d wood)

The free volume in the reactor and piping to UV-Vis detector are 265 mL and 96 mL, respectively (Ji, 2007). Therefore, the reactor volume V_r is 265 mL, while the residence time between the Berty reactor and UV detector, t_d, is

$$t_d = \frac{96}{\phi_v}\left[\frac{mL}{mL/min}\right] \qquad \text{Equation 4.4}$$

Thus the dissolved lignin concentration inside the Berty reactor at time t, $C(t)$, is equal to the concentration measured by UV spectroscopy at time $t + t_d$, $C_L(t + t_d)$:

$$C(t) = C_L(t + t_d) \qquad \text{Equation 4.5}$$

By substituting Equation 4.5 into Equation 4.3:

$$r(t) = \frac{\phi_v}{m_p} C_L(t + t_d) + \frac{V_r}{m_p}\frac{dC_L}{dt}\Big|_{t+t_d} \qquad \text{Equation 4.6}$$

The amount of lignin removed from the wood at time t is:

$$m_L(t) = \frac{\phi_v}{m_p}\int_0^{t+t_d} C_L(t)dt + \frac{V_r}{m_p}C_L(t+t_d) \qquad \text{Equation 4.7}$$

Thus, the residual amount of lignin remaining in wood at time t is:

$$m_L(t) = m_L^0 - \frac{\phi_v}{m_p}\int_0^{t+t_d} C_L(t)dt + \frac{V_r}{m_p}C_L(t+t_d) \qquad \text{Equation 4.8}$$

where m_L^0 is the initial lignin amount in the original wood in mg/g o.d. wood.

A typical dissolved lignin concentration profile is displayed in Figure 4.1(a). Application of Equation 4.6 leads to the rate of delignification versus time shown in Figure 4.2(b).

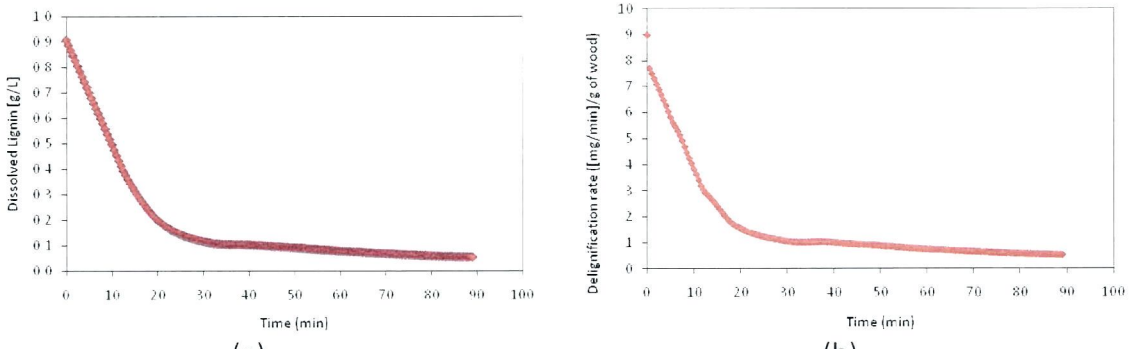

(a) (b)

Figure 4.1. Concentration (a) and removal rate (b) of lignin

As customary for interpretation of kinetics, the removal rate of lignin can be plotted against the amount of lignin remaining in the wood by applying Equation 4.8 (Figure 4.2).

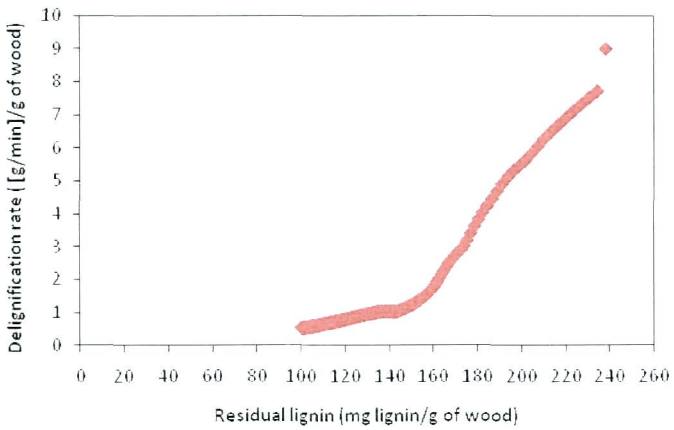

Figure 4.2. Removal rate vs. residual lignin

4.3.2 Smoothing the Monosaccharide Concentration Data

Liquid samples were taken at 2, 4, 6, 10, 20, 30, 40, 50, 60, 70, 80, and 90 minutes, for one minute long each time, and stored in plastic containers at 4°C. An aliquot was taken from each bottle to determine the monosaccharide concentration. Results are expressed as milligram of monosaccharide per gram of dry wood (Figure 4.3). However, the sampling time interval was too big to obtain a smooth behavior of the first order time derivative of the polysaccharide concentration, dCX/dt which is needed in equation 4.6. Thus, more points were generated via Mathcad functions between the actual xylan concentration measurements. All of the points of the xylan concentration were connected to form a smooth curve by using a cubic spline interpolation function in Mathcad (*cspline* and *interp*). With this approach the curve is guaranteed to go through

all of the data points. All data points created at a 0.5 minute interval together with the actual measurement points (only for xylan concentration) are shown in Figure 4.4.

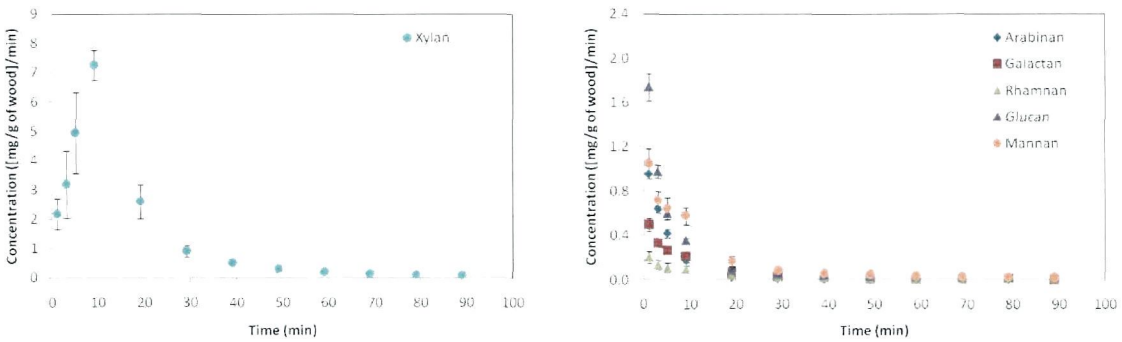

Figure 4.3. Concentration of monosaccharides in extract samples.

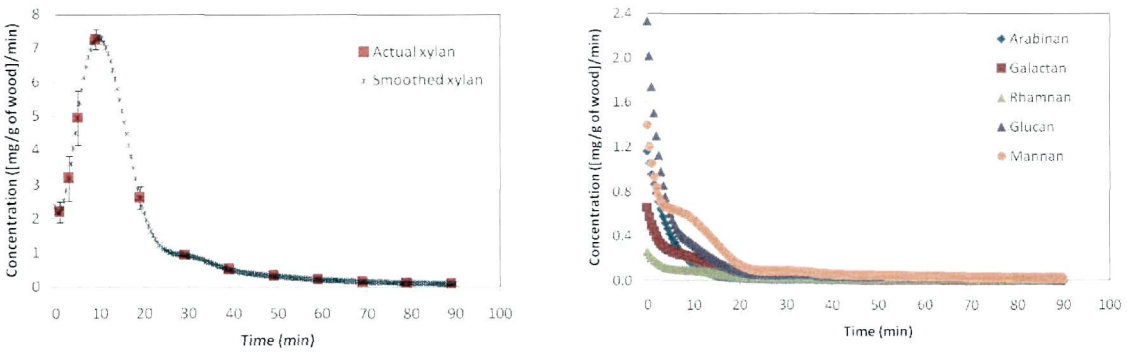

Figure 4.4. Concentration of monosaccharides after smoothing.

4.3.3 Xylan Removal Rate

Once the concentration for xylose has been smoothed, the removal rate for xylan can be obtained similarly to the delignification rate by applying Equation 4.6. Figure 4.5(a) shows the xylan removal rate versus time after applying Equation 4.6. Similarly, the xylan removal rate can be plotted against the residual xylan concentration in wood by applying Equation 4.8 in which the variable m_L is replaced by m_X, the residual xylan concentration, and with m_X^0 the original concentration of xylan in the wood (Figure 4.5(b)).

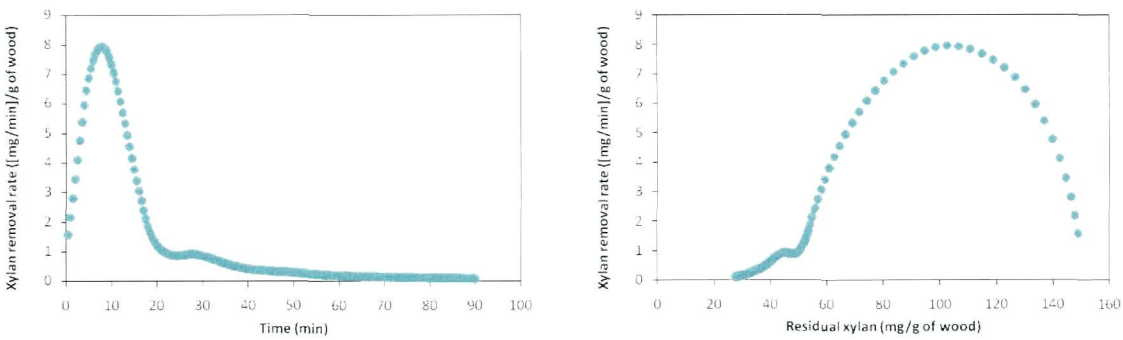

(a) (b)

Figure 4.5. Removal rate of xylan with time (a) and residual concentration (b).

4.4 Validation of Continuous Mixed Batch Reactor (CMBR) Operation

In order to validate the operation of the CMBR system the following experiments were completed:

i. A mass balance verification between the solid and liquid phase

ii. Repeatability of the experimental results

iii. Influence of feed flow rate and wood particle size on lignin and xylan removal rate

4.4.1 Mass balance study

A mass balance study was performed between the solid and liquid phase at two different temperatures: 160°C and 170°C. The total monomeric content for each sugar and the total lignin content were determined in the total extract as well as the extracted wood. The calculation for the total monomeric concentration for each sugar was calculated with the following equation:

$$C_i = \frac{1}{m_p}\left[v \cdot \sum_j C_j + C_k \cdot V\right] \qquad \text{Equation 4.9}$$

where C_i is the total concentration of the individual monosaccharide "i" $[\frac{mg}{g\ of\ wood}]$

m_p is the amount of the dry original wood $[gram]$

v is the volume of the extract sample, the same for each time "j" $[mL]$

C_j is the concentration of monomeric concentration for sugar "i" in the extract sample at time j $[\frac{mg}{mL}]$

C_k is the concentration of monomeric concentration for sugar "i" in the final total extract volume $[\frac{mg}{mL}]$

V is the final total extract volume $[mL]$

The monomeric concentration of sugars in the original/extracted wood was determined as described in section 3.2.3. The lignin concentration in the liquid phase was determined using Equation 4.8. The concentration of lignin in the solid phase was determined as the sum of Klason and ASL. Results are shown in Table 4.3. Values for original and extracted wood are based on an average of three and two replicates, respectively.

Table 4.3. Mass balance for liquid and solid phase. Values in mg/g of wood.

		160C			170C		
Polysaccharide	Original wood	Liquid	Solid	**Total**	Liquid	Solid	**Total**
Arabinan	8.5 ± 0.3	7.3	0.2	**7.6**	7.2	0.2	**7.4**
Galactan	9.4 ± 0.2	5.9	0.3	**6.2**	6.1	0.2	**6.2**
Rhamnan	4.3 ± 0.1	3.2	0.0	**3.2**	5.4	0.0	**5.4**
Glucan	441 ± 16	15.4	435	**450**	18.0	426	**444**
Xylan	156 ± 4	126	30.2	**157**	131	23.1	**154**
Mannan	21.1 ± 0.5	14.8	8.3	**23.1**	16.6	6.3	**22.9**
Lignin	266 ± 1	175	92	**266**	190	78	**268**

From Table 4.3 it can be observed that there is a good agreement for the mass balance for the major polysaccharides, namely glucan, xylan, and mannan, and also for lignin, which accounts for almost 90% of the total mass balance. However, for the minor polysaccharides the mass balance is not that close (arabinan, galactan, and rhamnan). Looking at the values for those sugars it can be noted that most of the total amount is coming from the liquid phase, and that the concentration in the solid phase is very low.

Therefore, the difference may be explained in part by degradation of these sugars to furfural and hydroxymethylfurfural (HMF) during the two step acid hydrolysis of the solid samples.

4.4.2 Data Repeatability

All extractions in this thesis were done at least in duplicate. The temperature effect section considered a set of three experiments for each condition. An analysis of the data repeatability was performed in order to determine the experimental error of the experiments. Three experiments were performed at exactly the same operating conditions: flow rate around 100 mL/min, solvent 1 g/L acetic acid (pH ~3.2), temperature 160 °C, stirring speed 400 rpm, wood meal weight 10.0 g (70 ≤ x ≤ 40 mesh). Figure 4.6 shows the results for xylan (a) and lignin (b) concentrations. It should be noted that both lignin and sugar concentrations are normalized dividing by the initial amount of dry wood.

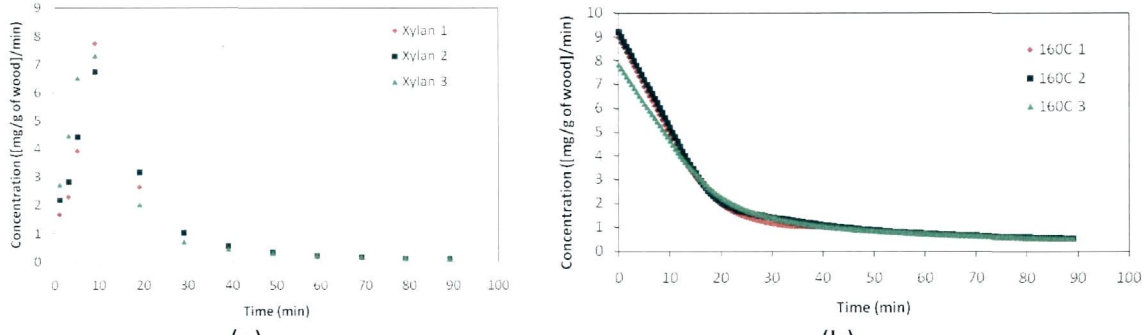

(a) (b)

Figure 4.6. Concentration of xylan (a) and lignin (b) with time for three different experiments.

In order to estimate the experimental error, it was decided to use the *standard error of the mean*, which is a simple estimation method of the standard deviation from the mean (Equation 4.10).

$$SE_{\bar{x}} = \frac{s}{\sqrt{n}} \qquad \text{Equation 4.10}$$

where s is the sample standard deviation

n is the number of experiments

Figure 4.7 shows the mean values for xylan and lignin concentrations including the standard error. Now, this standard error can be compared with the mean value ($\bar{x}$) through the *relative standard error* (RSE) by using Equation 4.11. It was found that for xylan concentration distribution there is a maximum error of about 20% and an average value of 8.3%. For lignin the error was below 7%.

$$RSE(\%) = \frac{SE_{\bar{x}}}{\bar{x}} \cdot 100 \qquad \text{Equation 4.11}$$

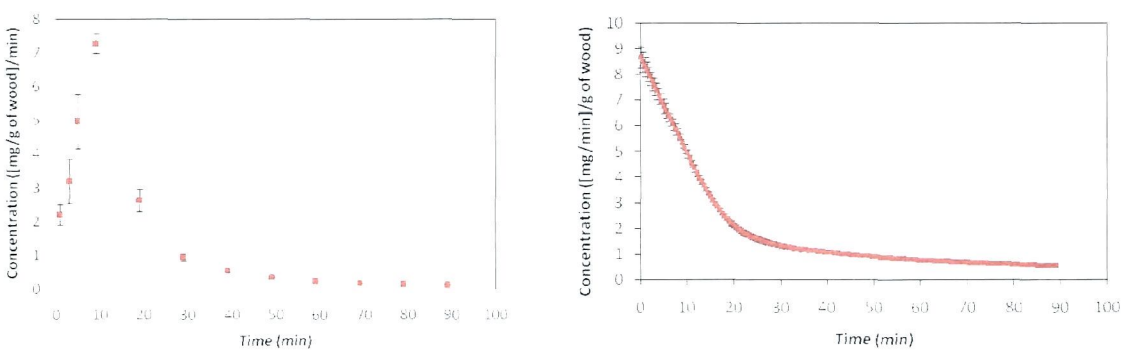

(a) (b)

Figure 4.7. Distribution of mean concentration with standard error bars for xylan (a) and lignin (b).

4.4.3 Effect of Different Flow Rates

With different flow rates the lignin and sugar concentrations in the product streams will be different. Higher flow rates reduce the concentrations because of the higher dilution, while a lower flow rate would lead to the opposite effect. However, for intrinsic dissolution kinetics, the rate of lignin and sugar removal from the wood should remain the same independent of flow rate changes.

The effect of flow rate is seen in Figure 4.8 (a&b) for xylan and lignin concentrations respectively. The removal rates are shown in Figure 4.9 (a&b). The results show that lignin and xylan removal rates are not considerably affected by the flow rate although the concentrations are different. Removal rate values are normalized by the initial amount of dry wood.

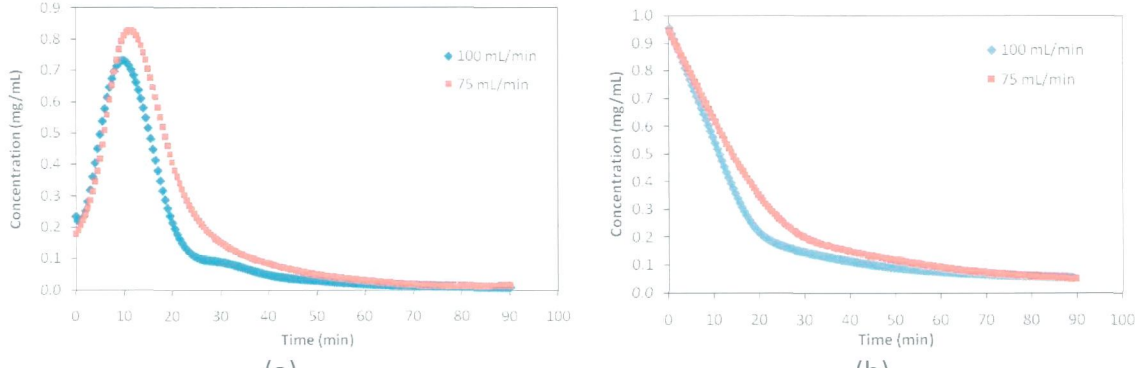

Figure 4.8. Concentrations of xylan (a) and lignin (b) at two different flow rates.

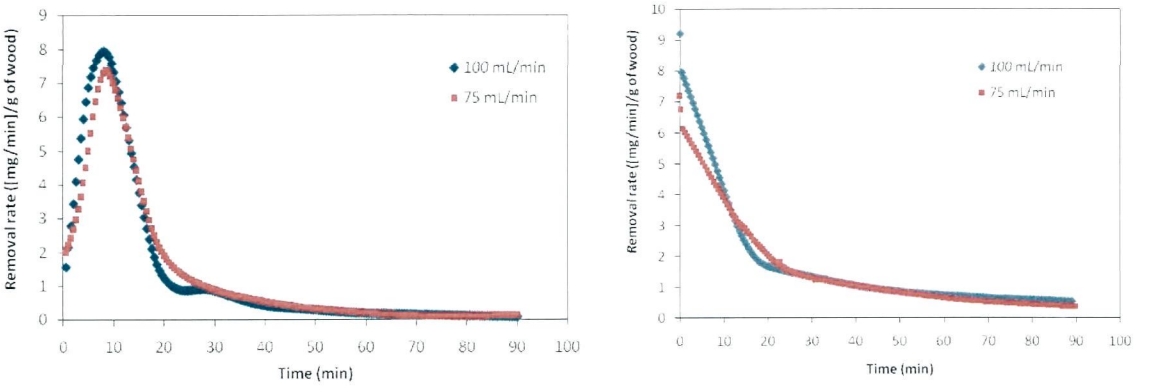

Figure 4.9. Removal rates of xylan (a) and lignin (b) at two different flow rates.

4.4.4 The effect of wood particle size on xylan and lignin removal rate

Experimental

Five different wood particle sizes were used: wood meal 70 ≤ x1 ≤ 40 mesh and 200 ≤ x2 ≤ 100 mesh, wood strands with 0.75 mm thickness, wood chips with 3 mm thickness, and wood chips with 6 mm thickness. The extraction solvent used was 1 g/L acetic acid solution. The extraction temperature was fixed at 160°C. Close to 10 grams of wood meal were placed in the reactor. The flow rate was set at 100 mL/min and samples were collected at different times (2, 4, 6, 10, 20, 30, 40, 50, 60, 70, 80, and 90 min) for one minute long in plastics containers and weighed to check the flow rate.

Wood component dissolution

Figure 4.10 shows the concentrations of xylan and lignin normalized by the original wood weight during the 90 minutes extraction time for the four different wood particle sizes. The wood meal fractions were labeled as 150 mesh and 55 mesh for fractions x2 and x1 respectively. The xylan concentration goes through a maximum at all conditions, with the maximum increasing and occurring earlier with decreasing particle size. Lignin on the other hand dissolves at a high concentration immediately from the start of the extraction at all conditions and then decreases linearly. Lignin concentration profile shows a drastic change in its slope and this change occurs earlier with increasing particle size.

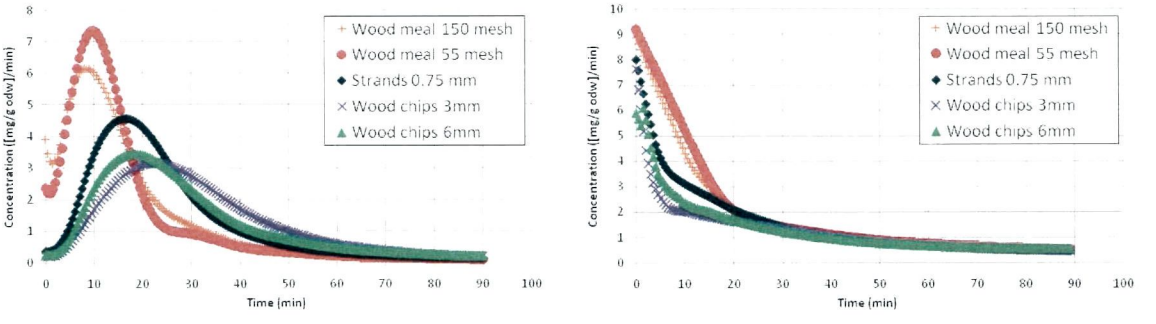

Figure 4.10. Concentration of xylan (a) and lignin (b) with time for two different wood meal particle sizes.

If the extraction were mass transfer limited for the particle size condition of wood meal 55 mesh one would expect to see higher concentration at 150 mesh for both xylan and lignin, which is not seen. The concentration of these two wood polymers in general decreases by increasing wood particle size. However this effect is not very clear

for wood chips showing almost no effect by increasing thickness from 3 to 6 mm. This situation will be explained later in this section.

The removal rate for xylan and lignin

For a better understanding of the extraction kinetics, the lignin and xylan concentrations in the extract are used to calculate their respective removal rates using Equation 5.19.

The removal rates of xylan and lignin are plotted in Figure 4.11 against percentage of residual xylan and lignin respectively in the wood for all wood particle sizes. It can be noted that the removal rate does not increase for particle size smaller than at 55 mesh and then a mass transfer limitation is not observed at this particle size condition of wood meal and even xylan removal rate at 150 mesh resulted in slightly smaller values. However, the final residual xylan value was almost the same for both wood size conditions. In general, it can be observed that both removal rates of xylan and lignin increase significantly with increasing wood particle size from 3 mm chips to strand to wood meal. However this is not seen between the two different size wood chips which was not expected.

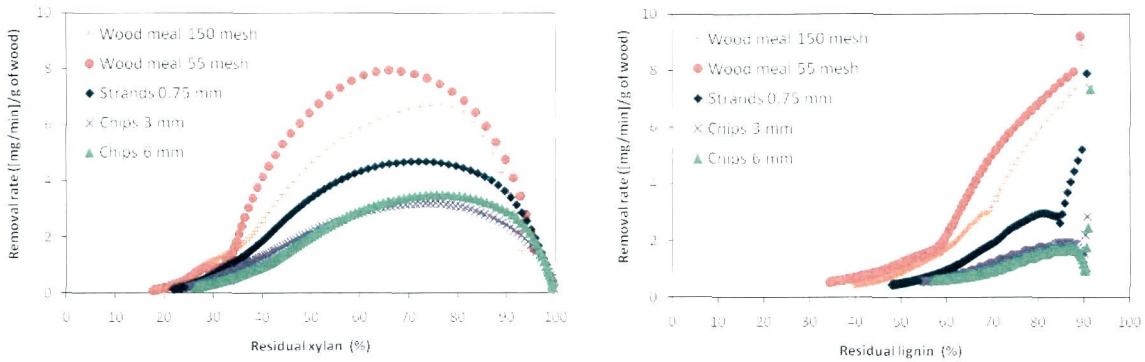

(a) (b)

Figure 4.11. Xylan and lignin removal rates versus their residual concentration in wood.

Effect of particle size and pore diffusion

A pore diffusion limitation study was performed to investigate the effect of particle size on the removal rate of xylan from wood. The Weisz modulus (M_w) is selected for interpretation of the kinetic data (Levenspiel, 2002).

$$M_w = \frac{-r_A''' L^2}{C_{As} \mathcal{D}_{eff}}, \qquad \text{Equation 4.12}$$

where, r_A''' is the removal rate for xylan dissolution, g/s L

L is characteristic length of the wood particle, m

C_{As} is the xylan concentration in the extract, g/L

$\mathcal{D}_{eff}$ is the effective diffusion coefficient in wood, ~1x10^{-9} m^2/s

For the estimation of the Weisz modulus the maximum removal rate value in Figure 4.11(a) is used. For wood meal, strands, and chips L is equal to half of the thickness. The xylan concentration selected for this analysis is the value determined as

saturation concentration in section 5.3.3. The values for the Weisz modulus are shown in Table 4.4.

Table 4.4. Weisz modulus for different wood samples.

Wood sample	L (m)	$-r_A'''$ (g/s L)	C_{As} (g/L)	M_w
Wood meal 55 mesh	$1.6x10^{-04}$	$4.7x10^{-02}$	2.0	0.6
Wood strands	$4.0x10^{-04}$	$3.0x10^{-02}$	2.0	2.4
Wood chips 3 mm	$1.5x10^{-03}$	$2.3x10^{-02}$	2.0	26.2

There is no resistance to pore diffusion when $M_w < 0.15$, and there is strong pore diffusion effects when $M_w > 4$ (Levenspiel, 2002). Then, from the values in Table 4.4 can be concluded that there is a strong pore diffusion limitation for wood chips, and there is a very small diffusion effect for the wood meal. Finally, there is an intermediate regime for wood strands.

The effect of rotational speed in the Berty reactor on the removal of xylan

The non-significant differences between the two wood chip size conditions on xylan removal rate were unexpected. As a way to eliminate the effect of a mass transfer limitation in the liquid phase, the rotational speed was varied during the extraction for 3 mm wood chips. Figure 4.12 depicts the xylan concentration, xylan removal rate, and xylan yield versus time ((a), (b), and (c) respectively) for extractions performed at two different rotational speeds (400 and 800 rpm). Figure 4.12(d) depicts the xylan removal rate versus the percentage of residual xylan in wood at these two rotational speeds. It is immediately noted that there is an important effect on the concentration and removal

rate profiles increasing 1.5 times for concentration and removal rate with doubling the rotational speed. Also, from Figures 4.12(a) and (b) it can be noted that a higher amount of xylan of about 5% more (based on the original xylan) is removed at the higher rotational speed (1% more on original wood). This increases on removal rate with increasing the rotational speed means there is still a mass transfer limitation at 400 rpm, more likely in the liquid phase. This may explain the reason that there is no significant difference on the removal rate between the two wood chips sizes (Figure 4.11). This behavior is not fully understood and requires further investigation.

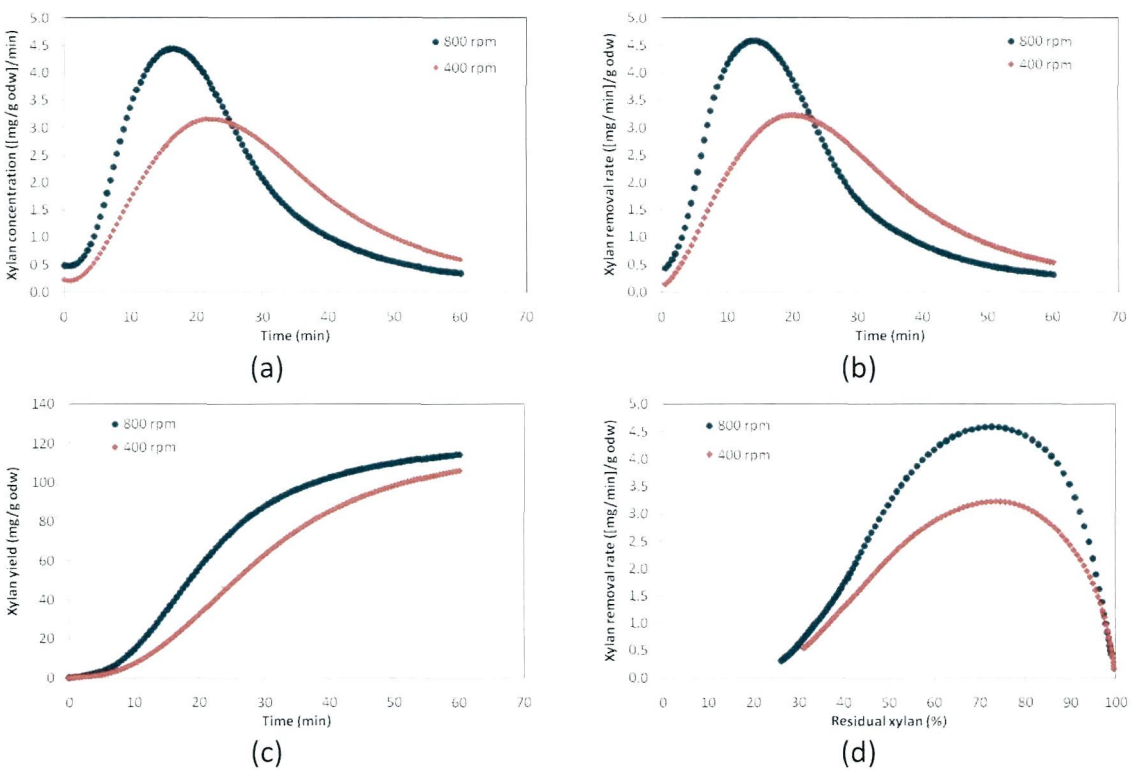

Figure 4.12. Comparison of xylan kinetics for two different rotational speeds in the Berty reactor during the extraction. Xylan concentration (a), xylan removal rate (b), and xylan yield (c) versus time and xylan removal rate versus the percentage of residual xylan in wood (d).

4.4.5 Conclusions

The operation of the CMBR system has been validated by showing:

i. A close mass balance between the solid and liquid phase

ii. A good repeatability of the experimental results

iii. A small influence of feed flow rate and wood particle size on lignin and xylan removal rates

CHAPTER

5 RESULTS AND DISCUSSIONS

5.1 Removal of wood components from OSB strands by hot water in a batch reactor

5.1.1 Introduction

The removal of hemicelluloses from wood chips prior to pulp production has been proposed in the literature (van Heiningen, 2006) for further production of chemicals and fuels to increase revenue of pulp mills in North America. Similarly the oriented strand board (OSB) industry can be suitable for this technical approach as it is composed of large centralized facilities (Paredes et al., 2008). Hydrothermal treatments at laboratory scale in a batch reactor (ASE-100, Dionex) were applied to red maple (*Acer rubrum*) strands, a hardwood wood species, with the objective to study the extraction yield. Complete mass balances for extracted wood and wood extracts have been performed by determining the cellulose, hemicellulose, and lignin content of both the solid and liquid phases generated at different extraction temperatures and times expressed combined in terms of the P-factor (Sixta, 2006). A complete chemical composition of the red maple wood strands used in the present study is shown in Table 3.1. In addition, in order to better understand the mechanism of wood dissolution, the molecular weight distribution of polysaccharides was determined for the dissolved hemicelluloses in the liquid phase and for cellulose in the solid phase. Details about the experimental procedure and analysis techniques are provided in Chapter 3.

5.1.2 Hydrothermal dissolution of wood components from OSB strands. The effect of P-factor on the extraction yield.

Extractions with DI-water were performed at different temperatures and times to investigate the effect on the total extraction yield. The extraction yield was determined from both the solid and liquid phase for comparison as described in Chapter 3. Results are shown in Figure 5.1 where it can be observed that the difference between the yield values calculated from solid and liquid phases increases with increasing time and temperature of the hydrothermal treatment. This may be due to release of volatile compounds during the extraction and also to decarboxylation of uronic acids (Leschinsky et al., 2007), which are part of pectins (galacturonic acid) and present as side chains in the xylan backbone (4-O-methyl glucuronic acid). Also, it can be seen in Figure 5.1 that similar extraction yields are obtained for different combinations of temperature and time. Different parameters have been proposed in order to combine the effect of these two operating variables into just one. The severity factor (R_0)., first proposed for Overend and Chornet (1987), has been widely used. On the other hand, the P-factor which has been used to control the hot water pre-extraction process of wood chips before pulp production (Sixta, 2006), is shown in Equation 5.1, where T is the temperature in Kelvin and t is time in hours.

$$P = Exp(40.78 - \frac{15106}{T}) \cdot t \qquad \text{Equation 5.1}$$

The activation energy used in this expression is typical of cleavage of glycosidic bonds of the carbohydrate material in wood. The activation energy value used is 125.6 kJ/mol (or 30 kcal/mol) which corresponds to the rate of fast-reacting xylan and is only slightly smaller than the Kraft cooking activation energy of 134 kJ/mol (or 32 kcal/mol) used in the H-factor for kraft delignification (Sixta, 2006).

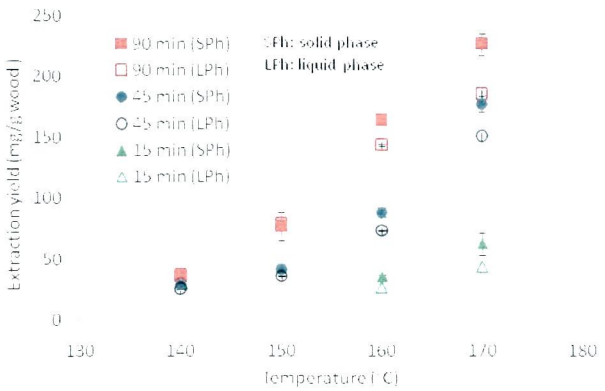

Figure 5.1. Extraction yield of red maple wood strands with DI-water.

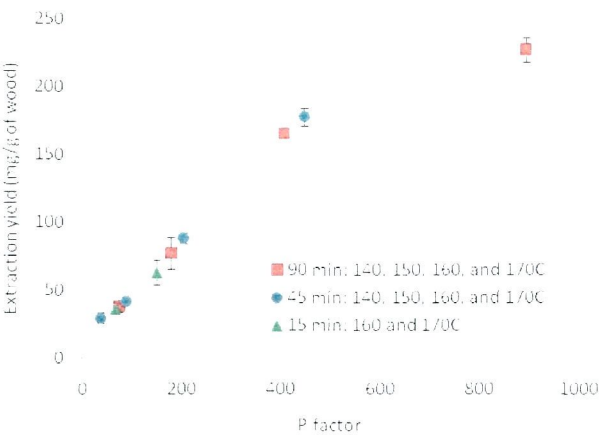

Figure 5.2. Extraction yield based on solid phase versus P-factor.

Figure 5.2 shows the extraction yield based on the solid phase versus the P-factor (see equation 5.1) showing that the P-factor approach can be used to analyze the

extraction yield for the hydrothermal treatment of red maple OSB strands. In this figure is noted that at a very high severity of the hydrothermal treatment, i.e. a P-factor value over 800 hrs., the wood removal rate slows down probably due to development of secondary reactions other than hemicellulose removal, i.e. carbohydrate degradation, lignin condensation.

Tunc and van Heiningen (2009) showed that the P-factor concept works for all three major wood components, namely cellulose, lignin and hemicellulose. Therefore, this factor will be used in the present study to describe the dissolution of the individual wood components. Lignin content can be calculated as the sum of Klason and acid soluble lignin (ASL). Lignin content was determined for freeze dried extracts at five different extraction conditions and lignin yield was plotted versus P-factor (Figure 5.3). The total lignin yield calculated from the extract is compared with that obtained from the solid phase. The results are given in percentage based on the original amount of lignin in wood. The total amount of lignin removed at the highest P-factor of 900 hrs. was around 12% of the original lignin content in wood, i.e. about 2.9% on original wood. The lignin removal increases linearly with P-factor up to a value of 400 hrs., reaching a plateau after that. This plateau can also be observed for the pH around a value of 3.5 (Figure 5.3) meaning that the dissolution of lignin is controlled by the pH rather than a combination of temperature and time (P-factor). The total lignin amount in the liquid phase includes a precipitate which is formed after storing the extracts over night at 4°C. This precipitate was quantified gravimetrically after separation by centrifugation. Since the material completely dissolves in 96% dioxane (Björkman, 1957), it is lignin-based.

The amount of precipitate increases with the P-factor and it is significant at a P-factor of 900 hrs. This may be explained by lignin condensation and formation of insoluble lignin by removal of the sugars from dissolved LCCs (Tunc et al., 2010).

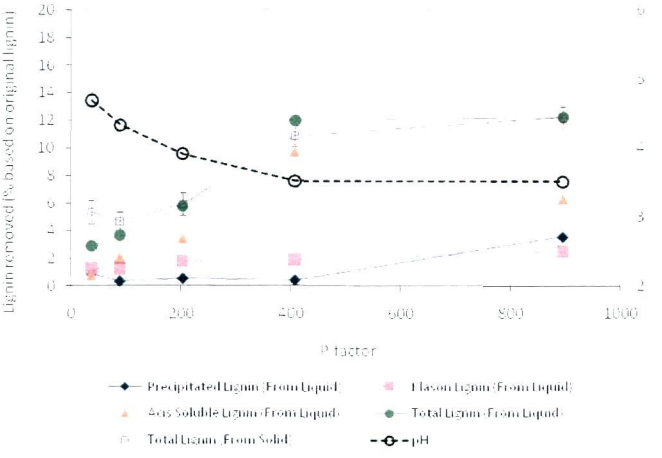

Figure 5.3. Total lignin in liquid extracts calculated as the sum of Klason lignin, acid soluble lignin, and lignin precipitate. Total lignin in solid phase is also included for comparison.

Figure 5.4 shows the concentration of free acetic acid and free formic acid found in wood extracts at different extraction conditions (P-factor). Based on the pK_a values for those acids (4.8 and 3.7, respectively; Fengel and Wegener, 1983) one can conclude that acetic and formic acids are the main acids contributing to the pH of the extracts. Formic acid can be formed from the degradation of glucose during acid hydrolysis (Sjöström, 1993).

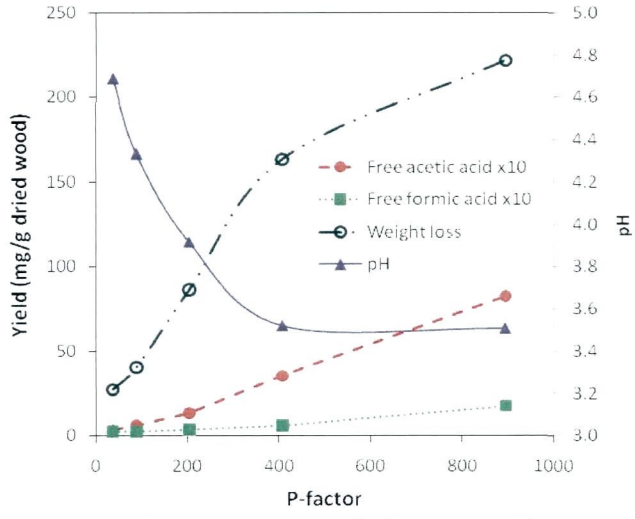

Figure 5.4. Free acetic and formic acids in extracts and its effect on the pH and extraction yield (weight loss)

A detailed mass balance for the liquid phase is presented in Figure 5.5. The minor wood components were split into two additional graphs (Figure 5.5 (b) and (c)) for improved presentation of the results. Figure 5.5 (a) includes the total mass balance which is the summation of all partial yields from the carbohydrates, total lignin, and minor wood components. This curve is compared with the total extraction yield calculated from the solid phase (weight loss). The xylan yield displays an S-shaped curve implying that the extraction yield of xylan is slow initially and then accelerates to reach a maximum at a P factor of 900 hrs. The slow initial removal of xylan may be explained by the initially low acidity of the solution and that xylan in the wood first needs to be degraded to a lower degree of polymerization before becoming soluble. The maximum amount of xylan removed at the highest P-factor was 64% based on the original content of xylan in wood. The total acetyl groups and methyl-glucuronic acid (Me-GUA) curves follow the same general behavior as that of xylan showing that these xylan side groups

are being released together with xylan as it is dissolved. At the highest P-factor the removal of acetyl groups reaches 63% and the maximum amount of Me-GUA is 41% at a P-factor of 408 hrs. showing a decreasing rate at a higher P-factor. This can be explained by decarboxylation of uronic acids at more severe conditions reported previously by Leschinsky et al. (2007).

The yield of minor wood components is shown in Figure 5.5(b) and (c) where sugars names are given as the polymeric form meaning that the monomeric amount values determined through acid hydrolysis/HPAEC are corrected to its anhydrous amounts as found in wood. Galactan increases to a maximum of 10 mg/g wood at the highest P-factor (896 hrs.). Arabinan shows a maximum at a P-factor of 200 hrs. followed by a constant decrease at higher P-factor, which is evidence of acid degradation (to furfural). Ash and proteins are totally extracted after a P-factor of 200 hrs. Galacturonic acid (GalUA) shows a maximum at a P-factor of 400 hrs. and presumably like methyl-glucuronic acid decreases due to decarboxylation.

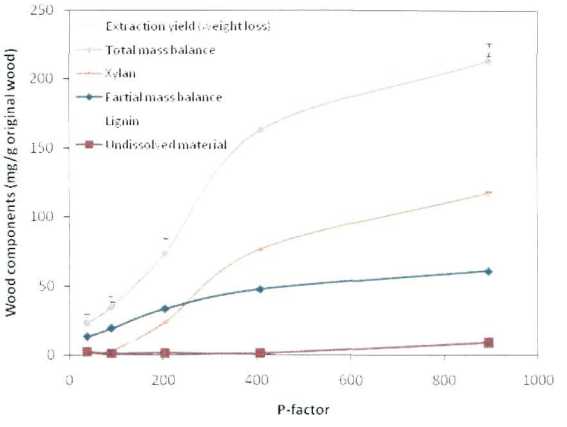

(a)

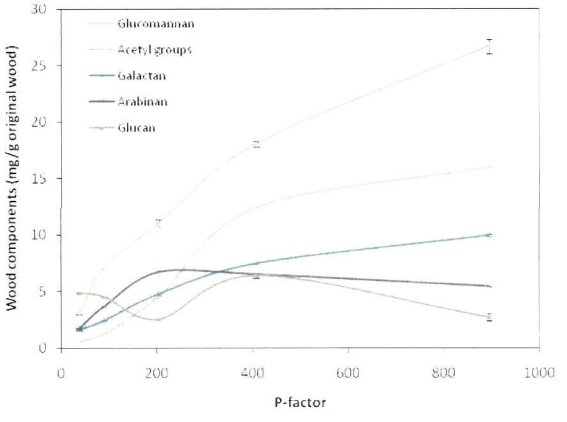

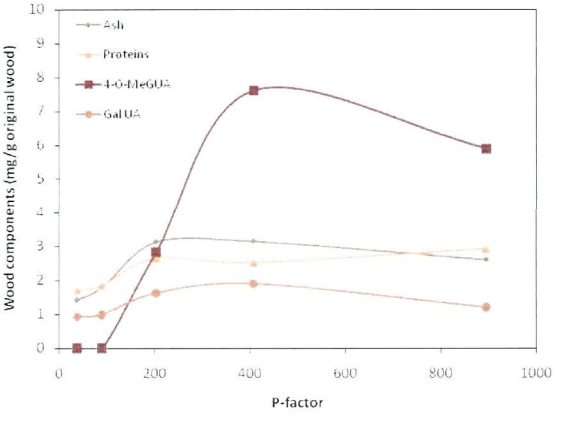

(b) (c)

Figure 5.5. Solid weight lost, total, main (a), and minor (b) wood components yield at different P-factor values (hrs.) in liquid phase. Proteins, acids, and ash yield (c).

The oligomeric and monomeric composition of dissolved xylan is depicted in Figure 5.6 which shows that xylan dissolves mostly as oligosaccharides up to a P-factor of 200 hrs. and then at more severe conditions the xylo-oligosaccharides depolymerize to monomeric xylose by acid hydrolysis (Conner and Lorenz, 1986). The same general behavior is obseved for acetyl groups. The bound acetyl groups reach a plateau after a P-factor of 400 hrs.; however, deacetalytion increases linearly with increasing extraction

severity (P-factor) above P-factor of 200 hrs. The dissolution of MeGUA shows a behavior similar to that for oligomeric xylan except that its concentration reaches a maximum at a P-factor of 400 hrs. most probably due to degradation of MeGUA by decarboxylation (Leschinsky et al., 2007). Figure 5.7 shows the molar ratio of bound acetyl groups and MeGUA per 10 anhydro xylose units. From the figure it is clear that the molar ratio of MeGUA to 10 xylose has a value of zero for mild extraction conditions up to a P-factor of about 100 hrs., and then increases to a maximun of 0.9 at a P-factor of about 200 hrs. followed by a linearly decreasing ratio to 0.4 at a P-factor of about 900 hrs. This decrease in the molar ratio is probably due to degradation of MeGUA by decarboxylation. The acetyl groups to xylose ratio presents a totally different behavior starting from a very high ratio value of about 25 at P-factor of 38 hrs. and then decreasing rapidly to a value of about 5 at a P-factor of 200 hrs. After this P-factor the ratio decreases slightly to a value of about 4 at 900 hrs. Based on these results the xylan fraction removed up to a P-factor of 200 hrs., which corresponds to about 13% of the original xylan in wood, is highly acetylated and low in MeGUA side groups and is mainly as oligomeric form.

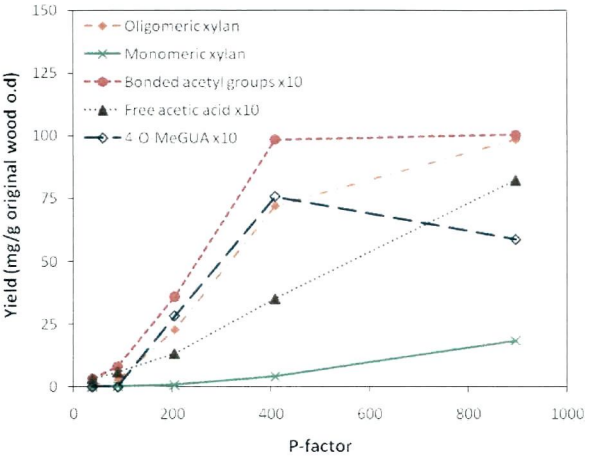

Figure 5.6. Oligomeric and monomeric xylan versus P-factor. MeGUA and bound acetyl side groups are also depicted.

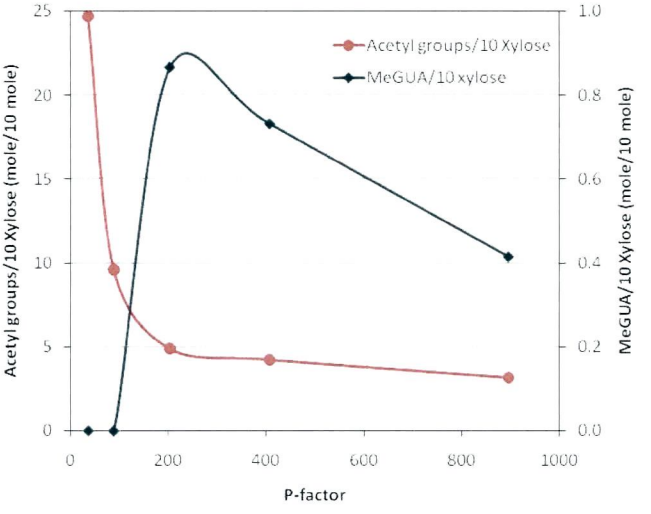

Figure 5.7. Molar ratio of acetyl and MeGUA side groups to 10 xylose units in wood extracts.

The molar ratio between glucan and mannan is depicted in Figure 5.8. The total glucan content is corrected for the amount of formic acid assumed to be the product of glucose degradation (Fengel and Wegener, 1983). From the graph it is clear there is a high amount of glucan at mild extraction conditions (P-factor up to about 90). It is believed that this high molar rate is due to the dissolution of glucan as starch (Tunc and

van Heiningen, 2010). In order to estimate the amount of starch being dissolved the following calculation was performed for the lowest P-factor value (38 hrs.) assuming that degradation of cellulose is negligible:

$$Starch = Total\ glucan - mannan \cdot 0.6 \qquad \text{Equation 5.2}$$

where the ratio glucan to mannan is assumed to be 0.6 according to the work of Janson (1974), and in agreement with ratios of about 0.5-0.7:1 reported for most hardwoods (Fengel and Wegener, 1983).

This amount of starch, which in wood is found to be less than 1% (Fengel and Wegener, 1983), was subtracted from the total glucan at higher P-factor values assuming that the same amount of starch is dissolved at all conditions considering that starch is much more soluble. Thus the molar ratio glucan:mannan was determined as follows:

$$\frac{glucan}{mannan} = \frac{Total\ glucan - starch}{mannan} \qquad \text{Equation 5.3}$$

This glucan:mannan ratio is shown in Figure 5.8 as glucomannan. This ratio slightly decreases from about 0.6 to 0.4 at P-factor of 200 hrs., and then increases to a plateau value of 0.8 at a P-factor of 400 hrs. This level may be explained by amorphous cellulose hydrolysis which starts to be noticeable at this severity, as will be discussed in subsequent sections. Thus the results in Figure 5.8 are consistent with rapid initial dissolution of starch, a food storage component of wood, before major dissolution of glucomannan.

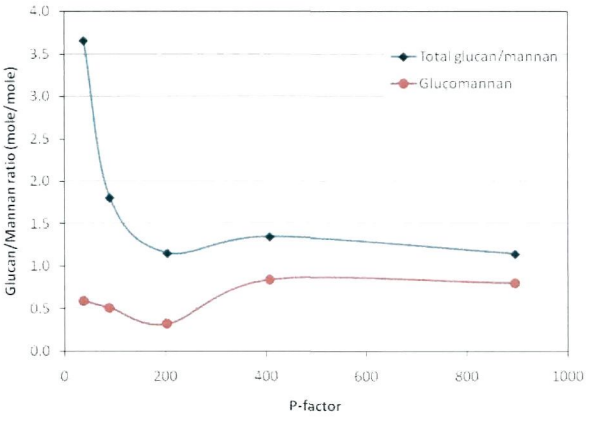

Figure 5.8. Molar ratio of glucan:mannan in wood extracts.

5.1.3 Hydrothermal dissolution of wood components from OSB strands. The effect of P-factor on the residual concentration of wood components.

The concentration of residual wood components of hardwood strands after hydrothermal pretreatments is depicted in Figure 5.9 for different extraction conditions (P-factor). The summation of all individual wood component yields is presented as "Total" in Figure 5.9(a). All values are in milligrams per gram of original wood. The summation of the "Total" value plus the wood weight loss value should give 1000 mg per gram or 100 percent. An excellent agreement is observed for the "Total + Weight Loss" at different conditions. Thus, it is clear that the residual cellulose concentration stays intact due to cellulose high molecular weight and crystalline nature, while lignin is only slightly dissolved. This behavior has been reported by others (Tunc and van Heiningen, 2009; Garrote et al., 1999). The data also shows that the majority of wood dissolution is due to xylan removal. Glucomannan is rapidly removed up to a P-factor of

200 hrs. and then the rate slow down lineraly reaching a final removal of about 47% of the original amount in wood at the highest P-factor (896 hrs.) (Figure 5.9(b)). Minor saccharides and ash are quickly dissolved before reaching a P-factor of 400 hrs. Galactan shows a different behavior dissolving to a lower rate during the first 200 hrs. Total uronic acid group decreases significantly with increasing P-factor dissolving about 83% of it at the most severe condition studied (P-factor of 896 hrs.). Close to 48% of acetyl groups dissolve at this P-factor.

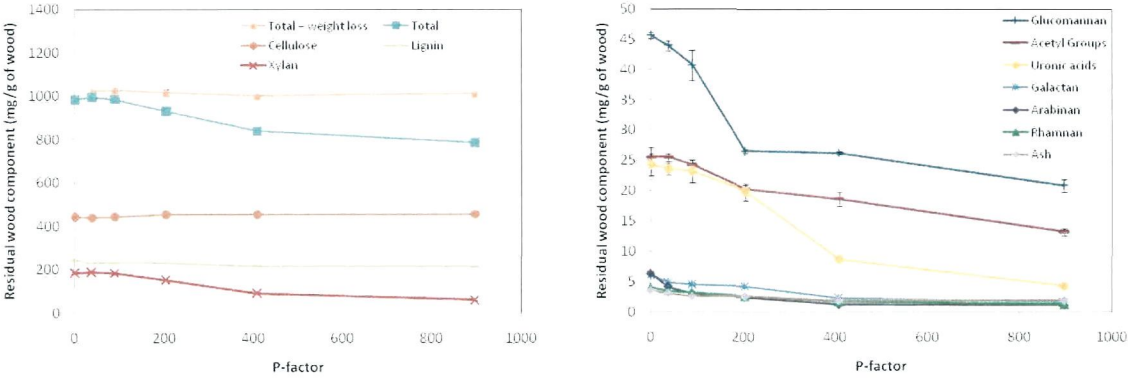

(a) (b)

Figure 5.9. Residual concentration for main (a) and minor (b) wood components as a function of P-factor.

The quantification of uronic acids was carried out by two analytical techniques: a colorimetric method (Scott, 1979) and methanolysis with gas chromatography (Li et al., 2007). Results are depicted in Figure 5.10 for the original wood and for extracted wood at different severities (P-factor). The colorimetric method quantifies the total amount of uronic acids but cannot identify the individual acids coming from pectin and hemicellulose. On the other hand, the methanolysis method is able to distinguish among

different types of acids, so it is possible to identify and quantify the 4-O-MeGUA originating from xylan. From the Figure 5.10 it is clear that both methods give very similar results. The results for the methanolysis method includes the amount of galacturonic acid (GalUA) and 4-O-methyl-glucuronic acid (4OMeGUA). GalUA is the monomeric unit of galacturonan which is a polysaccharide found in wood pectins. Rhamnose residues can be interspersed within the backbone of this polymer and some neutral polysaccharides can be found attached to the acidic pectic backbone as large side chains where the main structures known are arabinans and galactans (Teleman, 2009).

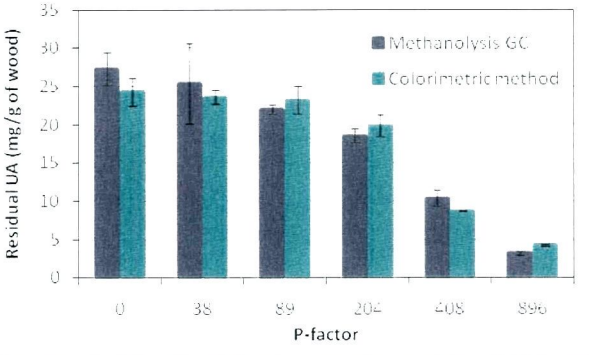

Figure 5.10. Residual uronic acids (UA) with two different analytical techniques: colorimetric method and methanolysis with gas chromatography. Values are given at different P-factor values.

The residual content of these two uronic acids is depicted in Figure 5.11. It is clear that the residual amount of both GalUA and 4OMeGUA in wood decreases dramatically with increasing P-factor. About 84% and 91% of initial GalUA and 4OMeGUA dissolve/degrade during the hot water extraction respectively at the highest severity condition (P-factor 896 hrs.). It can be concluded that the dissolution of GalUA

is significantly affected by the P-factor. On the other hand 4OMeGUA is a side group of xylan so its dissolution is closely associated to that of xylan.

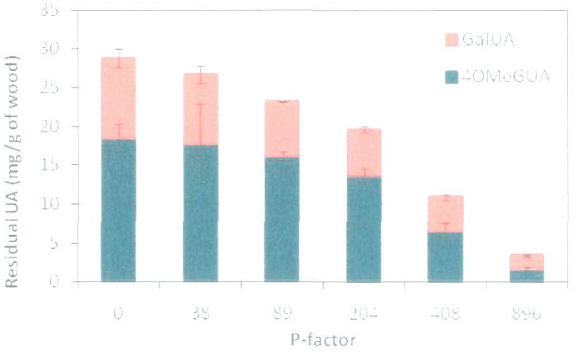

Figure 5.11. Residual galacturonic (GalUA) and 4-O-methyl glucuronic (4OMeGUA) acids in original and extracted wood at different P-factor values.

Table 5.1 show the results for the residual molar ratio of acetyl and 4OMeGUA side groups per 10 xylose units in the original and extracted wood samples at different P-factors. The acetyl/10 xylose molar ratio remains almost constant at 4.2 up to a P-factor of 200 hrs. and then increases up to a value of 7 at the most severe conditions (P-factor 896 hrs.). This implies that the residual xylan becomes more acetylated with increasing P-factor. On the other hand, 4OMeGUA exhibits a totally opposite behavior where the molar ratio remains constant up to a P-factor of about 200 hrs. and then decreases with increasing P-factor, i.e. these side groups are less prevalent on residual xylan with increasing P-factor.

Table 5.1. Residual molar ratio of acetyl and 4OMeGUA side groups per 10 anhydrous xylose units in original and extracted wood.

Temperature	Time	P-factor	Molar ratio	
(°C)	(min)		4OMeGUA/10 Xy	Acet/10 Xy
		Original wood	0.7 ± 0.1	4.3 ± 0.3
140	45	38	0.7 ± 0.2	4.2 ± 0.1
150	45	89	0.6 ± 0.1	4.1 ± 0.1
160	45	204	0.6 ± 0.1	4.1 ± 0.1
160	90	408	0.5 ± 0.1	6.4 ± 0.4
170	90	896	0.2 ± 0.1	7.0 ± 0.3

Finally, Table 5.2 shows the mass of the wood components present in the original wood and extracted wood, and that in the liquid phase. The summation of the amount of each wood component in the liquid and solid phases after hot water extractions performed at different P-factor values is a measure of the mass balance closure obtained in the present study. All values are given in milligram per gram of original wood. In general major wood components, namely cellulose, lignin and xylan, present a fair agreement in their mass balance for all P-factor conditions. The highest difference for cellulose and lignin was about 0.8% and 0.7% on wood, respectively. For xylan the highest difference was about 2%. For glucomannan the highest difference was about 0.8%. Acetyl groups show good agreement with a maximum difference of 0.6% on wood. 4-O-MeGUA and GalUA showed an increasing mass loss with increasing P-factor with 60% and 73%, respectively. As discussed in previous paragraphs this must be due to degradation by decarboxylation. The mass balance for arabinan does not agree very well for P-factor values of 408 hrs. and 896 hrs. The total arabinan content is higher than that in the original wood and is mostly caused by the higher arabinan content in the liquid

phase compared to that in the original wood. This has been reported before by Tunc and vanHeiningen (2008) who concluded that this is caused by acid degradation of arabinose during the two step acid hydrolysis for monosaccharide quantification in the solid phase leading to an underestimation of arabinan in wood.

Rhamnan was not determined in the liquid phase because the analytical method for its quantification was not implemented yet at this time. From Table 5.2 it is observed that the rhamnan content in the solid is decreasing with increasing P-factor as expected. On the other hand, the total galactan content is constantly increasing with P-factor. The explanation for this is that the galactan content also includes rhamnan as they co-eluted at the same retention time with the earlier HPAEC analytical method used for its quantification. Adding the amount of rhamnan to that of galactan one obtains 10.2 mg/g of wood in the original wood. Comparing this value with the sum of the total content for these two polysaccharides shows that there is a fair mass balance agreement, and thus it may be concluded that the galactan content in the liquid phase is overestimated because rhamnan is included in its quantification.

Table 5.2. Mass balance comparison between the liquid and solid phases at different P-factor values.

Wood component	**Original wood**	P-factor 38			P-factor 89			P-factor 204			P-factor 408			P-factor 896		
	(mg/g of wood)	Solid	Liquid	**Total**	Solid	Liquid	**Total**	Solid	Liquid	**Total**	Solid	Liquid	**Total**	Solid	Liquid	**Total**
Arabinan	**6.3 ± 0.2**	4.1	1.7	**5.9**	3.1	3.7	**6.7**	2.4	6.7	**9.1**	1.2	6.5	**7.7**	1.1	5.4	**6.5**
Galactan	**6.1 ± 0.1**	4.8	1.6	**6.4**	4.5	2.4	**6.9**	4.2	4.8	**8.9**	2.3	7.4	**9.8**	1.6	9.9	**11.5**
Rhamnan	**4.1 ± 0.1**	3.5		**3.5**	3.2		**3.2**	2.6		**2.6**	1.7		**1.7**	1.2		**1.2**
Glucan	**---**	---	4.9	**4.9**	---	4.6	**4.6**	---	2.6	**2.6**	---	6.4	**6.4**	---	2.7	**2.7**
Xylan	**183 ± 4**	187	0.5	**187**	183	2.8	**185**	151	23.5	**175**	89	76	**166**	58	117	**175**
Glucomannan	**45.6 ± 0.5**	43.9	3.0	**46.9**	40.7	7.1	**47.8**	26.5	11.0	**37.6**	26.2	18.0	**44.3**	20.8	26.7	**47.5**
Cellulose	**440 ± 4**	438		**438**	441		**441**	451		**451**	452		**452**	454		**454**
Acetyl groups	**26± 2**	26	0.6	**26**	24	1.2	**26**	20	4.6	**25**	18.6	13	**31**	13	16	**29**
4OMeGUA	**19 ± 2**	18	0.0	**18**	16	0.0	**16**	14	2.8	**17**	6.7	7.6	**14**	1.7	5.9	**8**
GalUA	**10 ± 1**	9	0.9	**10**	7	1.0	**8**	6	1.6	**8**	4.2	1.9	**6**	1.7	1.2	**3**
Lignin	**243 ± 3**	229	4.9	**236**	231	8.1	**240**	228	12.6	**242**	216	28.1	**245**	213	21.0	**242**
Lignin precipitate			2.1			0.8			1.3			1.0			8.5	
Ash	**3.5 ± 0.5**	3.1	1.4	**4.5**	2.5	1.8	**4.3**	2.6	3.1	**5.8**	1.9	3.2	**5.1**	1.9	2.6	**4.5**
Total	**986**	965	21.5	**987**	956	33.4	**989**	909	74.6	**983**	821	168.7	**989**	768	216.8	**985**

5.1.4 Hydrothermal dissolution of wood components from OSB strands. The effect of P-factor on the molecular weight distribution of wood extracts

The polymeric substances in the wood extracts were analyzed using a GPC system with three detectors namely spectrophotometer (UV-Vis), refractive index (RI), and intrinsic viscosity differential pressure (IV-DP). For analytical details one is referred to section 3.2.3. Figure 5.12 depicts the GPC traces for five different extracts produced at different temperature and time conditions (Table 5.1). The IV-DP trace of sample (a) in this figure shows a very shallow peak at a retention time of 21-23 min and this detector is sensitive to carbohydrates. At this location there is no peak in the UV trace. Since higher molecular weight material elutes at lower retention times, this fraction represents a high molecular weight carbohydrate polymer free of lignin dissolved at mild extraction conditions. At this condition the concentration of xylan is very low, around 0.05% on wood, and the glucan concentration is 10 times higher than that of xylan. As stated earlier when discussing Figure 5.8 which showed a relatively high concentration of glucan at mild extraction conditions, this high molecular weight fraction is glucan oligomers or starch. This peak is absent in the following samples, meaning that starch has been degraded to a lower molecular weight or DP. The IV-DP and RI traces show a peak between 23 and 25 minutes for P-factor 38 up to 204 hrs. (Figure 5.12(a), (b), and (c)). The RI signal increases with increasing P-factor which means the concentration of oligomers also increases. This peak does not line up with a UV peak which means that this peak corresponds to lignin-free oligomers. Xylan has the

highest concentration in the sample at P-factor 204 hrs. (Table 5.2) which means this peak corresponds to xylo-oligomers which are free of lignin. With increasing P-factor these xylo-oligomers show further hydrolysis to lower DP values since the peak shifts to longer elution times (Figure 5.12 (c) and (d)). This agrees with the increased dissolution of xylo-monomers shown in Figure 6.6 at high P-factor values (408 and 896 hrs.). The RI and IV-DP signals show a shoulder at a retention time between 26 and 27 minutes for all conditions and the UV signal starts showing this shoulder more clearly at P-factor of 204 hrs., and increases with increasing P-factor. Also, a peak is now observed at this P-factor value at a retention time between 21 and 22 minutes. All three detectors line up at these two peaks at 21-22 minutes and 26-27 minutes (shoulder), thus are identified as lignin-carbohydrate complexes or LCC. The earlier peak (21-22 minutes) is not present at higher P-factor values meaning this polymeric fraction degrades to lower DP values.

Because the RI trace is related to the concentration of carbohydrates in the different solutions and it was used to determine the average molecular weight of the hemicelluloses present in each wood extract. Method details are given in section 3.2.3.

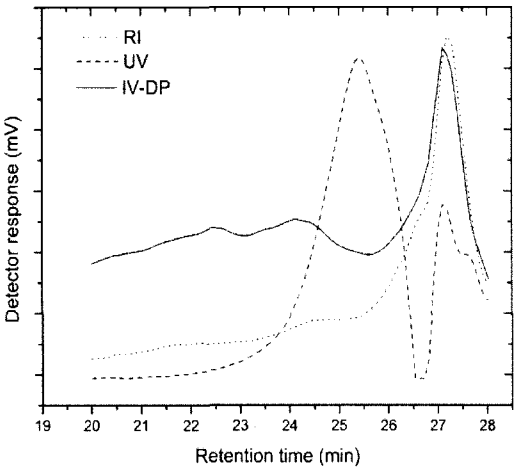

P-factor 38 hrs.

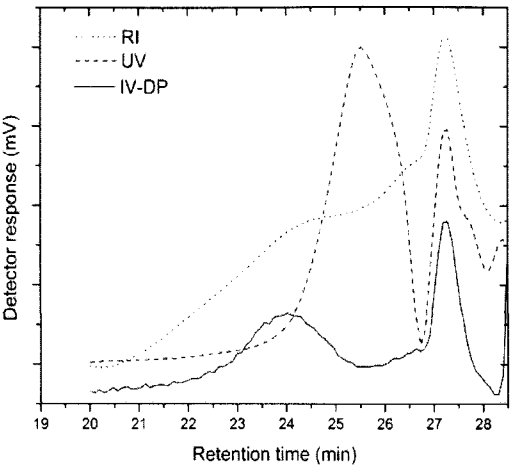

P-factor 89 hrs.

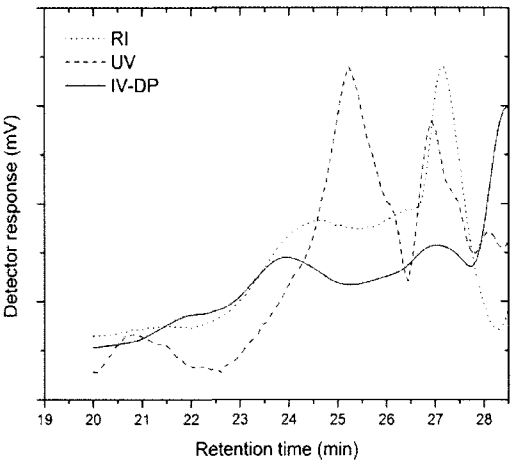

P-factor 204 hrs.

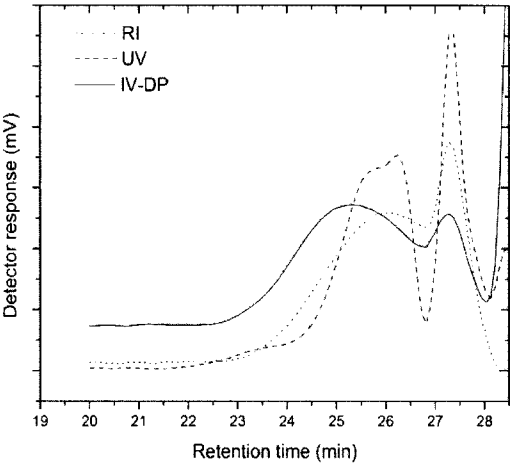

P-factor 408 hrs.

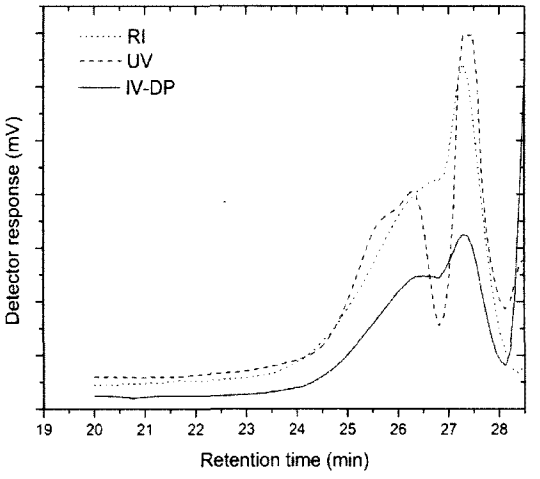

P-factor 896 hrs.

Figure 5.12. Gel permeation chromatography analysis of wood extracts at different extraction conditions.

Figure 5.13 depicts the RI detector response versus the logarithm of the molecular weight at each extraction condition. From this figure is can be seen that the hemicellulose concentration of higher molecular weight (log Mw between 3 and 4) increases with increasing P-factor and then at higher P-factor values (408 and 896 hrs.) shift to the left signifying there is hydrolysis degradation to lower DP values. Table 5.3 shows the results for the average molecular weight and degree of polymerization (DP) at each extraction condition (P-factor). The DP of hemicellulose reaches a maximum of 17 at a P-factor value of 89 hrs. and then decreases with increasing P-factor to a value of 6 for the most severe condition. The low DP value at a P-factor of 38 hrs. can be explained by the very low concentration of high molecular weight fraction of carbohydrates (23.5-25.5 min.) compared with the low molecular weight fraction (26-28 min.). Chen et al. (2010) found a maximum value of 25 for the DP of hemicellulose produced from DI-water extraction. This difference in DP values can be explained by the difference in liquid to wood ratio used by Chen (L/W=720) compared with that used in the present work (L/W=3). The lower value found at the present low L/W ratio means that the dissolution of hemicelluloses is also limited by the lower solubility of higher DP hemicelluloses during batch hot water extraction.

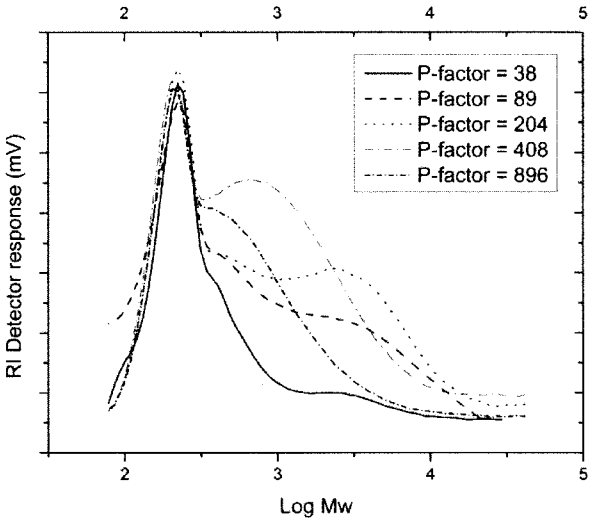

Figure 5.13. Molecular weight distribution for wood extracts at different extraction conditions.

Table 5.3. Average molecular weight (Mw) and degree of polymerization (DP) for wood extracts at different extraction conditions.

P-factor (hrs.)	Mw	DP
38	759	6
89	2,311	17
204	1,702	13
408	1,144	9
896	782	6

5.1.5 Effect of P-factor on degree of polymerization of cellulose in pulp

The goal of this section is to study the effect of hot water extraction of red maple strands on the total alkaline pulp yield, cellulose and xylan mass fractions, and the DP of cellulose in the alkaline pulp. The DP of cellulose was calculated through the determination of the intrinsic viscosity of cellulose in the pulp and corrected for hemicellulose content using the equation developed by da Silva Perez and van Heiningen (2002). The cooking temperature was kept at 170°C and the time adjusted for a final H-factor of 1,000 hrs. The alkali charge varies from 13 to 17% effective alkali (EA) and 30% sulfidity. The total yield was calculated based on the dryness of pulp, the total air dry pulp weight, and the dry weight of the wood strands added to the cook.

The intrinsic viscosity, kappa number, and mono sugar content of the alkaline pulps were determined as described in Chapter 3. The cellulose and hemicellulose content of pulp was determined from the mono sugar content as indicated in Table 5.4.

Table 5.4. Calculation of cellulose and hemicellulose content of pulp.

Eq. #	Description
5.4	Lignin (L) (g/g). Determined as 0.15*Kappa
5.5	Arabinan polymer (AR) (g/g) = arabinose (mg)*(132/150)/dry pulp (mg)
5.6	Galactan polymer (GA) (g/g) = galactose (mg)*(162/180)/dry pulp (mg)
5.7	Glucan polymer (GL) (g/g) = glucose (mg)*(162/180)/dry pulp (mg)
5.8	Mannan polymer (MA) (g/g) = mannose (mg)*(162/180)/dry pulp (mg)
5.9	Xylan polymer (XY) (g/g) = xylose (mg)*(132/150)/dry pulp (mg)
5.10	Total carbohydrate (TC) (g/g) = AR + GA + GL + MA + XY
5.11	Cellulose (G) (g/g) = GL – MA/b b = 1.7 (for hardwood, based on Janson (1974))
5.12	Hemicellulose (H) (g/g) = TC - G

Calculation of the DP of Cellulose from the Intrinsic Viscosity of Pulp

The DP of cellulose is calculated using the relationship of da Silva Perez and Van Heiningen (2002):

$$DP = \left\{\frac{1.65[\eta]-116H}{G}\right\}^{1.111} \qquad \text{Equation 5.13}$$

where [η] is intrinsic viscosity of the pulp in cm^3/g, and G and H are the mass fractions of cellulose and hemicelluloses in the (lignin containing) pulp respectively. This formula considers the actual weight of cellulose rather than that of the pulp weight being responsible for the viscosity, and also makes a correction for the small contribution of the hemicelluloses to the pulp intrinsic viscosity. The correction for the hemicelluloses (i.e. the term 116H) is based on a DP of hemicelluloses of 140.

The mass fractions of cellulose (Y_C), and xylan (Y_X) in the pulp made from the extracted woods can be expressed based on the original wood, respectively Y_C*, and Y_X*, by multiplication of respectively Y_C, and Y_X by the corresponding remaining wood mass fraction (f_i, Table 6.5). For example for the cellulose content of pulp based on the original wood, $Y_C^*=Y_C(f_i)$. Similarly Y_X^* is obtained as $Y_X(f_i)$. Y_C^* and Y_X^* are expressed in milligram per gram of original wood.

Table 5.5. Remaining wood mass fraction after hot water extraction. Values based on original wood.

P-factor (hrs.)	Remaining wood mass fraction (g/g of wood)	Final pH
38	$f_1 = 0.97$	4.7
89	$f_2 = 0.96$	4.3
204	$f_3 = 0.91$	3.9
408	$f_4 = 0.84$	3.5

Results and discussion

Figure 5.14 shows the kappa number (a) and the total alkaline pulp yield (b) based on the original wood (Y_T*) at different cook conditions for the original wood (P-factor 0 hr.) and extracted woods at different P-factor conditions. The value for Y_T* was calculated multiplying the total pulp yield by the remaining wood fraction for each extraction condition (Table 5.5). From the figure it can be noted how the kappa number and the pulp yield are greatly affected by the severity of the extraction. At the most severe condition the kappa number reaches a value of around 5 almost independent of the alkaline cook conditions. At this extraction condition the lignin has been much degraded so it is readily dissolved in the alkaline solution. On the other hand the pulp yield drops 2-3 percentage points even at low P-factor values (38 hrs.) dropping more than 10 at the highest P-factor (408 hrs.). This large drop in yield can be mostly explained by the much lower residual content of carbohydrates in these alkaline pulps.

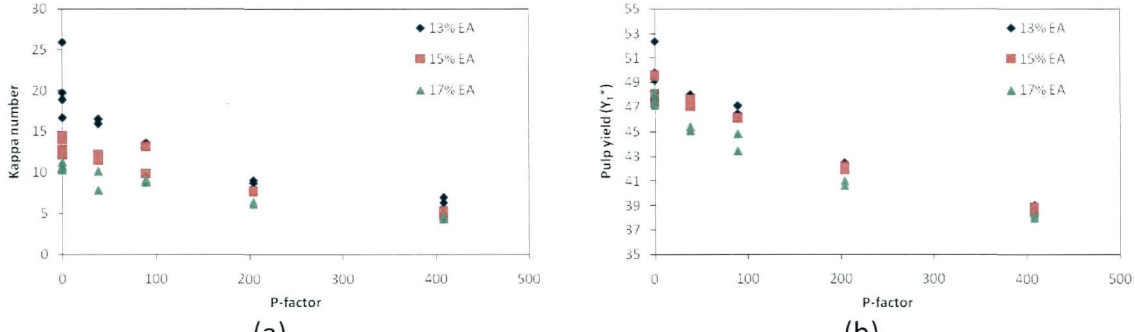

(a) (b)

Figure 5.14. Effect of severity of the pre-extraction (P-factor) on the kappa number (a) and pulp yield (b).

Figure 5.15 shows the effect of P-factor of the hot water extraction on the cellulose (a) and xylan (b) mass fractions of the pulp based on the original wood weight in mg/g of wood. It can be noted that for the lowest value of P-factor (38 hrs.) the cellulose mass fraction drops significantly and even more than that at the following extraction condition (P-factor 89 hrs.). This behavior was not expected and needs further investigation. After this maximum for cellulose fraction there is a linear decrease with increasing P-factor values. On the other hand, xylan displays an expected behavior showing a small effect at the lowest P-factor and then decreasing with increasing P-factor. It is noted that even though wood has been pretreated at a high severity (P-factor 900 hrs.) and has been cooked in strong alkali conditions there is still a non-removable amount of xylan in the final pulp. This is also observed in the production of viscous pulp by the sulfite process (Sixta, 2006) and it can be explained by a strong association between xylan and cellulose (Dammström et al., 2009).

The effect of P-factor on the DP of cellulose is shown in Figure 5.16. There is no a significant effect on the DP up to a P-factor of 90 hr. Then, the DP linearly decreases at more severe extraction conditions for all alkaline cooks showing that the P-factor has a major effect on the DP of cellulose. This decrease in DP can be explained by degradation of cellulose through acid hydrolysis because after a P-factor of 90 hrs. the pH drops under a value of 4. It is also observed that as degradation of cellulose increases xylan concentration decreases in the final pulp.

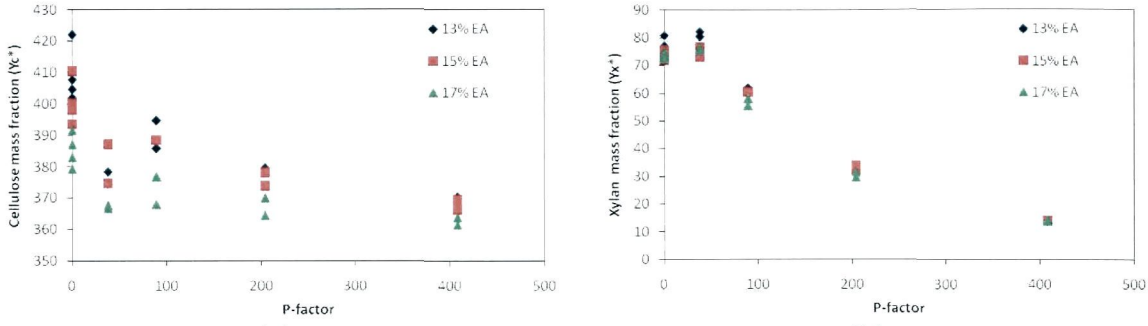

(a) (b)

Figure 5.15. The effect of the extraction severity on the cellulose (a) and xylan (b) pulp mass fractions.

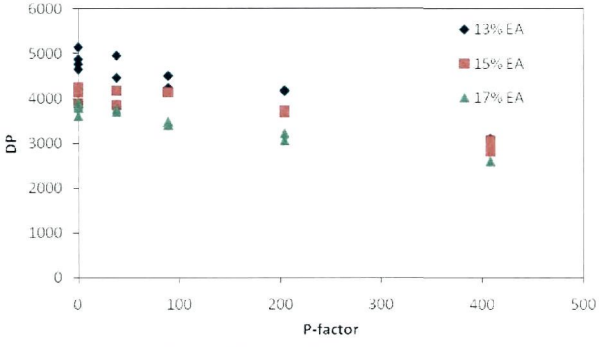

Figure 5.16. The effect of the extraction severity on the DP of cellulose.

5.1.6 Conclusions

The effect of P-factor on the extraction yield

- The P-factor was successful to describe the effect of time and temperature of all wood components dissolved during hydrothermal treatment of Red Maple.
- The maximum amount of wood material removed at the most severe condition (P-factor of 896 hrs.) was around 23%. 3% accounts for lignin removal. Xylan is the wood component that contributes the most to the total yield of removal.
- The pH of the final extract reaches a plateau after a P-factor of 400 hrs. with a value of 3.5. Free acetic acid is mainly responsible for lowering the pH.
- Xylan yield presents an S-shaped curve which can be explained by the initially low acidity of the solution and that xylan needs to be degraded to a lower degree of polymerization before become soluble.
- The maximum amount of xylan removed at the highest P-factor was 64% based on the original content of xylan in wood. Xylan dissolves mostly as oligosaccharides up to a P-factor of 200 hrs. and at more severe conditions the xylo-oligosaccharides depolymerize to monomeric xylose by acid hydrolysis.
- MeGUA is degraded at P-factor values over 400 hrs. probably due to decarboxylation.
- The high amount of glucan dissolved at mild extraction conditions (P-factor up to 89) corresponds to the dissolution of gluco-oligomers or starch.
- Arabinan starts degrading at P-factors above 200 hrs.

Effect of P-factor on the residual concentration of wood components

- Cellulose is not dissolved significantly at all P-factor values due to its high molecular weight and crystalline nature, while lignin shows a low degree of dissolution.
- The total uronic acid group content decreases about 83% at the most severe condition studied (P-factor of 896 hrs.).
- The molar ratio of acetyl groups per 10 xylose units increases with P-factor meaning the residual xylan becomes more acetylated. 4OMeGUA ratio decreases with increasing P-factor meaning that the number of these side groups becomes smaller on the residual xylan.
- When comparing the major wood components namely cellulose, lignin and xylan in the liquid and solid phases a good closed mass balance is obtained at all P-factor conditions.
- Higher mass balances differences are seen for the minor wood components probably due to acid degradation during sample preparation of the solid samples.

The effect of P-factor on the molecular weight of wood extracts

- A high molecular weight lignin-free carbohydrate fraction identified as gluco-oligomers (starch) is dissolved during the initial stage of hydrothermal treatment. This fraction decreases with increasing P-factor.

- Carbohydrate-free lignin was identified at all P-factor conditions. Lignin-free carbohydrates were identified with a maximum DP value of 17 at a P-factor of 89 hrs. The lowest DP value was 6 at the most severe conditions (P-factor of 896 hrs.) showing a high degradation of carbohydrates and lignin-carbohydrate oligomers.

Effect of P-factor on degree of polymerization of cellulose in pulp and wood

- Kappa and pulp yield after alkaline cooks of water extracted wood are greatly affected by increasing P-factor on the extraction of wood material. At the most severe condition the kappa number decreases around 75% and the pulp yield close to 10%. This is evidence of lignin and carbohydrates degradation.
- Cellulose mass fraction decreases between 2% and 4% in the final pulp at the highest P-factor (896 hrs.). Xylan mass fraction decreases about 6% at this condition.
- DP of cellulose is not affected significantly up to a P-factor of 90 hrs. At higher P-factors the DP linearly decreases with increasing P-factor, from 5,000 to around 3,000 at the most severe extraction conditions. This verifies that P-factor has a major effect on the DP of cellulose.
- A lower DP value of cellulose in pulp is found to be related to lower concentrations of xylan on it.

5.2 Intrinsic kinetics of the removal of wood components from hardwood (*Acer rubrum*) by hot water extraction in a continuous mixed batch reactor

5.2.1 Introduction

To date the kinetics and mechanism of hemicellulose dissolution with hot water from wood is not fully understood. Previous research for autohydrolysis was mostly carried out in batch reactors (Garrote et al., 1999; Jacobsen and Wyman, 2002; Mittal et al., 2009; Conner and Lorenz, 1986; Conner, 1983; Garrote et al., 2004; Nabarlatz et al., 2005). Unfortunately batch reactors are not best suited to study the intrinsic kinetics of xylan dissolution because the dissolved hemicelluloses are further degraded in solution. On the other hand, the use of flow-through systems has shown that xylan removal increases with flow rate which is inconsistent with intrinsic homogeneous kinetics (Liu and Wyman, 2003). In addition, studies on the degree of polymerization of xylan using the flow-through system suggest that lignin-xylan oligomers and their solubility could have a large effect on the rates of removal and yields of lignocellulosic biomass pretreatment (Yang and Wyman, 2008). More recently, a continuous mixed batch reactor (CMBR) was used to study the kinetics of removal of hemicelluloses and lignin from mixed southern hardwood (SHM) chips with hot water. The system was shown to be suitable to study the intrinsic kinetics of the autohydrolysis process because the wood component dissolution rates were independent of flow rate and wood-to-liquid mass ratio. (Chen et al., 2010). However, the rates were still affected by diffusional transport of the components out of the wood chips. Therefore the same continuous

mixed batch reactor was used in the present work but now wood-meal was used to study the temperature and pH effect on the kinetics of removal of hemicellulose from hardwood (*Acer rubrum*). In addition, the effect of wood particle size was also investigated.

5.2.2 Effect of temperature

Experimental

Three different extraction temperatures were studied: 150, 160C, and 170°C. The extraction solvent was a solution of 1 g/L acetic acid. Close to 10 grams of wood meal were placed in the reactor. Table 5.6 shows the composition for this new sample of wood produced as described in Chapter 4. The flow rate was set at 100 mL/min and samples were collected at different times (2, 4, 6, 10, 20, 30, 40, 50. 60, 70, 80, and 90 min) for one minute long in plastics containers and weighed to check the flow rate.

Wood component dissolution

Figure 5.17 shows the concentrations of hemicellulose polysaccharides and lignin normalized by the original wood weight during the 90 minutes extraction time, at the three different temperature conditions. The xylan concentration goes through a maximum for all conditions, with the maximum increasing and occurring earlier with increasing temperature. Lignin on the other hand dissolves starting with a high concentration at all conditions. The xylan concentration initially decreases and then

increases in the early stages of extraction (Figure 5.17) because dissolved xylan has accumulated in the reactor during the short temperature ramp-up time, and this xylan is then flushed out over time when solvent is fed to the reactor. However as will be shown later, this effect is eliminated when the xylan removal rate is calculated from the concentration versus time graphs. All other minor sugars start dissolving at a high concentration and then decrease over time except for arabinan at the lowest temperature (Figure 5.18) which increases slightly for a short time (3 min) and then decreases. This is indicative of more rapid hydrolysis of the side groups of the hemicelluloses as reported earlier by Tunc (2008).

Table 5.6. Chemical composition of original wood. Values in milligram per gram over dry wood.

Arabinan	Galactan	Rhaman	Glucan	Xylan	Mannan	Acetyl groups	Lignin
8.5	9.4	4.3	441	156	21.1	35.3	266

As observed in Figures 5.19 and 5.20, the contribution to the total extraction yield is mainly coming from xylan and lignin which increases with increasing temperature. It can be noted that the xylan concentration profile is S-shaped due to the initially slow dissolution of xylan oligomers which need to be degraded to a lower degree of polymerization (DP) in order to dissolve. This has been shown by Chen et al. (2010) who concluded that xylan needs to be degraded down to a DP value of about 25 in order to dissolve in DI-water at 160°C. Figure 5.19 shows the final weight loss measured from the quantification of the residual lignin and polysaccharides in extracted wood and does not include all minor wood components (glucuronic acids, ash, and

proteins). The difference between these two yields can be explained partially by not including these components on the total extraction yield values. Figure 5.20 shows the concentration of the minor polysaccharides. It can be observed how the total yield of arabinan and rhamnan at 170°C are lower than that at 150°C which is evidence of a degradation process. This is more pronounced for arabinan which is known to be more susceptible to acid degradation (Teleman, 2009).

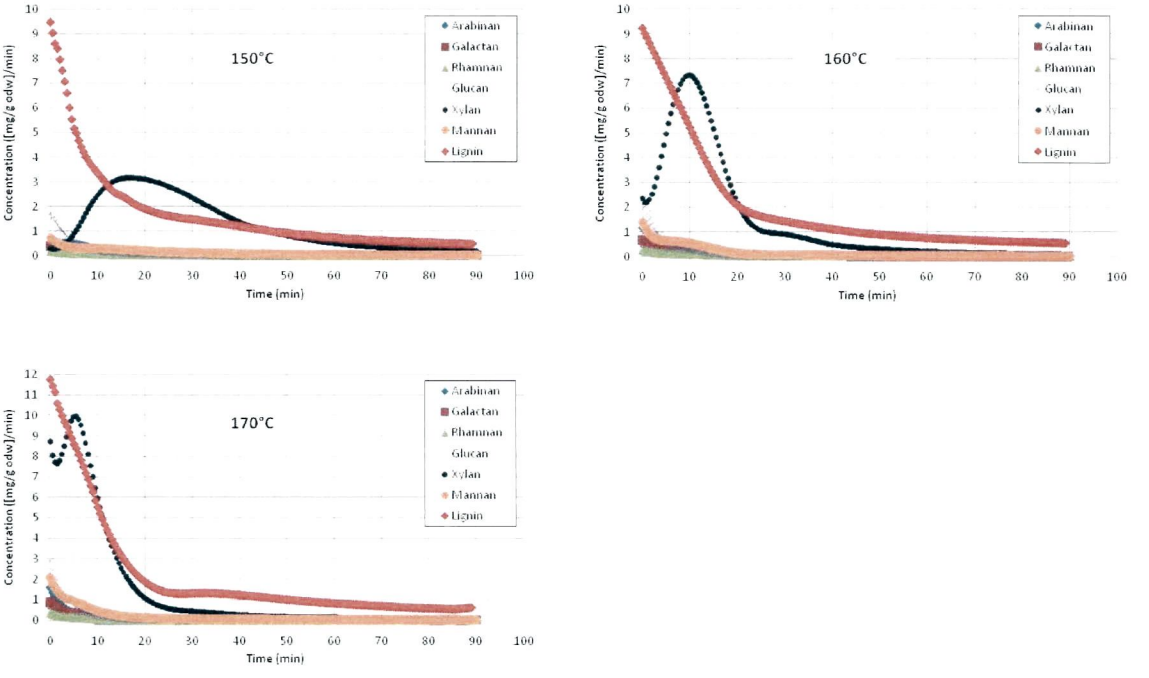

Figure 5.17. Concentration versus time for lignin and polysaccharides at three temperature conditions during the hot water extraction

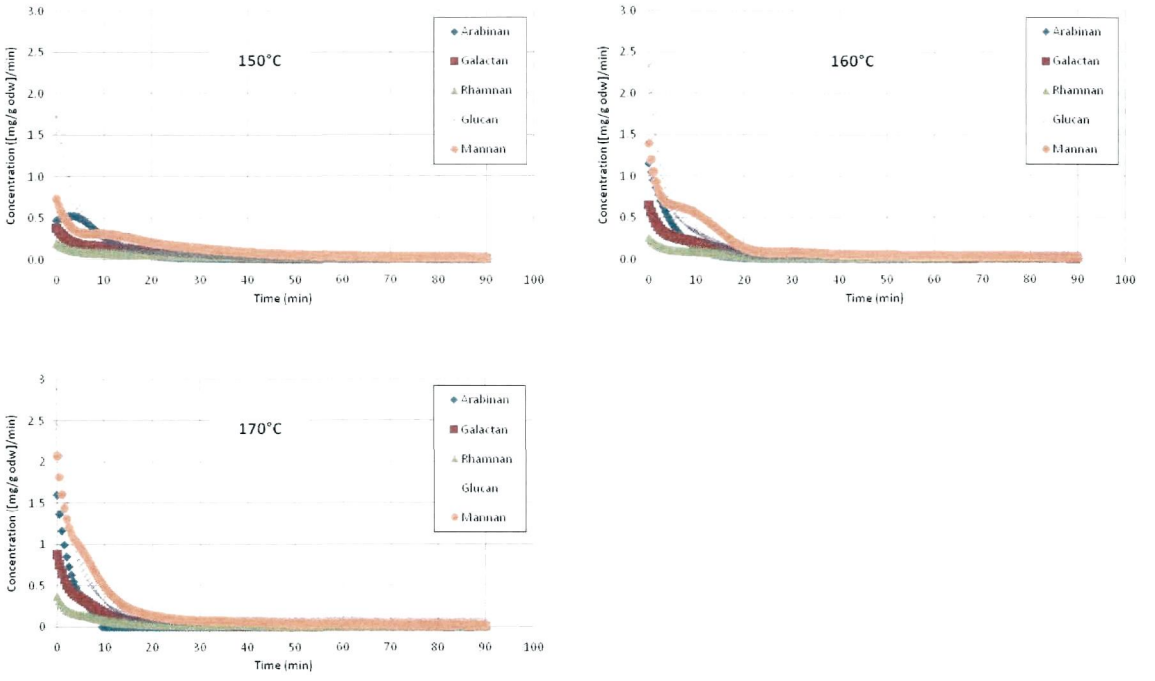

Figure 5.18. Concentration versus time for minor polysaccharides at three temperature conditions during the hot water extraction

Glucan and mannan show a higher concentration than xylan during the first 5 minutes of extraction at 150°C (Figure 5.18). It could be assumed that these sugars are part of a glucomannan type hemicellulose. In sugar maple (*Acer saccharum*) the molar ratio between mannan and glucan was found to be 2.3:1 (Fengel and Wegener, 1983). However, Figure 6.38 shows that glucan concentration is higher than that for mannan for all temperature conditions during the first 5 minutes of extraction. In recent work Tunc and van Heiningen (2010) have shown that during the early stage of hot water extraction of mixed southern hardwoods (SHM) chips high molecular weight oligo-glucan is removed and that most of this is actually starch.

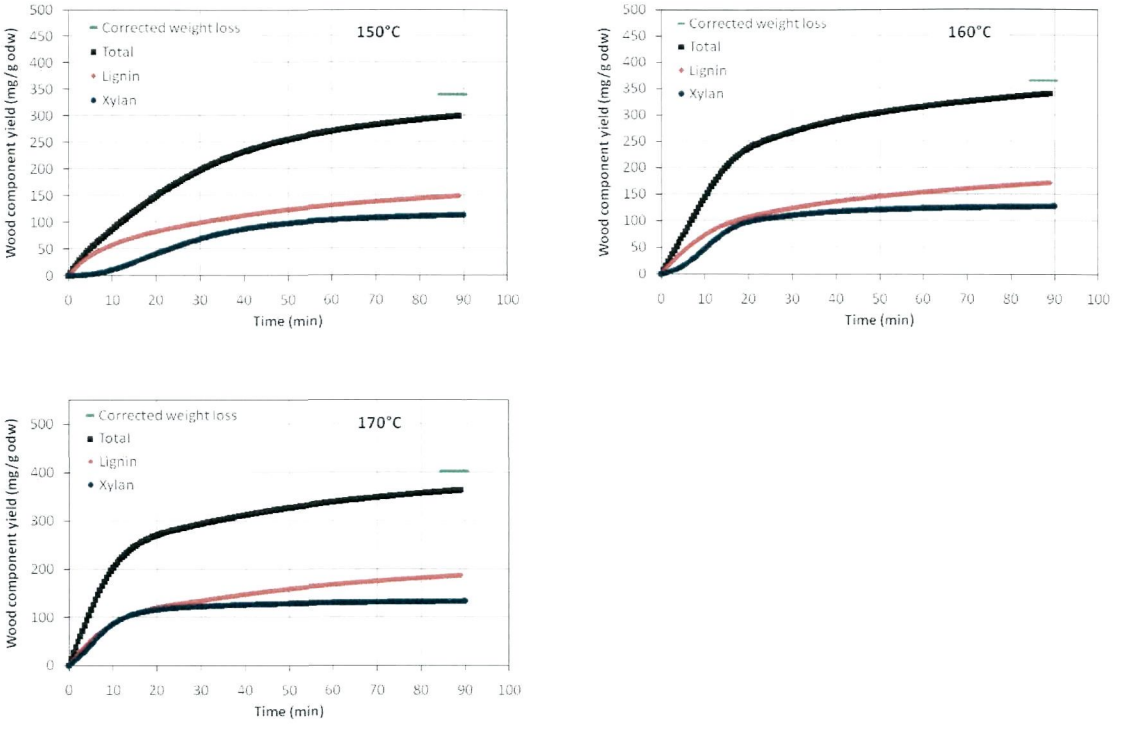

Figure 5.19. Extraction yield for lignin, xylan, and the overall process at different temperatures.

The extraction yield of the minor sugars is shown in Figure 5.20. It can be seen that the glucan yield is higher than that of mannan at 150°C during the entire extraction (Figure 5.20). This behavior changes at higher temperatures where the mannan yield now is higher than that of glucan. After 60 minutes at 150°C and 40 minutes at 160°C the glucan and mannan yields increase at the same rate. However, at 170°C the glucan yield starts to increase faster than that of mannan after 20 minutes of extraction. This continued glucan removal may be interpreted as cellulose degradation.

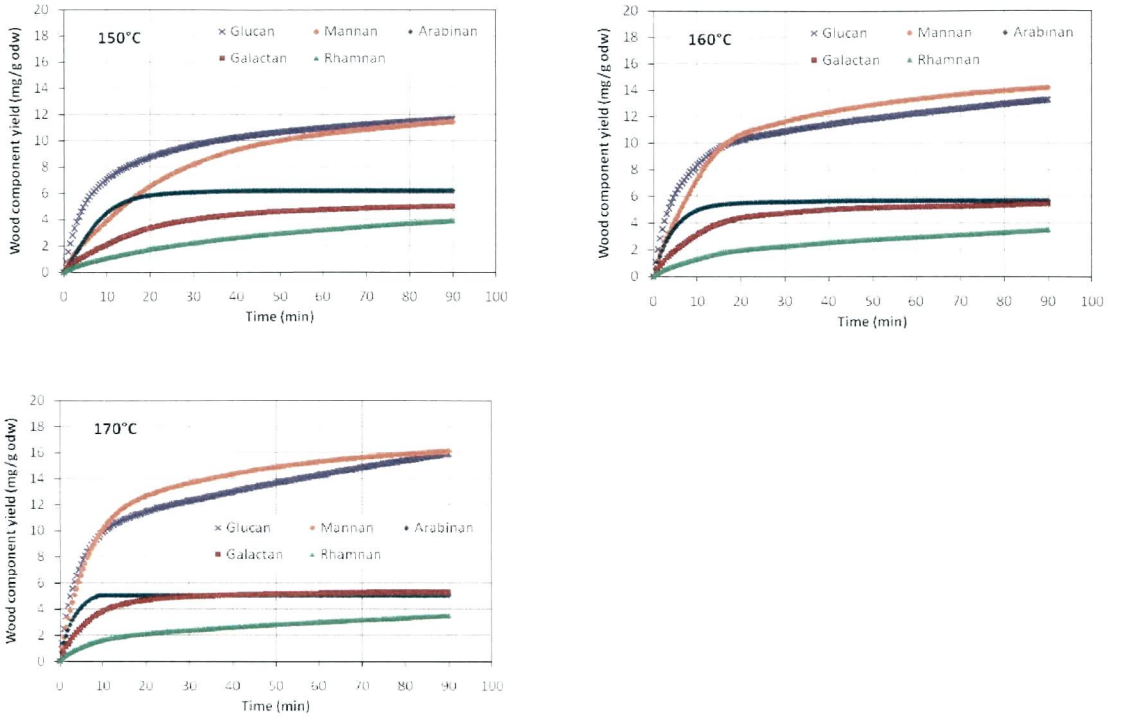

Figure 5.20. Extraction yield for minor polysaccharides at different temperatures.

In a different set of experiments, original and extracted wood at 160°C for 3 different extraction times (20, 40, and 90 minutes) were tested for its cellulose viscosity to determine the extent of cellulose degradation. Values were corrected for hemicellulose and lignin content and the degree of polymerization (DP) of cellulose was also determined by using the equation developed by da Silva Perez and van Heiningen (2002). The results in Table 5.7 show that before 10 minutes of extraction there is no cellulose degradation. At 40 and 90 minutes of extraction the DP value drops considerably. The number of cellulose chain scissions (S) is calculated as $10^4 x(1/DP-1/DP_o)$ (Sixta, 2006), with DP_o the degree of polymerization in the original wood (Table

5.7). These results show that a significant amount of cellulose chain scission takes place after 40 minutes of extraction due to acid hydrolysis.

Table 5.7. Intrinsic viscosity, degree of polymerization (DP) and scission number for described solid samples.

Description	Residual wood (g/g wood)	Lignin (g/g)	Hemicellulose (g/g wood)	Cellulose (g/g wood)	Intrinsic viscosity [h] (cm^3/g)	DP	Cellulose chain scission number (S)
Original wood		0.27	0.25	0.43	1,381	9,207	---
10 min	0.87	0.19	0.14	0.49	1,096	9,183	0.0
40 min	0.62	0.13	0.10	0.69	803	4,226	1.3
90 min	0.58	0.10	0.08	0.73	630	2,641	2.7

The removal rate for xylan and lignin

For a better understanding of the extraction kinetics, the lignin and xylan concentrations in the extract are used to calculate their respective removal rates using Equation 5.14 (Chen, 2009).

$$r(t) = \frac{\phi_v}{m_p} C(t + t_d) + \frac{V_r}{m_p} \cdot \left.\frac{dC}{dt}\right|_{t+t_d} \qquad \text{Equation 5.14}$$

where,

$r(t)$ is the component removal rate ([g / min]/ g of wood),

ϕ_v is the liquid flow rate (ml/min),

$C(t + t_d)$ is the dissolved concentration (g/ml),

V_r is the reactor volume (ml),

m_p is the wood weight (o.d wood), and

t_d is the residence time between the reactor and sample detection.

Figure 5.21 depicts the removal rate of xylan and lignin at all three temperatures during the extraction. The xylan removal rate shows a maximum at all conditions which increases and occurs earlier with increasing temperature. On the other hand, lignin shows a different behavior, starting always from a high value and then rapidly decreasing followed by a lower decreasing rate. It is interesting to note that the latter behavior starts just after the maximum xylan peak is reached and then both rates decrease almost in parallel. It is important to note that the amount of xylan removed when the maximum xylan removal rate is reached increases with increasing temperature. The highest amount removed was around 3.8-3.9% based on the original wood (25% on the original xylan) at the most severe condition (170°C), and the lowest amount was 2.2% on wood (14% on xylan) at the lowest condition (150°C). Thus, the total xylan amount removed up to the maximum rate is temperature dependent. A similar amount of 3-3.5% of xylan based on wood was found to be removed at the time of the maximum removal rate by Chen et al. (2010) who used deionized water at 160°C to study the removal of wood components from mixed southern hardwood (SHM) chips. They concluded that this fraction of xylan removed during the early stage of the extraction would correspond to lignin-free xylan. Chen findings would explain the different pattern between xylan and lignin rates during the initial extraction period. As a consequence the lignin removed during this initial period is also carbohydrate-free. The presence of carbohydrate-free lignin in hardwood was recently shown by Lawoko and van Heiningen (2010). Chen also concluded that all xylan removed after the maximum

xylan removal rate is in the form of lignin carbohydrate complexes (LCC) and that at this point the xylan removal rate is subsequently controlled by the hydrolysis of the lignin leading to the release of lignin fragments with covalently bound xylan. This mechanism has been also suggested by Conner (1983).

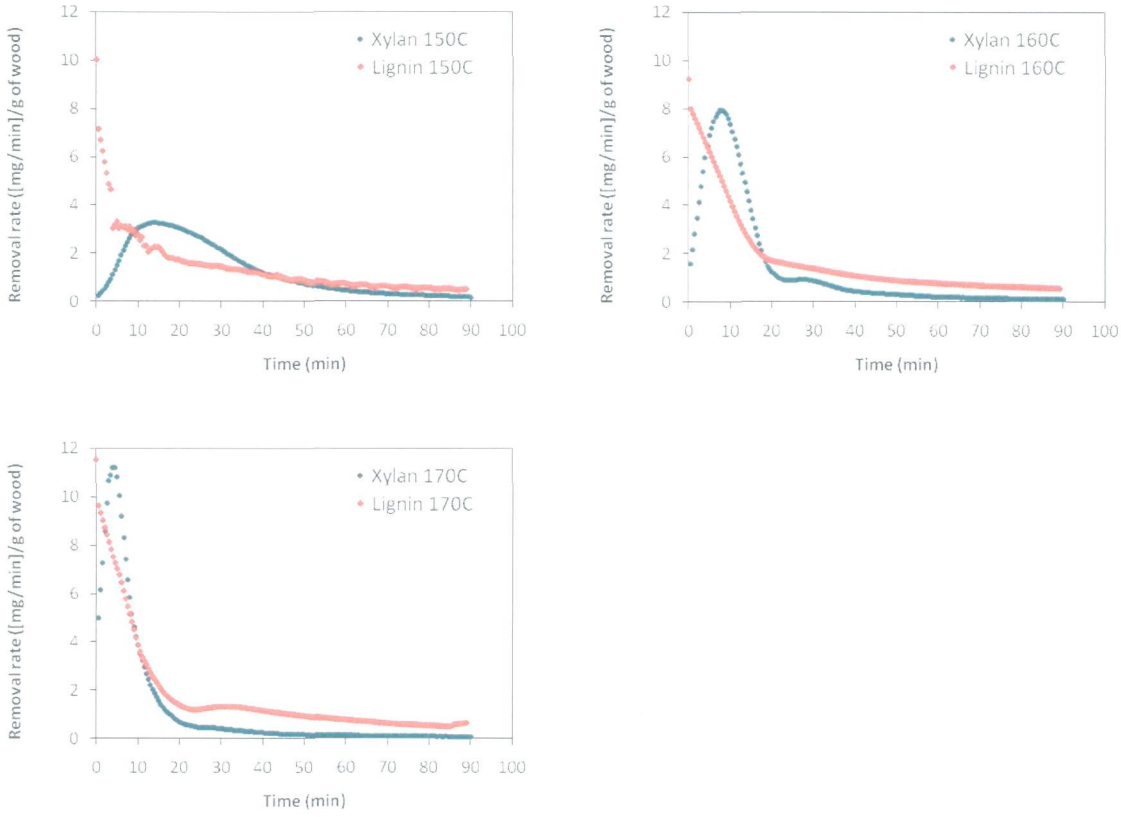

Figure 5.21. Removal rates for xylan and lignin at all three temperature conditions.

Following the conventional way of interpretating kinetics, the removal rates of xylan and lignin are plotted in Figure 5.22 against percentage of respectively residual xylan and lignin in wood for all temperature conditions. In general for all conditions the xylan removal rate increases initially until a maximum followed by an approximately

linearly decreasing rate. On the other hand, the removal rate of lignin can be separated into two different zones: an initial at high removal rate which decreases rapidly with decreasing residual lignin, followed by a second phase where the rate also decreases linearly but at a much smaller slope. The slope on this second phase seems to be independent of temperature. In general, it can be observed that both removal rates of xylan and lignin increase with increasing temperature.

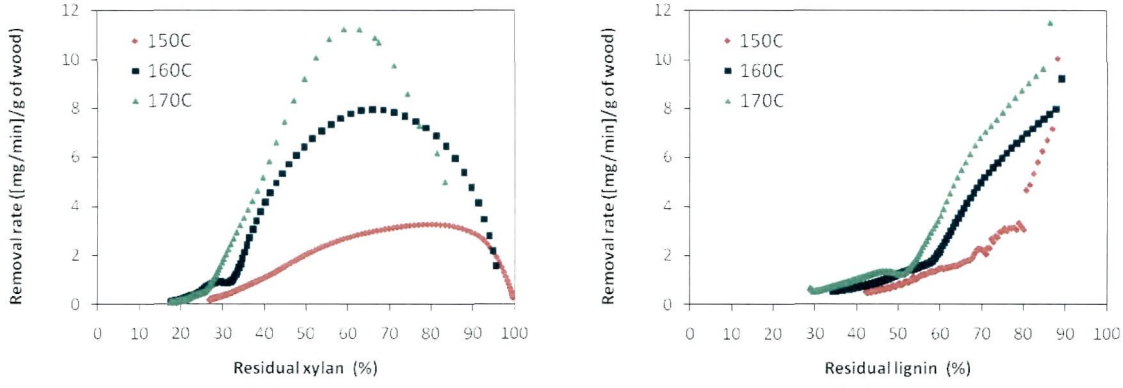

(a) (b)

Figure 5.22. Xylan (a) and lignin (b) removal rates versus their residual concentration in wood at different temperature conditions.

By extrapolating the xylan removal rate at the final stage in Figure 5.22(a) for all temperature conditions to a rate of zero it can be noted that there is a non-removable amount of xylan at 160 and 170 °C of about 18%, and 25% at 150 °C.

5.2.3 Effect of pH

Experimental

Four different solutions were prepared for different pH values: pH 2, 3, 4, and 5. The solutions were prepared by mixing formic acid (HFA), sodium formate (NaFA), and deionized water: 6.67 g/L HFA (pH 2.1 ±0.1), 1.00 g/L HFA + 0.33 g/L NaFA (pH 3.0 ±0.1), 1.00 g/L NaFA + 0.19 g/L HFA (pH 4.0 ±0.1), and 2.0 g/L NaFA + 3.7 mg/L HFA (pH 5.0 ±0.1).The extraction temperature was fixed at 160°C. Close to 10 grams of wood meal were placed in the reactor. The flow rate was set at 100 mL/min and samples were collected at different times for one minute long in plastics containers and weighed to check the flow rate.

Wood component dissolution

Figure 5.23 depicts the concentrations of hemicellulose polysaccharides and lignin normalized by the original wood weight during the 90 minutes extraction time at the four different pH conditions. As for different temperature conditions the xylan concentration goes through a maximum at all pH conditions, with the maximum increasing and occurring earlier with increasing acidity. However, a more evident effect is observed for pH as compared with the temperature effect. Lignin on the other hand dissolves at a high concentration immediately from the start of the extraction at all pH conditions. All other sugars start at the highest concentration and then decrease over time.

Figure 5.24 depicts the total and xylan and lignin yields with the length of the extraction. The total yield is compared with the final weight loss measured from the wood weight which is shown as a short horizontal line at the end of the experiment with applicable error bars. This value was corrected by subtracting the residual total acetyl groups amount in the extracted wood (Table 5.9) to allow a better comparison with the final total extraction yield determined from the liquid phase analysis. The difference between these two yields can be explained partially because the total yield curve does not include uronic acids which in original wood account for up to 3 percent. Figure 5.25 shows the extraction yield for the minor polysaccharides. It can be observed that the total yield of arabinan, galactan and rhamnan at pH 2 is lower than that at pH 3 which is evidence of degradation. This behavior was also observed when temperature increases (Figure 5.18).

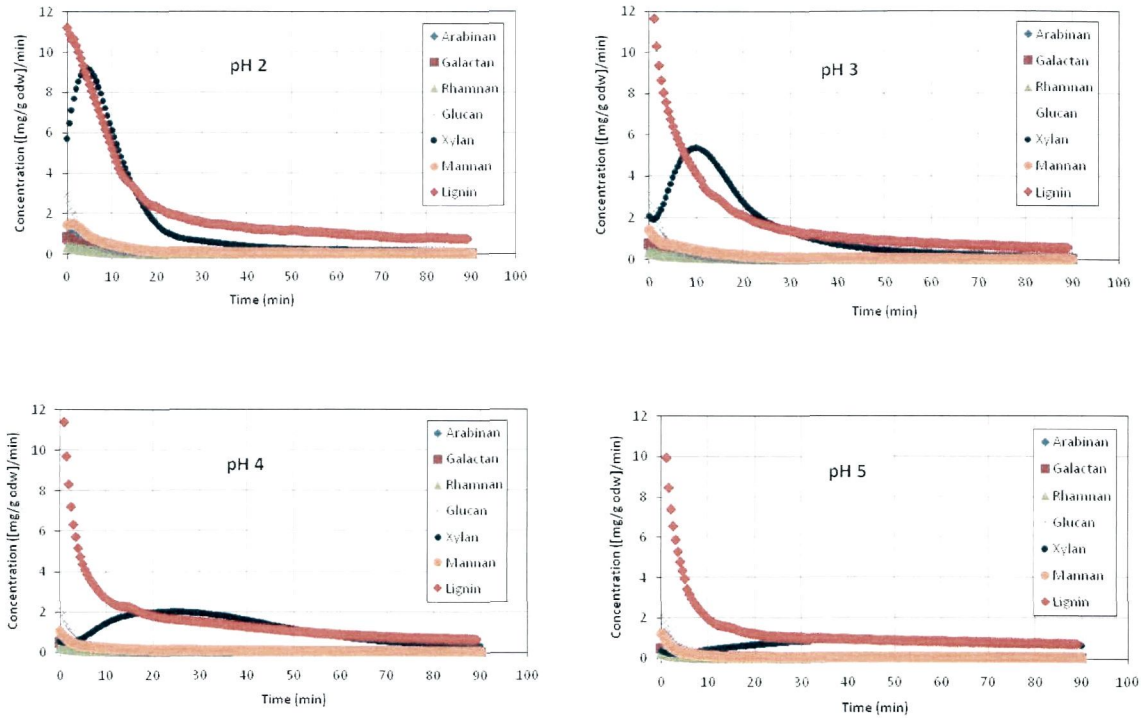

Figure 5.23. Concentration curves of lignin and polysaccharides for all four pH conditions along the extraction process.

It can be noticed from Figure 5.25 that glucan yield increases rapidly to about 10 mg/g (or 1% on wood) after 10 min of extraction at pH 2 and 3. This level is reached asymptotically after 90 minutes at pH 4 and 5, while the glucan yield keeps increasing after 10 minutes above this asymptotic level at the two lower pH levels, and at a higher rate at pH 2. This continued increase in glucan removed may be interpreted as cellulose degradation. Looking at the glucan to mannan ratio (Figure 5.26) it is clear there are two type of glucan being dissolved: one which is removed at an early stage of the process (starch) and another which is removed almost at a constant glucan/mannan ratio of 0.5. It is also clear that already at pH 3 this ratio starts increasing slightly after 30 minutes

and it is more evident after 20 minutes at pH 2, which reaffirms the hypothesis of cellulose degradation.

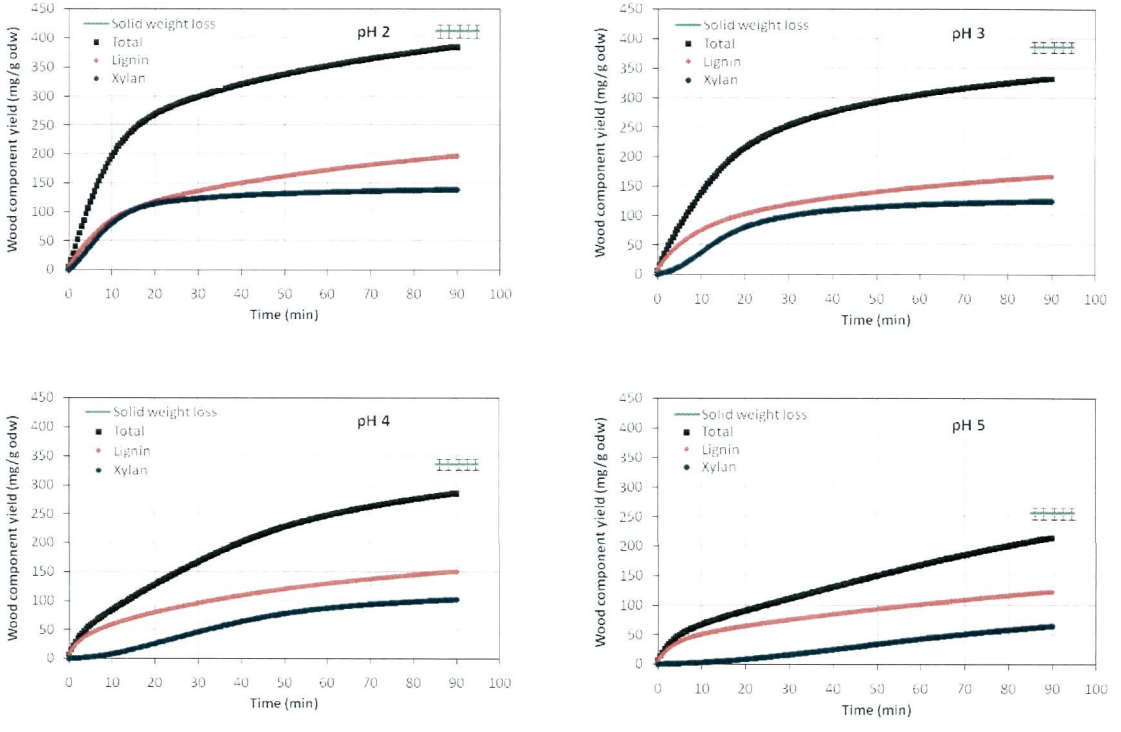

Figure 5.24. Extraction yield for lignin, xylan, and the overall process at different pH conditions.

In a different set of experiments, original and extracted wood at pH 3, 4, and 5, were tested for its cellulose viscosity as a way to determine the extent of cellulose degradation. Values were corrected for hemicellulose and lignin content and the degree of polymerization (DP) of cellulose was also determined by using the equation developed by da Silva Perez and van Heiningen (2002). The results in Table 5.8 show that the values at pH 4 and 5 are comparable showing there is only a modest degradation of cellulose; however at pH 3 the DP value drops considerably. These

results show that cellulose chain scission occurs at all pH values, but at pH 3 the rate triple the value determined for pH 4 and 5. However this is a small increase considering that acidity increases more than 10 times.

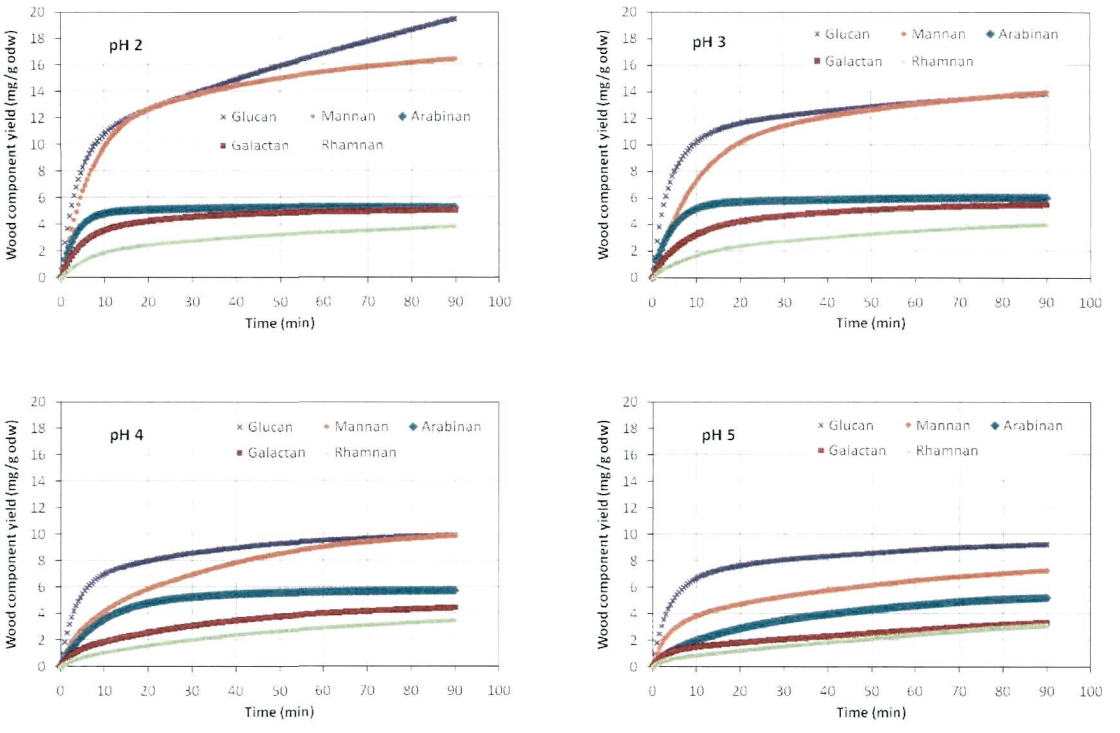

Figure 5.25. Extraction yield for minor polysaccharides at different pH conditions.

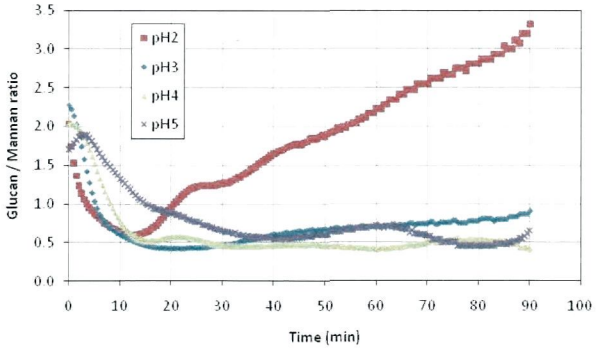

Figure 5.26. Molar ratio for glucan and mannan at different pH conditions.

Table 5.8. Intrinsic viscosity, degree of polymerization (DP) and scission number for described solid samples.

Description	Residual wood (g/g wood)	Lignin (g/g)	Hemicellulose (g/g wood)	Cellulose (g/g wood)	Intrinsic viscosity [h] (cm^3/g)	DP	Cellulose chain scission number (S)
Original wood		0.27	0.25	0.43	1,381	9,207	---
Wood pH 3	0.61	0.13	0.07	0.70	7,91	3,496	1.7
Wood pH 4	0.66	0.14	0.11	0.65	1,184	5,917	0.6
Wood pH 5	0.74	0.15	0.15	0.58	1,284	6,249	0.5

The removal of acetyl groups

Acetyl groups can be found as side groups in hardwood xylan with a general ratio of 7 acetyl units for every 10 xylose units (Sjöström, 1993). Figure 5.27 depicts the concentration of the total acetyl groups for every pH over the duration of the extraction. All curves show a maximum value at the same time as is seen for the xylan curves in Figure 5.23. Figure 5.28 shows the molar ratio between acetyl groups and 10 xylose units for all pH conditions. The ratio after 10 minutes extraction is close to 7-8 which is in agreement with literature. However, at times shorter than 10 minutes the values are surprisingly higher than expected with a high value of almost 24 at 2 minutes for pH 5. This high molar ratio was also found at the lowest P-factor (38 hrs.) in the hot water extraction of wood strands in a batch reactor shown in Figure 5.7 in section 5.1.2. The general trend is concordance with the work of Chen et al. (2010) starting from a high value of 7.5 and decreasing quickly at 5 minutes of extraction to about 2.5 after 20 minutes. However, these values are lower by more than a factor 2 than those obtained here.

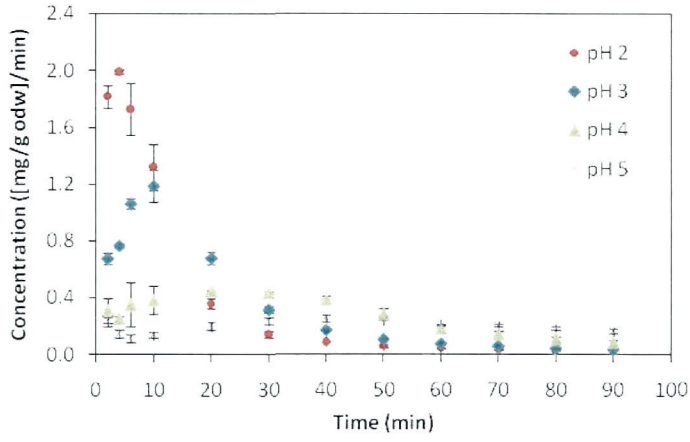

Figure 5.27. Concentration of acetyl groups along the extraction process at four different pH conditions.

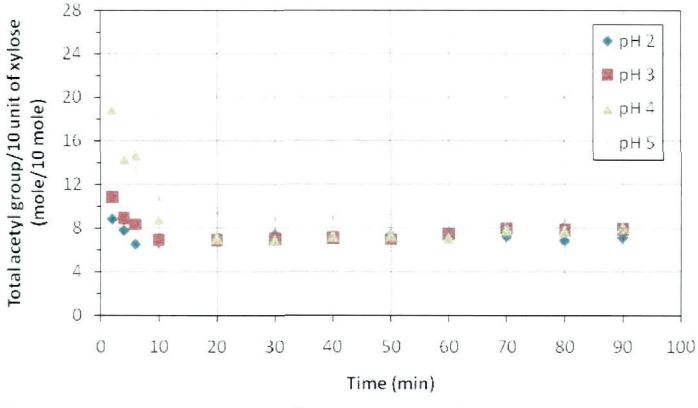

Figure 5.28. Amount of units acetyl groups per every 10 units of dehydrated xylose at four different pH conditions.

A mass balance study was performed to check the consistency of these results. The total volume of wood extracts was recorded for these experiments and homogeneous samples were taken, so it was possible to quantify the total amount of acetyl groups removed. In addition, the extracted solids samples were hydrolyzed in alkaline media to complete deacetylation and then the acetyl groups were quantified as acetic acid using the Megazyme kit described in section 3.2.3. The addition of these two

quantities should match the amount of acetyl groups in the original wood. The results are shown in Table 5.9. Also, the final acetyl group/10 xylose ratio is determined in the extracted wood.

Table 5.9. Mass balance for acetyl groups and final acetyl group/10 xylose ratio in extracted wood.

Condition	Acetyl groups (mg/g odw)		Mass balance (mg/g odw)	Remaining xylan (mg/g odw)	Acetyl/10 xylose (mole/10 mole)
	Wood	Extract			
Original wood	35.3±0.5	--		155.9	7.0
pH 2	3.4±0.1	30.0±0.5	33.4	17.0	6.1
pH 3	7.5±0.1	28.7±0.6	36.2	32.8	7.0
pH 4	11.8±0.1	23.0±1.8	34.8	55.1	6.6
pH 5	16.0±0.6	15.3±4.6	31.3	91.5	5.4

The results show that there is a reasonably good mass balance. It can also be seen that the acetyl/10 xylose ratio in the residual xylan in the extracted wood is about 6-7 for all pH values except pH 5 which is 5.4. Since almost 60% of the original xylan is still remaining at the end of the extraction at pH 5, this confirms that in fact more highly acetylated xylan is initially dissolved during the extraction process. This is also consistent with the results of Chen et al. (2010) showing that there is an initial dissolution of high DP acetylated xylan oligomers followed by lower DP oligomers with lower degree of acetylation. At low pH values the acetyl/10 xylose units in the small amount of remaining xylan in the extracted wood is similar to that of the original wood.

The removal rate for xylan and lignin

Figure 5.29 shows the removal rate of xylan and lignin for all four different pH values calculated by using Equation 5.14. At low pH of 2 both removal rates start from a maximum value. At higher pH conditions the xylan removal rate starts from about zero and increases to a maximum value and then decreases and occurs after a longer extraction time with increasing pH. On the other hand, lignin starts always from a high value and then gradually decreases. It is important to note that at all pH conditions the amount of xylan removed when the maximum xylan removal rate is reached is about 3.8-3.9% on original wood. At pH 5 it is clear xylan and lignin follow a different behavior during the first 40 minutes of extraction. As described in the previous section, this can be explained by the presence of lignin-free xylan and carbohydrate-free lignin. At lower pH conditions (3-4) the removal of lignin-free xylan would be so fast that it becomes difficult to see a clear difference between the removal rates of xylan and lignin.

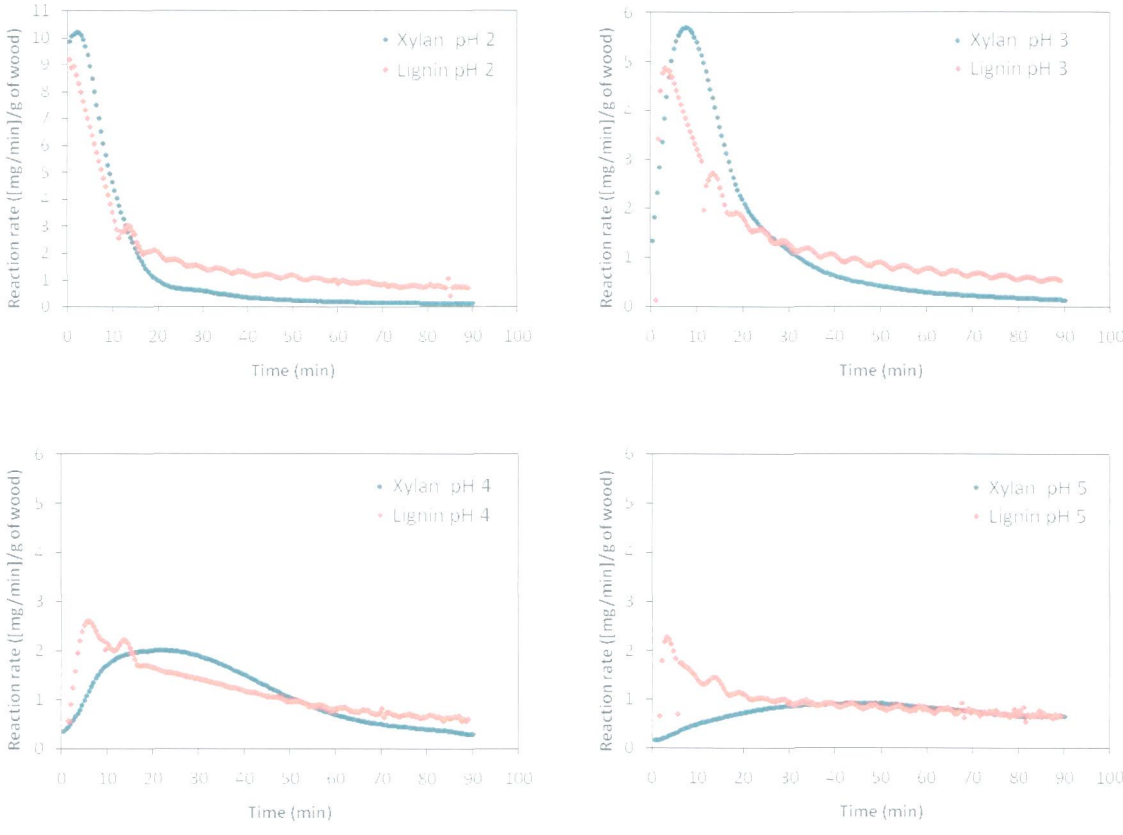

Figure 5.29. Removal rates for xylan and lignin at all four pH conditions.

The removal rates of xylan and lignin are plotted in Figure 5.30 against percentage of respectively xylan and lignin remaining in the wood for all pH conditions. For all pH conditions the xylan removal rate increases initially until about 25% of the original xylan, corresponding to 3.9% of xylan (on original wood), and then follows an approximately linear decreasing rate. As in the case for the temperature effect, lignin removal rate present two different zones which is more evident as the pH decreases. In general, it can be observed that both removal rates of xylan and lignin increase with decreasing pH.

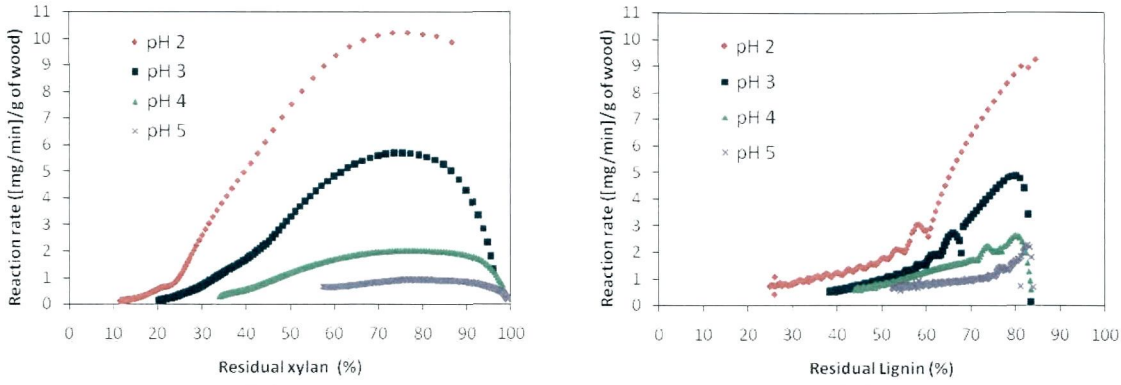

(a) (b)

Figure 5.30. Xylan (a) and lignin (b) removal rates versus their residual concentration in wood.

Extrapolating the final removal rate in Figure 5.30(a) for pH 3 to a value of zero it can be noted that there is a non-removable amount of xylan of around 20% based on the original xylan. This value decreases to 10% at pH 2 and is about 30% at pH 4. At pH 2 there is clear evidence at this stage of extraction of cellulose degradation. One possible mechanism is suggested in the following sections to explain the occurrence of this non-removable xylan based on recent findings of the interactions between cellulose and xylan in the hardwood fibre cell wall.

5.2.4 Conclusions

Effect of temperature

- Xylan shows an S-shape for its concentration profile which is explained by initially slow dissolution of xylan oligomers because they need to be degraded to a lower degree of polymerization (DP) in order to dissolve.
- There is a good agreement between the mass of dissolved organics in the liquid phase when compared with the weight loss of solid wood. Significant differences are found for the minor polysaccharides namely arabinan, galactan, and rhamnan, because of acid degradation during sample preparation.
- Glucan-oligomers (starch) are removed during the early stage of hot water extraction. Glucomannans show a molar ratio glucan/mannan equal to 0.5.
- Degradation of cellulose is observed after 10 minutes extraction at 160°C in 1 g/L acetic acid as solvent concentration. Cellulose degradation starts at an earlier time with increasing temperature.
- Xylan and lignin are the major wood polymers contributing to the total extraction yield. Total yield increases with increasing temperature.
- Two different xylan fractions were identified: lignin-free xylan and lignin-xylan oligomers (LCC). The former dissolves during the early stage of extraction up to a maximum in removal rate, and the later starts dissolving after this maximum has been reached. The total amount of xylan removed up to the maximum rate was found to be temperature independent

- Two different lignin fractions were identified: carbohydrate-free lignin removed early in the process at a high concentration and linearly decreasing to an inflection point when lignin starts dissolving at a much slower rate as LCCs controlled by cleavage of lignin.
- A non-removable xylan was identified which accounted for 18% of the original xylan at temperatures 160-170°C.

Effect of pH

- The concentration of dissolved wood components increases as the pH decreases.
- The contribution to the total extraction yield is mainly coming from xylan and lignin at all pH conditions.
- There is evidence of cellulose dissolution which increases and starts at an earlier time at lower pH. Cellulose degradation starts at pH 5 and increases when decreasing the pH to 3.0.
- Glucomannan present a glucan/mannan ratio of about 0.5 which is more evident when decreasing pH.
- Xylan with a higher degree of acetylation is dissolved during the early stage of water extraction. At low pH values the acetyl/10 xylose units in the small amount of remaining xylan in the extracted wood is similar to that of the original wood.
- The removal rate for lignin and xylan increases with decreasing pH.

- There is a non-removable amount of xylan of around 20% based on the original xylan for pH values from 3. This value decreases to 10% at pH 2 which can be related to additional cellulose degradation.

5.3 Chemical mechanism and rate determining step(s) in hemicellulose removal and kinetics study

5.3.1 Introduction

Our understanding of the chemical mechanism of the removal of wood components from wood by hot water extraction is presently still incomplete. However, some researchers have provided insight into the possible mechanism of the removal of hemicellulose from lignocellulosics with hot water. Conner (1983) proposed the existence of two types of xylan, both of them modeled through first order kinetics in a batch reactor. One fraction could be removed quickly and a second one was removed at a much slower removal rate due to an association with lignin. Wyman and coworkers have done systematic work to understand the mechanism of xylan removal with hot water. In one of these studies a flow-through reactor system was used (Liu and Wyman, 2003) and these results showed that xylan removal rate was affected by flow rate which is inconsistent with intrinsic homogeneous kinetics meaning there are other factors affecting xylan removal. Later, Gray et al. (2007) showed that solubility of xylo-oligomers is affected by their molecular weight (DP) and suggested that solubility of xylan from corn stover is affected by lignin covalently bound to xylan. In a recent study Chen et al. (2010) identified the presence of lignin-carbohydrate complexes (LCC) by gel permeation chromatography analysis of hemicellulose extracts produced from hot water extraction of mixed southern hardwood (SHM) chips in a CMBR system. Chen also identified two types of xylan and proposed two different mechanisms for the removal of

each of them. At the early stage of extraction lignin-free xylan is removed and its dissolution is controlled by the degradation of this xylan by acid hydrolysis until fragments are small enough that so that they become soluble in water. After most of the relatively easy to remove xylan (i.e. lignin-free xylan) is dissolved, the xylan dissolution rate is subsequently determined by the slower rate of cleavage of lignin to which xylan is attached, producing soluble LCC xylan. However, the rates were still affected by diffusional transport of the components out of the wood chips. Therefore, the same continuous mixed batch reactor was used in the present work but now wood-meal was used to study the kinetics of the removal of hemicellulose from hardwood (*Acer rubrum*)

This chapter attempts to develop a more complete mechanism than that proposed by Chen for the removal of wood components from wood by hot water extraction. Also, a modified P_H-factor is proposed to model the effect of pH in addition to time and temperature on the xylan yield during hot water extraction. The main tool to bring new insight in the mechanism used in this chapter is SEC (Size Exclusion Chromatography) applied to the water extracts.

5.3.2 Molecular weight distribution in hemicellulose extracts

Experimental

The extractions were performed on the CMBR system using acetic acid 1 g/L as solvent (pH = 3.2). The extraction temperature was setup at 160°C and samples were collected at three different ranges of time: 0-20 (sample 1), 21-50 (sample 2) and 51-90 (sample 3) minutes. Close to 10 grams of wood meal were placed in the reactor. The flow rate was set at 100 mL/min. The liquid phase was collected in a plastic container and then weighed for each range of time.

A size exclusion chromatography (SEC) system from Viscotek equipped with spectrophotometric (UV-Vis), refractive index (RI), and intrinsic viscosity differential pressure (IV-DP) detectors was used to analyze each sample. For the molecular weight distribution study samples were dissolved in alkali with a final dissolved wood concentration of 10-15 mg/mL. A commercial Birch xylan (Sigma) was also prepared for comparison with a final concentration of 10 mg/mL. Since the UV signal is far more sensitive than the other detectors, such concentrations result into an overshoot of the UV signal. Thus another SEC analysis is performed at dissolved wood concentrations as low as 0.2mg/ml in order to have a readable UV response. A direct calibration was performed using Pullullan standards dissolved in 0.4M NaOH. For method details refer to section 3.2.3.

Molecular weight distribution on wood extracts

The main components in all these three different fractions are xylan and lignin as shown in Tables 5.10 and 5.11. The molar molecular weight distribution analysis was made only on the first two fractions because the dissolved wood concentration was too low in the last fraction (sample 3: 51-90 min). The analysis of sample 1 (fraction 0-20 min, Figure 6.31) shows that there are clear IV-DP and RI signals in the retention time range of 17 and 21 minutes indicating a high concentration of carbohydrates. This portion consists of two distributions: one with a relatively higher molar mass (between 17 and 18 minutes) and the other, which is more dominant, with a relatively lower molar mass (between 18 and 21 minutes). A shallow UV signal is identified in the retention volume range 18 and 19 minutes which indicates a low concentration of high molecular weight lignin which could be part of lignin-xylan oligomers. Also, only RI and UV signals can be observed at a retention time between 21 and 22 minutes, with no IV-DP signal, indicating the presence of free lignin. In a very recent work Lawoko and van Heiningen (2010) have shown that the IV-DP detects only carbohydrates and lignin-carbohydrate complexes (LCC).

Table 5.10. Chemical concentration of wood extract fractions.

Extraction time (min)	Arabinan (mg/mL)	Galactan (mg/mL)	Rhamnose (mg/mL)	Glucan (mg/mL)	Xylan (mg/mL)	Mannan (mg/mL)	Lignin (mg/mL)
Sample 1: 0-20	0.028	0.019	0.012	0.058	0.375	0.049	0.416
Sample 2: 21-50	0.001	0.003	0.004	0.008	0.117	0.012	0.103
Sample 3: 51-90	0.000	0.001	0.003	0.004	0.016	0.003	0.110

Table 5.11. Chemical composition of wood extract fractions based on original dry wood. All values in mg per gram of original wood.

		Arabinan	Galactan	Rhamnose	Glucan	Xylan	Mannan	Lignin	Sub-total
Original wood	(mg/g wood)	8.5	9.4	4.3	441	156	21.1	266	**906.0**
Birch xylan	(mg/g xylan)	12.6	27.2	--	29.5	833	14.7	--	**--**
Extracts	P-factor*								
Sample 1	91	5.8	3.9	2.4	11.8	76.4	10.1	102	**212**
Sample 2	227	0.4	1.0	1.3	2.4	36.7	3.6	39	**84**
Sample 3	408	0.0	0.3	1.1	1.6	6.8	1.2	56	**67**
Sub-total	**--**	**6.2**	**5.2**	**4.8**	**15.7**	**119.9**	**14.9**	**197**	**364**

*This P-factor is calculated with the highest value of time range. Total sugar and lignin yields should sum up previous values for a given P-factor.

Sample 2 (fraction 21-50 min) shows same behavior as the case of sample 1 (Figure 6.32). A carbohydrate-rich portion is eluting first, followed by a free lignin portion and then low molar mass LCC. The RI signal shows a small peak between 17 and 18 minutes which is also observed on the IV-DP signal showing a shoulder. A shallow UV signal is also identified in this sample in the retention time range 18 and 19 minutes which could be part of lignin-xylan oligomers. However, the IV-DP signal in Sample 2 does not exhibit a trimodal distribution as clear as observed in Sample 1.

In general both samples present a similar pattern, with an early peak (Z1), and then an important carbohydrate-rich portion (Z2) followed by a lignin free portion, and finally a low molar mass LCC (Z3). The three zones are indicated on Figures 5.31 and 5.32.

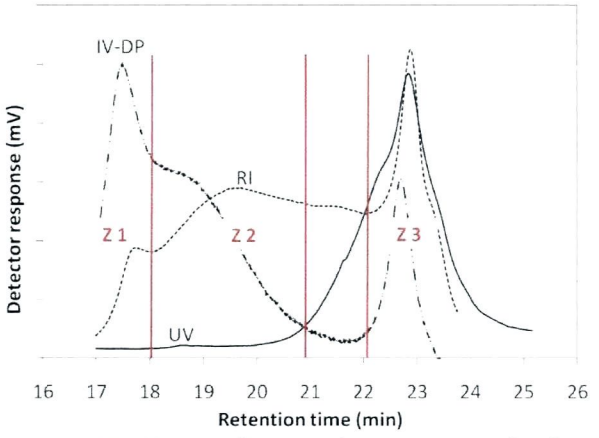

Figure 5.31. Size exclusion chromatography (SEC) analysis for Sample 1.

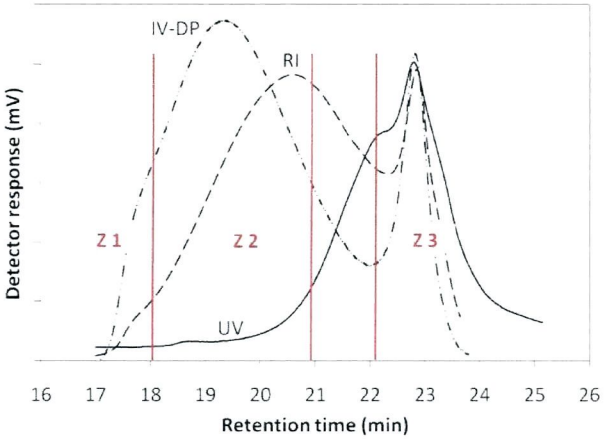

Figure 5.32. Size exclusion chromatography (SEC) analysis for Sample 2.

From the equation of the calibration curve in Figure 3.8, the retention volume in Figures 5.31 and 5.32 can be converted to Log M_W to permit plotting molar mass distributions relative to pullulan standards (Figure 5.33). The absolute molar mass was then determined by applying the relationship

$$M_W = \frac{\sum_i A_i \cdot M_i}{\sum_i A_i} \qquad \text{Equation 5.15}$$

where M_W and M_i are the average molecular weight and molecular weight at each retention volume respectively and A_i is the area under the chromatogram between each retention volume interval. The DP was determined relative to that of a xylose unit (132 g/mol)

Figure 5.33 shows the normalized RI signal for samples 1 and 2, and also for commercial Birch xylan (Sigma). The three zones are also indicated here (Z1, Z2, and Z3). The average degree of polymerization ($\overline{DP}$) was determined using Pullulan standards for calibration and the results are shown in Table 5.12. Also, the DP was determined for each zone on both samples.

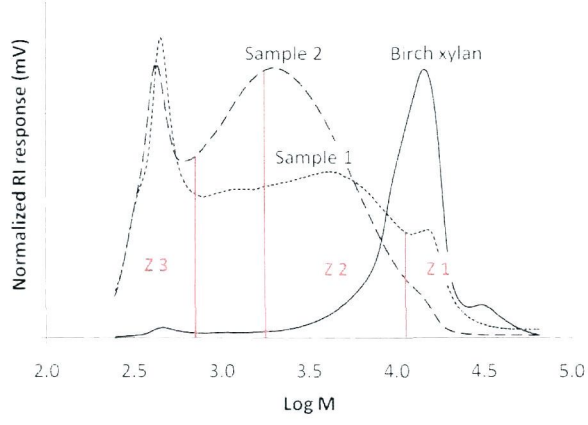

Figure 5.33. Molar Mass Distributions of the samples relative to pullulan standards.

Table 5.12. Molar Mass (Mw) of studied samples

Sample ID	$\overline{Mw}$	$\overline{DP}$	DP_{Z1}	DP_{Z2}	DP_{Z3}
Birch xylan	13,735*	104			
Sample 1	3,953	30	130	38	4
Sample 2	2,660	20	115	34	3

*Literature value is 16500 for birch glucuronoxylan (Teleman, 2009).

The four major components in Sample 1 are lignin, xylan, glucan and mannan (Table 5.11). The total and monomeric composition for these polysaccharides was determined in a different experiment at the same conditions than those for samples 1 and 2 (Figure 5.34). The results show that all three polysaccharides are mainly in the form of oligomers. Based on the recent work of Tunc and van Heiningen (2010) it is concluded that the high molecular weight peak at Z1 is related to starch.

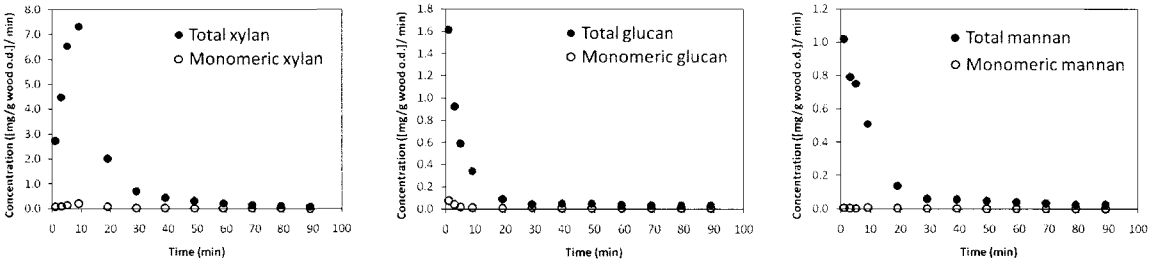

Figure 5.34. Total and monomeric concentration for xylan, glucan, and mannan during water extraction (1 g/L acetic acid, pH 3.2, and 160°C)

Chen (2009) studied the hot DI water extraction of a mixture of southern hardwoods (SHM) chips using the CMBR system. He concluded that lignin free xylan is extracted during the first 40 minutes of the extraction at 160°C (flow rate of 60 mL/min), which corresponds to the time when the maximum xylan concentration is reached, and he also found that the xylan oligomers will not dissolve until the DP is reduced to below 25. Sample 1 in the current work has a DP of 38 for the carbohydrate-rich fraction (zone Z2) and the concentration of xylan in this sample is 76.4 (mg/g odw), i.e. almost 50% of the original xylan in wood, which is almost the same as found by Chen et al. (2010). However, the extraction conditions in the present work are different: wood

meal; solvent 1 g/L acetic acid solution (pH 3.2); flow rate of 100 (mL/min); wood specie red maple. Deionized water was used on Chen's study and a flow rate of 60 (mL/min). It is interesting to notice that although the pH used in the current study was slightly acidic the DP value for xylan (38) is higher than of Chen (22). However, Chen was using wood chips so that the xylo-oligomers could degrade further during the time when diffusing out of the wood structure before being flushed out of the CMBR. This could explain at least partially the difference in DP values.

5.3.3 Solubility of hemicellulose extracts

Experimental

Three samples were collected from one extraction performed on the CMBR system using acetic acid 1 g/L as solvent. Final concentration of the different samples is shown in Table 5.11.

Different amounts of water were evaporated consecutively from each sample at 50°C using a vacuum rotary evaporator. The reduced volumes were recorded and the turbidity was determined at the different new concentrations (room temperature). Turbidity is a measurement of the amount of light scattered by suspended particles and is typically reported as NTU (nephlometric turbidity units) and increases with solid concentration but near the saturation point it increases exponentially. Saturation point is defined as the point at which no more solute can be dissolved in a solution. The

saturation point depends on the temperature of the liquid as well as the chemical nature of the substances involved.

Solubility of wood components

Table 5.13 shows the initial concentration for xylan, lignin, and the total amount corresponding to the sum of both polymers. The turbidity values are given for the initial concentration of each sample. It can be observed that turbidity increases with concentration, as expected. Figure 5.35 depicts the change in turbidity values as the concentration of the solution is increasing. It can be noted that turbidity for sample 1 (0-20 min) increases quickly with increasing concentration indicating that the saturation point is close to the initial concentration (0.9 mg/mL at room temperature) of the sample. Figures 5.36 and 5.37 depict the effect of the xylan and lignin concentration effect on the turbidity respectively. Both wood polymers show the same behavior due to the fact that they have similar initial concentrations.

Table 5.13. Initial concentration and turbidity for xylan and lignin in extract fractions.

Sample	Xylan (mg/mL)	Lignin (mg/mL)	Total (mg/mL)	Turbidity (NTU)
Sample 1: 0-20 min	0.38	0.50	0.88	45.8
Sample 2: 21-50 min	0.12	0.12	0.24	6.4
Sample 3: 51-90 min	0.02	0.13	0.15	2.4

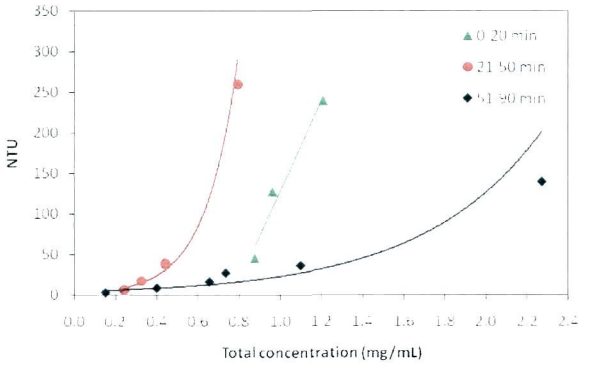

Figure 5.35. Effect of total wood polymers concentration on wood extracts turbidity.

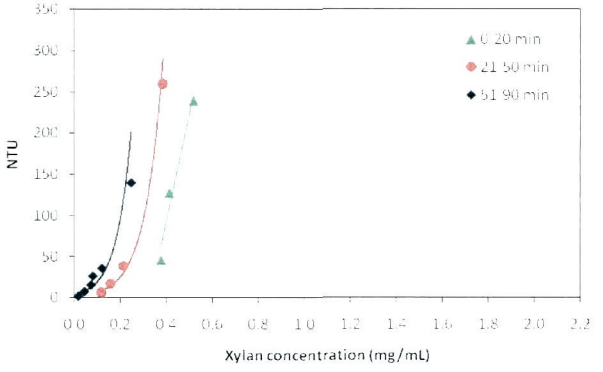

Figure 5.36. Effect of xylan concentration on wood extracts turbidity

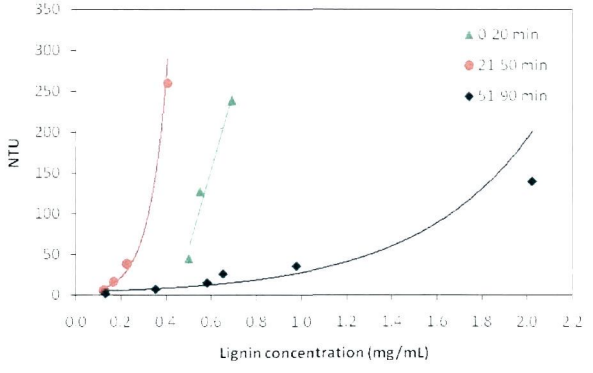

Figure 5.37. Effect of lignin concentration on wood extracts turbidity

The saturation point can be estimated as the concentration value where a deflection occurs on the curve of turbidity versus concentration (Table 5.14). Sample two shows a saturation point lower than that for Sample 1 with a value around 0.5 mg/mL. Now, the saturation points for xylan and lignin estimated from Figures 5.36 and 5.37 is the same for both wood polymers and half of that for the total concentration; this is because the initial concentration is the same for both polymers. It is interesting to notice that the saturation point is in general lower for Sample 2 compared with Sample 1 because the $\overline{DP}$ of Sample 1 (30) is higher than that for Sample 2 (20) (Table 5.12). Sample 1 has a higher amount of lignin-free xylan than Sample 2 which has a higher proportion of lignin-xylan oligomers. This difference in chemical structure leads to a different response in solubility. Sample 3 corresponds to LCC and shows the highest value for the saturation point (around 1.6 mg/mL). This means wood polymers have been further degraded to lower DP values. The saturation point in this sample is determined by lignin because xylan concentration is very low in this sample and this is covalently bond to lignin.

Table 5.14. Estimated saturation point values.

Sample	Total (mg/mL)	Xylan (mg/mL)	Lignin (mg/mL)
Sample 1: 0-20 min	0.8-1.0	0.4-0.5	0.5-0.6
Sample 2: 21-50 min	0.5	0.3	0.3
Sample 3: 51-90 min	1.6	0.1	1.3

The present solubility analysis shows that the solubility of xylan is highly affected for lignin, which can be covalently bound to xylan.

5.3.4 Possible chemical mechanism and rate determining step(s) in hemicellulose removal using DI-water

Effect of temperature

From Figure 5.21 it is possible to observe clearly two different behaviors for lignin removal rate at all three temperatures studied. The removal rate for lignin starts from a high value decreasing rapidly until a point of inflection is reached. This inflection point occurs exactly when the xylan removal rate also slows down at 160 and 170°C. At the lowest temperature condition (150°C) this is not that evident; now the inflection point occurs close to the maximum xylan concentration. Chen et al. (2010) concluded that lignin-free xylan is removed during this initial step and thus this lignin must be carbohydrate-free. These two different behaviors for lignin removal rate must correspond to different mechanisms of lignin degradation. It has been shown that mild acid conditions with acetic acid are effective enough to cleave the labile benzyl ether bonds (α-O-4) and preserve the propane side chains and β-O-4 linkages without condensation under formation of new C-C bonds (Fengel and Wegener, 1984). Therefore, the high lignin removal rate portion may correspond to acid cleavage of (α-O-4) lignin bonds. The second part showing a slow lignin removal rate is almost not affected by temperature (Figure 5.22(b)) meaning the reaction order is the same for all

three temperatures. β-aryl ether bonds are the major ether bonds found in lignin (Sjöström, 1993) and they are rather stable under acidic conditions (Sixta, 2006). Therefore, it is proposed that lignin removal during this second step is not controlled by a chemical reaction mechanism but more likely by a physico/chemical mechanism, i.e. by solubility. During the first step acid degradation occurs cleaving labile benzyl ether bonds (α-O-4). This step corresponds to an acid hydrolysis mechanism which is known to be temperature dependent so when the temperature increases the fast initial removal rate of lignin also increases. Then, during this second phase, lignin fragments formed during the acid degradation step dissolve slowly. Lawoko (2005) also concludes that two different forms of lignin are present in the wood fibre wall, with one linked to xylan and consisting largely of β-O-4 structures and having a rather linear structure. So it is proposed that this fraction of lignin bound to xylan oligomers is representing the lignin which is removed in the second phase. This is also in agreement with results of Chen et al. (2010).

The xylan removal rate is plotted against its residual content in wood (Figure 5.38). The xylan removal rate shows a maximum at all three temperatures, but the maximum is located at a lower residual xylan content and increases in magnitude at increasing temperature. The increasing removal rate data starting from 100% residual xylan follows approximately a straight line for all temperature conditions as depicted in Figure 5.38. This means that the removal of this fraction has the same reaction order for all temperatures. Then, it is proposed that the removal of this fraction is mainly due to solubility. Also important is that a higher amount of this xylan fraction is obtained by

increasing temperature from around 20% at 150°C to 60% at 170°C. This agrees with a literature study on the solubility of hemicellulose oligomers showing an increase with increasing temperature (Gray et al., 2003). After the maximum removal rate value is reached lignin is sufficiently degraded and lignin-xylan oligomers start to dissolve. Also, because of the slightly acid conditions cleavage of lignin-xylan bonds also take place. The cleavage of LCC bonds in acidic conditions has been demonstrated by Lawoko (2005). Near the end of the xylan removal rate peak in Figure 5.38 an inflection is observed which coincides with the beginning of the second part of lignin degradation discussed previously. Thus it is proposed that this final xylan removal rate period is due to lignin dissolution with xylan attached to it through lignin-xylan bonds. It is also noted that there is a non removable amount of xylan amount which is around 18% of the original xylan at 160 and 170 °C, and about 25% at 150 °C.

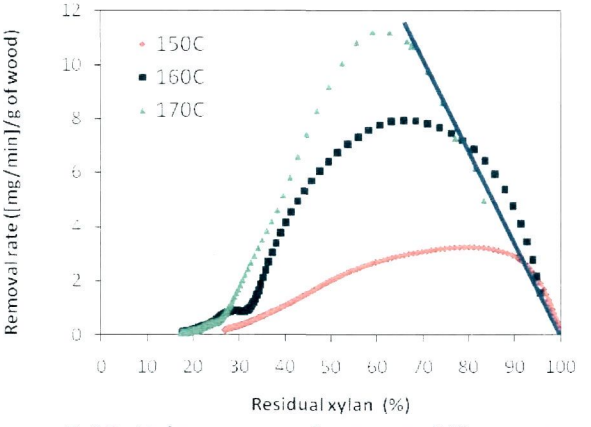

Figure 5.38. Xylan removal rate at different temperatures.

Effect of *pH*

Figure 5.30(b) depicts the lignin removal rate versus residual lignin content in wood. It can be seen that the lignin removed in the second phase as described previously is pH dependent. Since the initial phase of lignin removal is thought to be controlled by acid hydrolysis it is expected that this lignin removal is also pH dependent. For the second phase one reasonable explanation is that at high pH values acid hydrolysis slow down and then a longer time is required for the cleavage of labile benzyl ether bonds, and thus the dissolution of lignin fragments. By lowering the pH the hydrolysis speeds up and the removal rate curve at pH 3 for the second part of lignin removal becomes parallel to that at pH 2. This means that the proton concentration is only affecting the first phase of lignin degradation at pH values lower than 3 and then the mechanism of dissolution of lignin becomes controlled by solubility.

The xylan removal rate is depicted in Figure 5.30(a) versus its residual content in wood. The removal rate exhibits a maximum for all pH conditions and it is located at around the same xylan residual concentration for all pH (25% xylan removal). The removal rate shows a high pH dependence increasing with decreasing pH. A logical explanation for this behavior is that xylan dissolves only after it is degraded to a low enough DP value because high DP xylan oligomers have a low solubility. The first phase of xylan removal is based on the cleavage of glycosidic bonds by acid hydrolysis. This requires the presence of protons and thus a low acidity leads to a lower removal rate.

As discussed for the temperature effect in previous paragraphs it is proposed that after most of lignin-free xylan has been dissolved (maximum in removal rate) xylan

starts dissolving as lignin-xylan oligomers but also cleavage of LCC bond can take place. In wood, three main types of lignin carbohydrate linkages have been suggested: benzyl ester, benzyl ether, and phenyl glucosidic types (Fengel and Wegener, 1984). Lawoko (2005) studied the susceptibility of the latter two structures to acid hydrolysis by using model compounds. He found that both structures can be hydrolyzed and that the benzyl ether structure was more stable than the phenyl glucoside.

It was shown in section 5.2.4 that cellulose is degraded significantly at pH 2 and 3. This was evident after 20 minutes of extraction for pH 2 and after 30 minutes for pH 3 (Figure 5.26). However, cellulose chains are degraded before glucan dissolves. This can be inferred from the scission number (S) in Table 5.8 for pH 4 and 5. Also, from Figure 5.26 is possible to deduce that the degree of cellulose degradation at pH 2 is much larger than that at pH 3. The residual xylan after 20 minutes of extraction is about 23% and after 30 minutes about 36% at pH 2 and 3 respectively (Figure 5.24). From Figure 5.30 it is clear that there is a non-removable xylan of around 20% extrapolating curves at pH 3, 4, and 5 to a reaction rate value of zero. However, at pH 2 there this non-removable xylan decreases to a value of around 10%. It is suggested that this non removable amount of xylan is associated strongly with cellulose and is difficult to remove. A higher yield of xylan dissolution beyond this point could be achieved only through a large extent of cellulose degradation.

A very close association between cellulose and glucurono-xylan (GX) has been recently proposed (Reis and Vian, 2004) where cellulose and xylan associate with each other forming a cellulose/GX composite, which is charged and highly anisotropic as a

consequence of the carboxylic groups of the glucuronoxylans. This close association can explain the behavior previously discussed. Figure 5.39 taken from Dammström et al. (2009) work shows three types of xylan: glucuronoxylans tightly coated to the surface of cellulose microfibrils, free xylan, and xylan attached to lignin by LCC bonds.

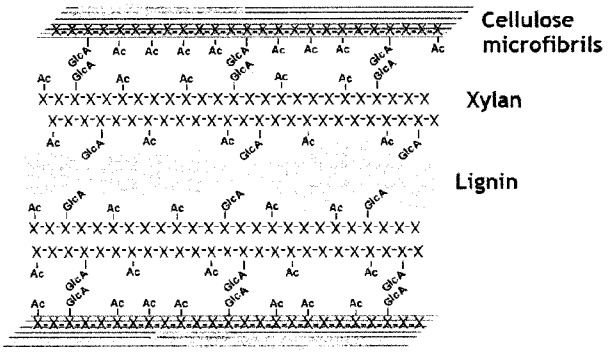

Figure 5.39. Model for the arrangement of cellulose, xylan, and lignin in the secondary cell walls of aspen wood (Dammström et al. 2009).

Effect of molecular weight distribution

Table 5.15 shows a comparison between the parameters and results obtained from the extraction of hemicelluloses performed in batch and CMBR systems. Wood strands were used for the water extractions performed on the batch system while wood meal was used on the CMBR system. The important difference on the range of degree of polymerization (DP) between the two extraction systems being 3-4 times larger for the CMBR system (DP_{Z2}corresponds to a carbohydrate-rich portion and DP_{Z3} to lignin-xylan oligomers or LCC) is immediately obvious. The amount of xylan removed at comparable P-factor values is also higher for the case of the CMBR system. At a P-factor of 227 hrs. the amount of xylan removed in the CMBR system was 4.7 times higher than that for the

batch system at a comparable P-factor of 204 hrs. (also 4.6 times higher when using wood strands on the CMBR system). For a P-factor of 408 hrs. the amount of xylan removed was 1.6 times higher in the CMBR system (practically the same when using wood strands). Even though the pH in the CMBR system was lower during the total length of the extraction, the DP values are much higher than those for the batch system. This can be partially explained because after dissolution of xylo-oligomers in the batch system they can further degrade to shorter chains while in the CMBR system the dissolved xylo-oligomers are flush out from the reactor and immediately cooled down avoiding further degradation. However, special attention should be given to the liquid to wood ratio (L/W) which can be a key factor for xylan dissolution. The values of L/W for the CMBR system are about 3 orders of magnitude higher than those for the batch system.

On the other hand, the amount of lignin removed in the batch reactor system is much lower than that removed in the CMBR system. For a P-factor of 204 hrs. 5% of the original lignin has been removed in the batch system while at a P-factor of 227 hrs. 53% (42% for wood strands) was removed in the CMBR system. At a P-factor of 408 hrs. the CMBR system removes 6.8 (4.6 for wood strands) times more lignin than in the batch system. When considering now the xylan to lignin ratio it can be noted how different this ratio is for both systems. For the batch system the xylan/lignin weight ratio increases from 1.7 to 3.9 with P-factor increasing from 200 to 900, while the xylan/lignin weight ratio in the CMBR system is about 0.7 from 90 to 210 P-factor. At a P-factor of 896 hrs. the amount of xylan removed in the batch reactor is 150% higher

than that at a P-factor of 408 hrs.; however, the amount of lignin remains almost unchanged. In addition, the DP value at a P-factor of 896 hrs. was 6 in the batch system while for a similar xylan yield (P-factor of 227 hrs.) the DP of carbohydrate-rich portion in the CMBR system was 34 and that for the LCC fraction was 3. A reasonable explanation for results in the batch system (L/W ratio 3) is that lignin has a much lower solubility than xylan and it is known that a significant amount of lignin is covalently bound to xylan (Lawoko and van Heiningen, 2010). Therefore, xylan remains in the wood until it is degraded to short enough oligomers which are soluble in the solution. This explains the low concentrations for xylan in the batch system compared with the CMBR system (P-factor of 204 and 408 hrs.). In order to increase the xylan yield lignin-xylan oligomers needs to degrade to lower DP xylan fragments with high enough solubility to compensate for the limited solubility of the attached lignin. This explains the high xylan concentration (117 mg/g wood) with a small DP (6) and low lignin concentration (30 mg/g wood) at the highest P-factor (896 hrs.) in the batch system. As observed in Figure 5.12 carbohydrates are located in the low molecular weight region where most of LCCs are present. On the other hand, a higher L/W ratio in the CMBR system enhances lignin solubility resulting in higher amounts of lignin removed and larger lignin-xylan oligomers released into solution. This explains the larger values in terms of concentration and DP shown in Table 5.15 for the CMBR system. Also, a shallow UV peak is observed on Figures 5.60 and 5.61 for a retention time of 18-19 minutes where a high IV-DP signal is located indicating the presence of large lignin-xylan oligomers (LCC) which confirm the proposed mechanism.

Table 5.15. Comparison of results for the removal of xylan an lignin on two different systems (batch and CMBR).

Reactor (wood material)	Temperature (°C)	Time (min.)	P-factor (hrs.)	Lignin* (mg/g odw)	Xylan* (mg/g odw)	$\frac{\text{Xylan}}{\text{Lignin}}$	DP	Final pH	L/W
Batch	160	45	204	14	24	1.7	13	3.9	3
(wood strands)	160	90	408	29	76	2.6	9	3.5	3
	170	90	896	30	117	3.9	6	3.5	3
CMBR	160	20	91	102(73)	76(58)	0.7(0.8)	DP_{Z2}: 38	3.2	200
(wood meal)							DP_{Z3}: 4		
	160	50	227	141(111)	113(111)	0.8(1.0)	DP_{Z2}: 34	3.2	500
							DP_{Z3}: 3		
	160	90	408	197(134)	120(121)	0.6(0.9)	--	3.2	900

*Results in parenthesis correspond to extractions with wood strands.

Solubility of hemicellulose extracts

The xylan concentration in the extract produced using the batch reactor system was around 40 mg/mL at the severest condition (170°C and 90 minutes) and its average degree of polymerization was 6. At a milder condition (160°C and 45 minutes) the xylan concentration was around 10 mg/mL and its average DP was 13. These concentrations are one order of magnitude higher than the saturation points estimated for xylan dissolution (Table 5.14) which then explains the much lower DP values of the dissolved xylan in the batch reactor as compared to that dissolved in the CMBR. This agrees with results found by Gray et al. (2007) who conclude that L/W ratio during the extraction of hemicelluloses from wood by hot water has a significant effect on xylose recovery.

Possible mechanism for xylan dissolution by hot water

Xylan dissolution is a very complex process which is affected by many factors: temperature, pH, solubility, lignin-xylan bonds, and physical association with cellulose. Based on all points discussed above the following general mechanism is proposed for xylan dissolution by hot water:

i. Hydronium ions randomly attack xylan glycosidic bonds and acid degradable lignin breaking down the heterogeneous polymer structure of the fibre cell wall. However, because of a very low solubility of high DP oligomers, free xylan only dissolves after they are degraded to a low DP value.

ii. Because hydrolysis is a random process it takes time before a significant amount of low DP xylo-oligomers are formed, explaining the initial increase in xylan dissolution rate with time. The liquid to wood ratio (L/W) used in the reactor system determines the degree of polymerization necessary for xylan dissolution. At high L/W ratios the xylan removal rate will be mostly controlled by the solubility of xylo-oligomers which can be enhanced by increasing temperature. However, at low L/W ratio (3-4) the removal rate will be controlled by hydrolysis of xylo-oligomers.

iii. Because lignin has a much lower solubility than xylan, xylan that is attached to lignin through LCC bonds would need to be degraded to a lower DP to compensate for the lower solubility of the attached lignin fragments or to break free from the lignin. Thus the removal rate of xylan as part of LCCs is then determined by the low solubility of lignin-xylan oligomers in water.

iv. Because of pore diffusion limitations of the wood polymers being dissolved, the dissolution rate of free xylan and lignin-xylan oligomers will be slower as the wood particle size increases.

v. Acetyl groups are released from the dissolved acetylated xylan forming acetic acid and producing a drop in pH to around 3.5. High temperatures and long extraction times will lead, at these conditions, to cellulose degradation thereby breaking the close association between cellulose and xylan and thus decreasing the unremovable xylan level.

5.3.5 Modeling xylan dissolution from hardwood by DI-water

The P-factor approach will be used to model the xylan yield because its simplicity and ease of implementation is practical for process control. The expression of P-factor has been previously proposed to control the water prehydrolysis process (Sixta, 2006). The expression for this factor is:

$$P_{factor} = \int e^{\left(\frac{E_a}{R \cdot 373.15} - \frac{E_a}{RT}\right)} dt \qquad \text{Equation 5.16}$$

where E_a is the activation energy for cleavage of glycosidic bonds, in $\frac{J}{mol}$

R is the gas constant, 8.314 $\frac{J}{mol\,K}$

T is the temperature in Kelvin, K

t is the time in hours

Effect of temperature

A kinetic analysis is performed on the xylan which dissolves after the maximum dissolution rate is obtained, and for which the dissolution rate follows approximately a straight line (Figure 5.22(a)), and represents about 40-45% of the xylan in wood. Also, as was mentioned previously none of these straight lines pass through zero meaning there is a non-removable amount of xylan. By extrapolating to rate zero it is found that the non removable portion of xylan is about 18% or 28.1 mg/g wood at 160 and 170 °C. Correcting for this non-removable xylan portion for a first order reaction it is possible to write the following expression for the loss of xylan from wood:

$$r_{xy} = k \cdot e^{\frac{-E_a}{RT}} \cdot C_H^n \cdot (C_{xy} - 28.1) \qquad \text{Equation 5.17}$$

where r_{xy} is the rate of xylan dissolution, [mg/min]/g of wood

k is the reaction rate constant, min^{-1} $[mol/L]^{-n}$

E_a is the activation energy, J/mol

R is the gas constant, 8.314 J/mol K

T is the temperature, K

C_H is the concentration of protons, mol/L

n is reaction order with respect to C_H

C_{xy} is the fraction of residual xylan in wood, mg/g of wood

At a constant pH condition (3.2) C_H^n would be a constant. Then, at a fixed temperature T_1 if r_{xy} is plotted versus $(C_{xy} - 28.1)$ the slope m_1 would be equal to $k \cdot e^{\frac{-E_a}{RT_1}} \cdot C_{H1}^n$. At a different temperature but the same pH extraction condition the

slope m_2 would be equal to $k \cdot e^{\frac{-E_a}{RT_2}} \cdot C_{H2}^{n}$ (Figure 6.40). Thus, it is possible to plot $\ln(m)$ versus $\frac{1}{\mathrm{T}}$ (Figure 5.41), and the slope of the curve is equal to the value of $\frac{-E_a}{R}$. By this analysis it was found that $E_a = 120.2\ kJ/mol$. A higher value of $125.6\ kJ/mol$ has been suggested for the P-factor (Sixta, 2006). However, this value was probably determined on a system with a low liquid to wood ratio where the xylan removal rate is controlled by the hydrolysis of the glycosidic bonds. In the present CMBR study the dissolution of xylan is controlled by the solubility of xylo-oligomers because a much larger L/W ratio is used during the extraction. In addition, the higher activation energy of $125.6\ kJ/mol$ does not take into consideration the effect of pH which is changing during the process.

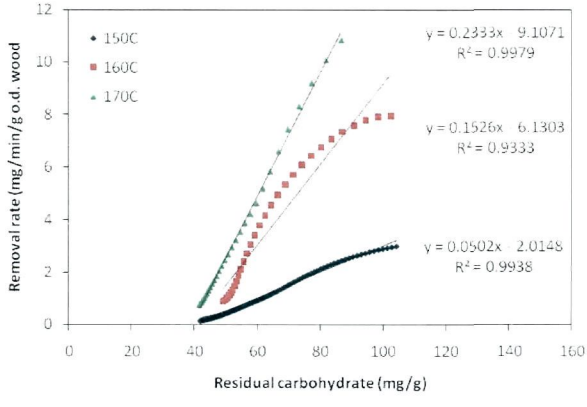

Figure 5.40. Xylan removal rate at different temperatures versus its residual concentration in wood.

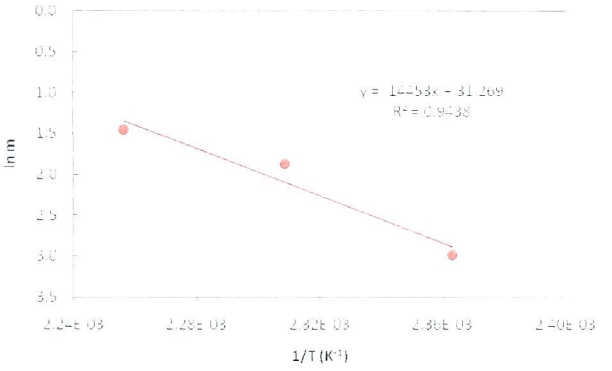

Figure 5.41. Determination of the activation energy for the cleavage of gycosidic bonds in xylan.

Effect of pH

The effect of pH on the kinetics is also studied for the portion of xylan which is removed after the maximum removal rate value is reached and then decreases linearly with decreasing xylan content in wood (Figure 5.30(a)). The non removable portion of xylan determined by extrapolating to rate zero was about 20% or 31.2 mg/g wood. Again for a first order reaction is possible to express the loss of xylan from wood as:

$$r_{xy} = K_{xy} \cdot C_H^n \cdot (C_{xy} - 31.2) \qquad \text{Equation 5.18}$$

where r_{xy} is the rate of xylan dissolution, [mg/min]/g of wood

K_{xy} is the overall hydrolysis rate constant for xylan removal,

C_H is the concentration of hydronium ions, mol/L

n is reaction order with respect to C_H

C_{xy} is the fraction of residual xylan in wood, mg/g of wood

If at a constant pH_1 condition r_{xy} is plotted versus $(C_{xy} - 31.2)$ the slope m_1 would be equal to $K_{xy} \cdot C_{H1}^{n}$. At a different constant pH condition and same extraction temperature the slope m_2 would be equal to $K_{xy} \cdot C_{H2}^{n}$. Thus, by plotting $\ln(\frac{1}{m})$ versus $\ln(\frac{1}{C_H})$, the slope of the straight line is equal to the reaction order . By doing so it was found that $n = 0.45$ (Figure 5.42).

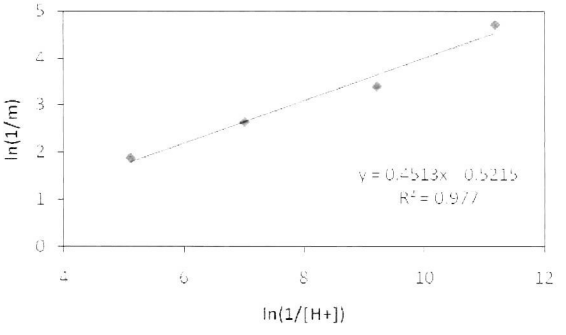

Figure 5.42. Determination of the reaction order with respect to the proton concentration.

Modeling the xylan yield with the P-factor approach

Figure 5.43 depicts the xylan yield as a function of the P-factor for pH (a) and temperature (b), using the activation energy value determined in this study (120.2 kJ/mol). The expression for the P-factor for isothermal conditions is:

$$P_{factor} = e^{\left(38.74 - \frac{14,458}{T(K)}\right)} \cdot t(hr) \qquad \text{Equation 5.19}$$

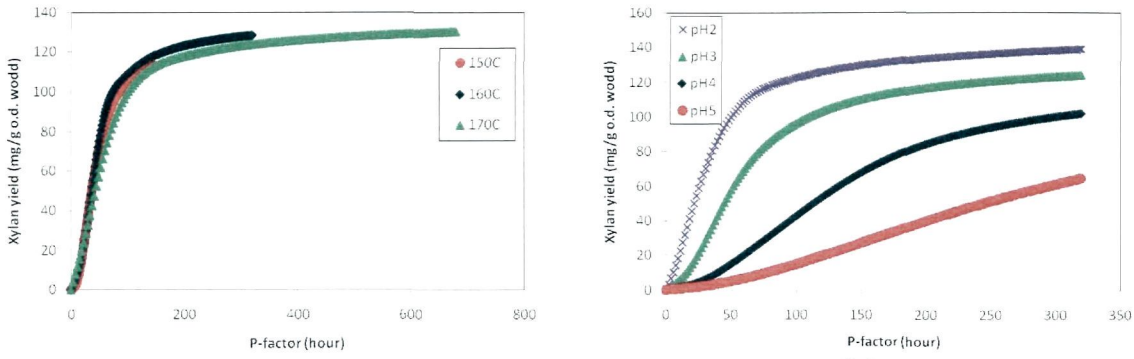

(a) (b)

Figure 5.43. Xylan yield versus P-factor for the temperature (a) and pH effect (b).

This expression (Equation 5.20) does not take into account the effect of pH. Therefore the expression is modified by including the earlier determined reaction order in proton concentration as:

$$P_H = e^{\left(38.74-\frac{14,458}{T(K)}\right)} \cdot \frac{C_H^{0.45}}{C_{3.5}^{0.45}} \cdot t(hr) \qquad \text{Equation 5.20}$$

The proton concentration has been divided by the concentration of protons at a pH value of 3.5, which was taken as reference level. This pH value was chosen also because this is the final pH during extraction in a batch system.

Figure 5.44 depicts now the xylan yield versus the modified P_H-factor which collapses all data into one single curve for all temperatures and pHs studied. Thus the P_H-factor now includes the effect of pH in addition to the effect of temperature and time. It should also be noted that at the most severe temperature condition (170°C) the value was much higher (1,100 hrs.) than for the unmodified expression (700 hrs.) and this is mainly due to the pH effect.

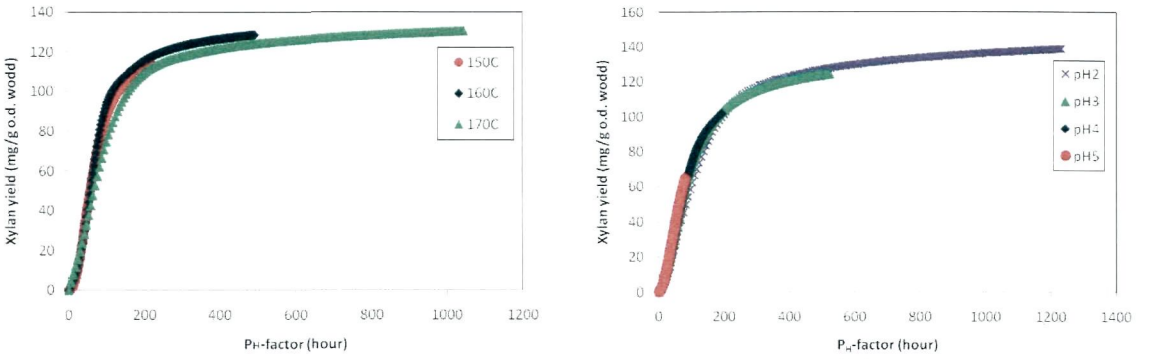

(a) (b)

Figure 5.44. Xylan yield versus the modified P_H-factor for the temperature (a) and pH effect (b).

Figure 5.45 displays the xylan yield for temperature and pH effects versus the modified P_H-factor. It can be observed that all data now are described by a single curve demonstrating that the proposed modified expression for the P-factor can be a useful and practical model for industrial scale process control. However, this modified factor does not include the effect of pore diffusion when increasing the wood particle size.

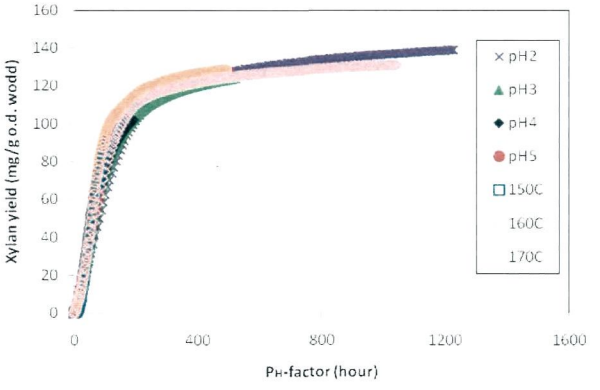

Figure 5.45. Xylan yield versus P_H-factor for the temperature and pH effect.

5.3.6 Conclusions

Molecular weight distribution in hemicellulose extracts

- High molecular weight glucan oligomers were identified (DP 130) as starch. These oligomers are degraded with increasing extraction time.
- A second carbohydrate- fraction free of lignin is identified having a lower DP (38) which is also degraded to lower DP with extraction time.
- A fraction with a low DP of about 3-4 is identified as dissolved lignin-carbohydrate complexes.

Solubility of hemicellulose extracts

- The dissolved wood polymers produced during the early stage of extraction (first 20 minutes) are close to the saturation point (0.8 to 1.0 mg/mL) showing that solubility is controlling wood dissolution at this stage.
- The wood polymers dissolved at a later stage (21-50 minutes) the saturation point decreases to a value around 0.5 mg/mL most probably because high molecular weight LCC begin to dissolve which have a lower solubility than the lignin-free hemicelluloses which dissolve during the initial phase.
- Wood polymers dissolved during the latest stage of the extraction (51 to 90 minutes) show the highest value for the saturation point (around 1.6 mg/mL) which means they have been further degraded to lower DP values thereby increasing their solubility.

Possible chemical mechanism and rate determining step

- The lignin removal rate show two different regimes each representing a different mechanism. It is proposed that during the first phase of extraction lignin fragments are dissolved following acid hydrolysis of α-O-4 ether linkages in the lignin. Since this process in controlled by chemical kinetics, the lignin removal rate during this phase is dependent on the temperature and pH. Lignin removal during the second phase is not controlled by chemical reaction mechanism but more likely by a physico/chemical mechanism, i.e. by solubility.
- The removal of xylan exhibits three different phases. It is proposed that the initial removal of xylan is mainly controlled by solubility of lignin-free xylan-oligomers formed after acid hydrolysis of xylan in the wood. The second phase of xylan dissolution occurs after the removal rate maximum is reached and lignin has been significantly degraded. Then lignin-xylan oligomers start to dissolve and also cleavage of lignin-xylan bonds takes place. The last phase of xylan dissolution is related only with dissolution of lignin-xylan complexes. About 20% of the original xylan cannot be removed when extracting with hot water in the range of pH 3-5. Only when the extraction severity in terms of temperature, time and acidity are so high that cellulose is significantly hydrolysed this resistant final xylan may be removed.
- The liquid to wood ratio (L/W) highly affects the solubility of both xylo-oligomers and lignin. The removal rate of the lignin-free xylan fraction is controlled by

solubility when the extraction is performed at a high enough L/W ratio. On the contrary, when a low L/W ratio is used (3-4) the removal rate of this xylan fraction is controlled by acid hydrolysis of xylan. The removal rate for the fraction of xylan covalently attached to lignin is controlled by lignin solubility.

- A modified P_H-factor is proposed which incorporates the effect of acidity in addition to time and temperature on xylan removal during hot water extraction of hardwood.

CHAPTER

6 SUMMARY OF CONCLUSIONS AND RECOMMENDATIONS FOR FUTURE WORK

6.1 Conclusions

6.1.1 Removal of wood components from OSB strands by hot water in a batch reactor

- Xylan is the dominant component contributing to the total dissolved yield of wood polymers, and is present mostly in the form of xylo-oligomers. Lignin only contributes 3% (on wood) to the total yield at the severest autohydrolysis condition (P-factor of 896 hrs.).
- Residual cellulose concentration in solid phase stays intact at all P-factor values due to its high molecular weight and crystalline nature.
- The total uronic acid group content in extracted wood decreases by about 83% at the severest condition (P-factor of 896 hrs.). This mass loss is probably due to decarboxylation of the uronic acids.
- The sum of the mass of the individual major wood components, cellulose, lignin and xylan, quantified in the extract and extracted wood at all P-factor conditions, are in fair agreement with the corresponding mass in the original wood.

- Minor wood components show larger differences mass balance closure probably due to underestimation of their content in original wood because of acid degradation during sample preparation.
- A high molecular weight, lignin-free, gluco-oligomeric fraction dissolved during the initial phase of autohydrolysis is identified as starch. This fraction decreases with increasing P-factor due to acid hydrolysis and increasing dissolution of other wood polymers.
- Carbohydrate-free lignin, lignin-free carbohydrates, and lignin-carbohydrate complexes (LCCs) were the three different fractions identified in the extract by GPC analysis. A maximum DP value of 17 (calculated as anhydro-xylose) was determined at a P-factor of 89 hrs.
- Kappa number and pulp yield decrease between 50-75% and about 10% at the most severe extraction condition (P-factor 408 hrs.) respectively when performing alkaline cooks on extracted wood. Cellulose and xylan mass fractions on pulp decrease 1.5-10% and 7% respectively at the same condition. Also, DP of cellulose decreases from 5,000 to 3,000 at the highest P-factor. This is evidence of lignin and carbohydrate degradation.
- The DP of cellulose in wood decreases with increasing P-factor values on the hot water extraction of wood strands.

6.1.2 Intrinsic kinetics of removal of wood components from hardwood (*Acer rubrum*) by hot water extraction in a continuous mixed batch reactor (CMBR)

- Xylan dissolution shows an S-shaped concentration profile which is caused by initially slow dissolution of xylan oligomers because they need to be degraded to a lower degree of polymerization (DP) in order to become soluble.
- There is good mass balance when comparing the dry solids in the liquid phase with the weight loss in wood. Major differences in mass balance are found for the minor polysaccharides namely arabinan, galactan, and rhamnan, probably because underestimation of their content in original wood due to acid degradation during sample preparation.
- Gluco-oligomers (starch) are removed during the early stage of hot water extraction. The dissolved glucomannans have a glucan/mannan molar ratio of 0.5.
- Xylan and lignin are the major wood polymers contributing to the total extraction yield. Total yield increases with increasing temperature and decreasing pH.
- Two different xylan fractions were identified: lignin-free xylan and lignin-xylan oligomers (LCC). The former dissolves during the early phase of extraction up to a maximum rate and the latter starts dissolving after this maximum has been reached. The xylan amount removed up to the maximum rate was found to be temperature dependent.

- Two different lignin fractions were identified: carbohydrate-free lignin starting with a high concentration and linearly decreasing during the first phase of extraction followed by lignin in the form of LCCs at a much slower rate in the second phase.
- A non-removable xylan was identified which accounted for 18-20% of the original xylan at 160°C and a pH of 3.
- The removal rate for lignin and xylan increases with decreasing pH and/or increasing temperature.
- There is evidence of significant cellulose dissolution at 160°C and at a pH of 3, which increases and becomes noticeable at an earlier time with increasing temperature and/or decreasing pH. Cellulose hydrolysis is noticeable at pH 5 and increases with decreasing pH.
- Xylan with a high degree of acetylation is dissolved during the early stage of the extraction. At low pH the acetyl/10 xylose units in the small amount of remaining xylan in the extracted wood is similar to that of the original wood.

6.1.3 Chemical mechanism, rate determining step(s) and kinetics of wood polymer removal during hot water treatment of hardwood

- Three different polymer fractions were identified by GPC analysis of the wood extract. A high molecular weight, lignin-free, gluco-oligomeric fraction dissolved identified as starch (DP 134). A second xylan-rich fraction with a lower DP (38). Both fractions degrade to lower DP during the course of the extraction. A third fraction with a low DP (around 3-4) identified as lignin-carbohydrate complexes.
- Solubility of the wood polymers was found to be very important during the early phase of extraction when lignin-free xylan and hemicellulose free lignin is dissolved, because the concentration of xylan and lignin are close to their respective saturation point (0.9 to 1.2 mg/mL).
- The changing chemical composition of the lignin-xylan complexes leads to different solubilities, as seen in the saturation point which decreases to around 0.5 mg/mL at 21-50 minutes extraction. At the final stage of extraction the saturation point increases to around 1.6 mg/mL, because the wood polymers have been further degraded to lower DP values thereby increasing their solubility.
- The lignin removal rate shows two different behaviors depending on both temperature and pH, which can be explained by different mechanisms. It is proposed that during the first phase of extraction lignin fragments are dissolved following acid hydrolysis of α-O-4 ether linkages in the lignin. Since this process in controlled by chemical kinetics, the lignin removal rate during this phase is

dependent on the temperature and pH. Lignin removal during the second phase is not controlled by chemical reaction mechanism but more likely by a physico/chemical mechanism, i.e. by solubility.

- The removal of xylan exhibits three different phases. It is proposed that the initial removal of xylan is mainly controlled by solubility of lignin-free xylan-oligomers formed after acid hydrolysis of xylan in the wood. The second phase of xylan dissolution occurs after the removal rate maximum is reached and lignin has been significantly degraded. Then lignin-xylan oligomers start to dissolve and also cleavage of lignin-xylan bonds takes place. The last phase of xylan dissolution is related only to dissolution of lignin-xylan complexes. About 20% of the original xylan cannot be removed when extracting with hot water in the range of pH 3-5. Only when the extraction severity in terms of temperature, time and acidity are so high that cellulose is significantly hydrolysed this resistant final xylan may be removed. The liquid to wood ratio (L/W) highly affects the solubility of both xylo-oligomers and lignin. The removal rate of the lignin-free xylan fraction is controlled by solubility when the extraction is performed at a high enough L/W ratio. On the contrary, when a low L/W ratio is used (3-4) the removal rate of this xylan fraction is controlled by acid hydrolysis of xylan. The removal rate for the fraction of xylan covalently attached to lignin is controlled by lignin solubility.

- A modified P_H-factor is proposed which incorporates the effect of acidity besides time and temperature on xylan removal during hot water extraction of hardwood.

6.2 Recommendation for future work

- The effect of wood particle size on the removal rate of hemicelluloses from wood by hot water extraction should be further studied and quantified in order to include this effect in the modified expression of P_H-factor. The effect of mixing (stirring rate) in the CMBR in combination with wood particle size needs to be investigated.
- Solubility of xylan and lignin were shown to be important for their respective removal from wood. A more complete study should be done on the effect of liquid to wood (L/W) ratio, pH, and temperature on this subject. Also, the solubility of LCCs should be studied.
- Related to the above point the degree of polymerization of both xylan and lignin should be studied in a more systematic way. It is recommended to investigate the effect of temperature and pH on the DP of these wood polymers.
- Based on the new knowledge produced in the present work new ways to fractionate wood/biomass into its main constituents may be proposed. In particular the focus should be on the operating conditions of the removal of hemicellulose prior to pulp production.

- Xylan oligomers can be a feedstock for many further applications. However, a key step is being able to produce a clean fraction of this polysaccharide. It is highly recommended to investigate the separation and purification of these oligomers from the wood extract.
- The fundamentals of hot water extraction of softwoods should be studied in combination with subsequent pulp production.

REFERENCES

Abatzoglou, N., & Chornet, E. (1998). Acid hydrolysis of hemicelluloses and cellulose: theory and applications. In S. Dumitriu, *Polysaccharides: structural diversity and functional versatility* (pp. 1007-1045). New York: Marcel Dekker, Inc.

Abatzoglou, N; Chornet, E; Belcacemi, K. (1992). Phenomenological kinetics of complex systems: the development of a generalized severity parameter and its aplication to lignocellulosics fractionation. *Chem. Eng. Sci., 47* (5), 1109-1122.

Abatzouglou, N., Bouchard, J., & Chornet, E. (1986). Dilute acid depolymerization of cellulose in aqueous phase: Experimental evidence of the significant precense of soluble oligomeric intermediates. *Can. J. Chem. Eng., 64*, 781.

Abatzouglou, N., Koeberle, P. G., Chornet, E., Overend, R. P., & Koukios, E. G. (1990). Dilute acid hydrolysis of lignocellulosics. An application to medium consistency suspensions of hardwoods using a plug flow reactor. *Can. J. Chem. Eng., 68*, 627.

Bikova, T., & Treimanis, A. (2002). Problems of MMD analysis of cellulose by SEC using DMA/LICl: A review. *Carohydr. Polym., 48* (1), 23-28.

Björkman, A. (1957). Studies on finely divided wood. Part 3. Extraction of lignin-carbohydrate complexes with neutral solvents. *Svensk. Papperstidn., 60*, 243-251.

Casebier, R. L., Hamilton, J. K., & Hergert, H. L. (1969). Chemistry and mechanism of water prehydolysis on southern pine wood. *Tappi, 52* (12), 2369-2377.

Casebier, R. L., Hamilton, J. K., & Hergert, H. L. (1973). The chemistry and mechanism of water prehydrolysis on black gumwood. *Tappi, 56* (3), 135-139.

Chen, X., Lawoko, M., & van Heiningen, A. (2010). Kinetics and mechanism of autohydrolysis of hardwoods. *Bioresource Technology, 101*, 7812-7819.

Chua, M., & Wayman, M. (1979). Characterization of autohydrolysis aspen (P. tremuloides) lignins. Part 3: Infrared and ultraviolet studies of extracted autohydrolysis lignin. *Canadian Journal of Chemistry, 57*, 2603-2610.

Conner, A. (1983). Kinetic modeling of hardwood prehydrolysis. Part I. Xylan removal by water prehydrolysis. *Wood and Fiber Science, 16* (2), 268-277.

Conner, A., & Lorenz, L. (1986). Kinetic modeling of hardwood prehydrolysis. Part III. Water and dilut acetic acid prehydrolysis of southern red oak. *Wood and Fiber Science, 18* (2), 248-263.

Dammström, D., Salmén, L., & Gatenholm, P. (2009). On the interactions between cellulose and xylan, a biomimetic simulation of the hardwood cell wall. *Bioresources , 4* (1), 3-14.

Davis, M. (1998). A rapid modified method compositional carbohydrate analysis of lignocellulosics by high pH anion exchange chromatography with pulsed amperometric detection (HPAEC/PAD). *Journal of Wood Chemistry and Technology , 18* (2), 235-252.

Effland, M. J. (1977). Modified procedure to determine acid-insoluble lignin in wood and pulp. *Tappi , 60* (10), 143-144.

Fengel, D., & Wegener, G. (1983). *Wood chemistry: chemistry, ultrastructure, reactions.* Germany: Walter de Gruyter.

Forss, K. (1961). *The composition of a spent spruce sulfite liquor.* Helsingfors, Finland: The Finnish pulp and Paper Research Institute.

Garrote, G., Domínguez, H., & Parajó, J. C. (1999). Mild autohydrolysis: an environmental friendly technology for xylo-oiligosaccharide production from wood. *Journal of Chemical Technology & Biotechnology , 74*, 1101-1109.

Garrote, G., Domínguez, H., & Parajó, J. C. (2004). Production of substituted oligosaccharides by hydrolytic processing of barley husks. *Industrial & Engineering Chemistry Research , 43*, 1608-1614.

Gray, M., Converse, A., & Wyman, C. (2007). Solubilities of oligomer mixtures produced by the hydrolysis of xylan and corn stover in water at 180C. *Industrial & Engineering Chemistry Research , 46*, 2383-2391.

Gray, M., Converse, A., & Wyman, C. (2003). Sugar monomer and oligomer solubility. Data and predictions for application to biomass hydrolysis. *Applied Biochemistry and Biotechnology , 105-108*, 179-193.

Henriksson, G. (2009). Lignin. In M. Ek, G. Gellerstedt, & G. Henriksson, *Pulp and Paper Chemistry and Technology. V1 Wood Chemistry and Wood Biotechnology* (pp. 121-145). Berlin: Walter de Gruyter GmbH & Co. KG.

Jacobsen, S., & Wyman, C. (2002). Xylose monomer and oligomer yields for uncatalyzed hydrolysis of sugarcane bagasse hemicellulose at varying solids concentration. *Industrial & Engineering Chemistry Research , 41* (6), 1454-1461.

Janson, J. (1974). Analytik der Polysaccharide in Holz und Zellstoff. *Faserforschung und Textiltechnik , 25* (9), 375-382.

Ji, Y. (2007). *Kinetics and mechanism of oxigen delignification.* Orono, Maine: University of Maine, Chemical Engineering Department.

Lawoko, M. (2005). *Lignin-polysaccharide networks in softwood and chemical pulps: characterization, structure and reactivity.* Stockholm, Sweden: KTH Chemical Science and Engineering.

Lawoko, M., & van Heiningen, A. (2010). Fractionation and characterization of completely dissolved ball milled hardwood. *Journal of Wood Chemistry and Technology* , Article in press.

Lawoko, M., Henriksson, G., & Gellerstedt, G. (2003). New method for the quantitative preparation of lignin-carbohydrate complex from unbleached softwood Kraft pulp: Lignin-polysaccharide networks I. *Holzforschung , 57*, 69-74.

Leschinsky, M., Patt, R., & Sixta, H. (2007). Water prehydrolysis of E. globulus with the main emphasis on the formation of insoluble components. *PulPaper Conference 2007.* Helsinki, Finland.

Levenspiel, O. (2002). *The Chemical Reactor Omnibook.* Oregon: OSU Book Stores, Inc.

Li, J., Kisara, K., Danielsson, S., Lindström, M. E., & Gellerstedt, G. (2007). An improved methodology for the quantification of uronic acid units in xylans and other polysaccharides. *Carbohydr. Res. , 342* (11), 1442-1449.

Liu, C., & Wyman, C. (2003). The effect of flow rate of compressed hot water on xylan, lignin, and total mass removal from corn stover. *Industrial & Engineering Chemistry Research , 42* (21), 5409-5416.

Mao, H., Genco, J. M., Y. S.-H., van Heiningen, A., & Pendse, H. (2008). Technical Economic Evaluation of a Hardwood Biorefinery Using the "Near-Neutral" Hemicellulose Pre-Extraction Process. *Journal of Biobased Materials and Bioenergy , 2*, 177-185.

McCormick, C. L. (1981). *Patent No. US patent 4,278,790.* USA.

McMillan, J. D. (1994). Pretreatment of lignocellulosic biomass. *Enzymatic conversion of biomass for fuels production. 566*, pp. 292-324. Washington, DC: ACS Symposium Series.

Mittal, A., Chatterjee, S., Scott, G., & Amidon, T. (2009). Xylan solubilization during autohydrolysis of sugar maple wood meal: reaction kinetics. *Holzforschung , 63*, 307-314.

Monsoor, M., & Proctor, A. (2001). Preparation and functional properties of soy hull pectin. *Journal of the American Oil Chemists Society , 78* (7), 709-713.

Morjanoff, P. J., & Gray, P. P. (1987). Optimization of steam explosion as a method for increasing susceptibility of sugarcane bagasse to enzymatic saccharification. *Biotechnol. Bioeng. , 29*, 733-741.

Mosier, N., Wyman, C., Dale, B., Elander, R., Lee, Y. Y., Holtzapple, M., et al. (2005). Features of promising technologies for pretreatment of lignocellulosic biomass. *Bioresour. Technol. , 96*, 673-686.

Nabarlatz, D., Farriol, X., & Montané, D. (2005). Autohydrolysis of almond shells for the production of xylo-oligosaccharides: product characteristics and reaction kinetics. *Industrial & Engineering Chemistry Research , 44*, 7746-7755.

Overend, R. P., & Chornet, E. (1987). Fractionation of lignocellulosics by steam-aqueous pretreatments. *Philos. Trans. R. Soc. London, Ser. A , 321*, 523-536.

Paredes, J., Shaler, S., Jara, R., & van Heiningen, A. (2008). Influence of hot water extraction on the physical and mechanical behavior of OSB. *Forest Prod. J. , 58* (12), 56-62.

Puri, V. P., & Mamers, H. (1993). Explosive pretreatment of lignocellulosic residues with high-pressure carbon dioxide for the production of fermentation substrates. *Biotechnol. Bioeng. , 25*, 3149-3161.

Reis, D., & Vian, B. (2004). Helicoidal pattern in secondary cell walls and possible role od xylan in their construction. *Comptes Rendus Biologies , 327*, 785-790.

Rydholm, S. (1965). *Pulping Processes.* New york: John Wiley and Sons.

Scott, R. W. (1979). Colorimetric determination of hexuronic acids in plant materials. *Anal. Chem. , 51* (7), 936-941.

Sixta, H. (2006). P-factor concept. In H. Sixta, *Handbook of pulp* (pp. 343-345). Weinheim: WILEY-vch.

Sixta, H. (2006). Pulp properties and applications. In H. Sixta, *Handbook of pulp* (pp. 1009-1067). Weinheim: WILEY-vch.

Sixta, H. (2006). Sulfite chemical pulping. In H. Sixta, *Handbook of pulp* (pp. 392-482). Weinheim: WILEY-vch.

Sjöström, E. (1993). *Wood Chemistry: Fundamentals and Applications.* San Diego, CA, USA: Academic Press.

Song, T., Pranovich, A., Sumerskiy, I., & Holmbom, B. (2008). Extraction of galactoglucomannan from spruce wood with pressurised hot water. *Holzforschung , 62* (6), 659-666.

Springer, E., & Harris, J. (1985). Procedures for determining the neutralizing capacity of wood during hydrolysis with mineral acid solutions. *Industrial and Engineering Chemistry, Product Research and Development , 24*, 485-489.

Sun, Y., & Cheng, J. (2002). Hydrolysis of lignocellulosic materials for ethanol production: a review. *Bioresour. Technol. , 83*, 1-11.

Teleman, A. (2009). Hemicelluloses and pectins. In M. Ek, G. Gellerstedt, & G. Henriksson, *Pulp and Paper Chemistry and Technology. V1 Wood Chemistry and Wood Biotechnology* (pp. 102-120). Berlin: Walter de Gruyter GmbH & Co. KG.

Tunc, M. (2008). *Hemicellulose extraction of mixed southern hardwoods.* Orono, Maine: University of Maine, Chemical Engineering.

Tunc, M. S., & van Heiningen, A. R. (2009). Autohydrolysis of mixed southern hardwoods: effect of P-factor. *Nordic Pulp an Paper Journal* , (accepted for publishing).

Tunc, M., & van Heiningen, A. (2010). Characterization and molecular weight distribution of carbohydrates isolated from the autohydrolysis extract of mixed southern hardwoods. *Carbohydrate Polymers , Article in Press.*

Tunc, M., Lawoko, M., & van Heiningen, A. (2010). Understanding the limitations of removal of hemicelluloses during autohydrolysis of a mixture of southern hardwoods. *Bioresources , 5* (1), 356-371.

Tunc, S., & van Heiningen, A. (2008). Hemicellulose extraction of mixed southern hardwood with water at 150C: effect of time. *Industrial & Engineering Chemistry Research , 47* (18), 7031-7037.

Van Heiningen, A. (2006). Converting a kraft pulp mill into an integrated biorefinery. *Pulp Pap. Can. , 107* (6), T141-T146.

Watanabe, T. (2003). Analysis of native bonds between lignin and carbohydrates by specific chemical reactions. In T. Koshijima, & T. Watanabe, *Association between lignin and carbohydrates in wood and other plant tissues.* Springer.

Wayman, M., & Parekh, S. (1988). Sulfur dioxide prehydrolysis for high yield ethanol production from biomass. *Appl. Biochem. Biotechnol. , 17*, 33-43.

Wayman, M., Parekh, S., Chornet, S., & Overend, R. P. (1986). SO2-Catalysed prehydrolysis of coniferous wood for ethanol production. *Biotechnol. Lett. , 8* (10), 749-752.

Yang, B., & Wyman, C. (2008). Characterization of the degree of polymerization of xylooligomers produced by flowthrogh htdrolysis of pure xylan and corn stover with water. *Bioresource Technology , 99*, 5756-5762.

Yoon, S. H., MacEwan, K., & van Heininhen, A. (2006). Pre-extraction of southern pine chips with hot water followed by kraft cooking. *TAPPI EPE Conference 2006.* Atlanta, Georgia, USA.

APPENDIX: HYDROLYSIS OF XYLAN MODEL COMPOUND (BIRCH XYLAN) IN SULFUR DIOXIDE (SO_2) AQUEOUS SOLUTIONS

I. INTRODUCTION

During the pre-extraction process hemicelluloses are partially extracted as oligomers (mainly xylan-oligomers) and monomers from the wood material. Because oligomers cannot be directly metabolized by microorganism during the fermentation process for the production of ethanol, they must be hydrolyzed to monomers. Acid hydrolysis using dilute sulfuric acid is a traditional hydrolysis process. After hydrolysis the solution is neutralized with lime to allow fermentation to proceed. There are two major problems with this technology: the spent acid is not recovered and gypsum is produced which must be disposed off at a cost. As an alternative to sulfuric acid, sulfur dioxide (SO_2) may be used to catalyze the hydrolysis of hemicellulose oligomers. After hydrolysis the SO_2 may be recovered and then recycled to significantly reduce operational costs.

Two simulated hemicellulose extracts were tested: a simulated hot water extract (HWE) and a near neutral extract (NNE). During the extraction of hemicelluloses by using only water as solvent acetyl groups are cleaved from xylan backbone and released into solution where they form acetic acid. On the other hand, in a near neutral process sodium carbonate is used in the solvent to neutralize the acetic acid formed from the cleavage of acetyl groups from xylan resulting in the formation of sodium acetate. This

chapter is focused on the kinetics of xylo-oligomers hydrolysis using SO_2. The effect of temperature and SO_2 concentration is also investigated. The kinetics and the pressure study are investigated on both simulated hemicellulose extracts.

II. EXPERIMENTAL DESIGN

2.1 Hydrolysis kinetics study

Material and equipments

Hydrolysis was performed in an Oil Bath Laboratory Multi-digester (OBLMD) system. The OBLMD system consists of eight high-pressure bombs (220 mL volume) which can rock back and forward in a hot oil bath (Figure 1). The system is designed to operate at high temperatures and employs polyethylene-glycol (PEG 400, BAKER) as a heater source that is temperature controlled through an Isotemp 2150 controller (Fisher Scientific).

Chemicals used in this study: de-ionized (DI) water (Milli-Q Millipore Corporation); glacial acetic acid (99.9%, Fisher Scientific); sodium acetate anhydrous (99.7%, Fisher Scientific); Birchwood Xylan (Sigma-Aldrich); and sulfur dioxide (100%, Metheson Tri-gas).

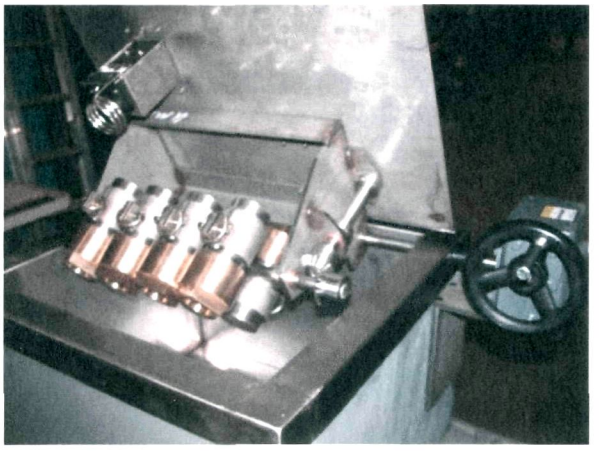

Figure A.1. Multireactor-system for the kinetic study of hydrolysis of xylo-oligomers.

Experimental

Two simulated hemicellulose extracts were tested: a simulated hot water extract (HWE) and a near neutral extract (NNE). Both HWE and NNE extract use commercial birch xylan (SIGMA) as model compound. The hydrolysis was performed using the multi-batch reactor system over a range of conditions of 130-160 °C, 30 and 60 minutes, and 3-12% SO_2. Xylose concentrations are determined by High Performance Anion Exchange Chromatography (HPAEC) with PAD detector. Ion Chromatography (IC-Dionex) is used to quantify SO_2 in the hydrolisate.

Dissolution of SO_2 into the simulated extracts.

Compositions for the two different simulated extracts are shown in Table A.1.

Table A.1. Composition of simulated extracts (values in weight %).

Simulated extract	Composition	
Hot water extract (HWE)	Birch xylan	1%
	Acetic acid	1%
	Water	98%
Near Neutral extract (NNE)	Birch xylan	1%
	Sodium acetate	2%
	Water	97%

The SO_2 gas is bubbled directly into the simulated extracts already prepared and placed into small reactors (vessels with total volume of 220 mL) according with Figure A.2. The excess/undissolved SO_2 goes to a trap which contains a solution N molar of hydrogen peroxide. In this way all SO_2 is converted to sulfuric acid. This solution is later neutralized to pH 5-8 to dispose.

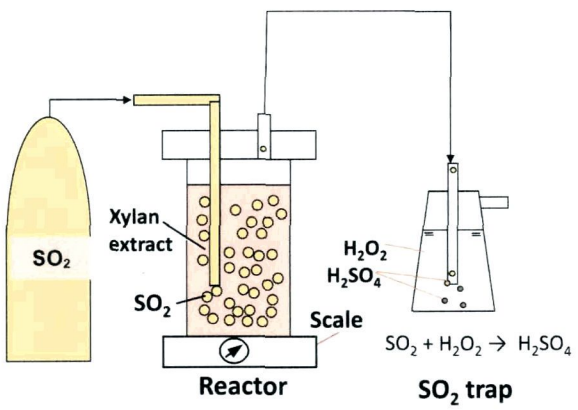

Figure A.2. Dissolution of SO_2 into simulated extracts.

After the reaction is finished the hydrolisate is prepared according with the analytical scheme shown in Figure A.3 (Forss, 1961). The hydrolisate is degassed with nitrogen at 45°C for 4 hours. The gas stream is bubbled in a hydrogen peroxide solution N molar where all SO_2 is converted to sulfuric acid. Then m milliliter from this solution is diluted with HPLC grade water and run on the Ion Chromatographer for SO_4^{-2} quantification.

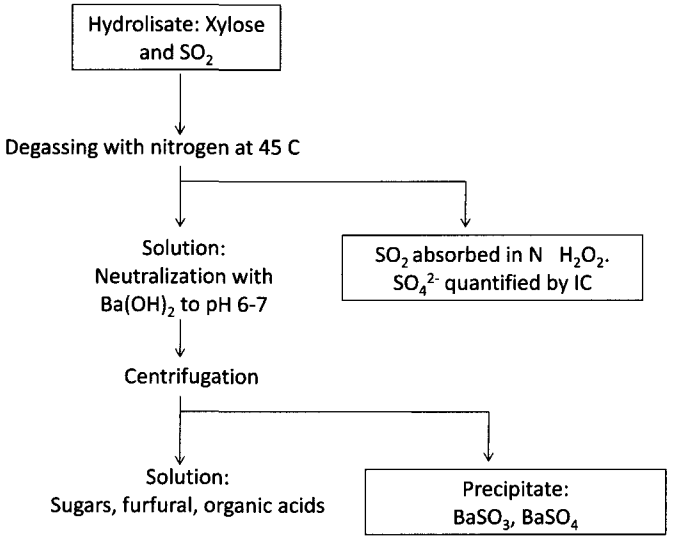

Figure A.3. Analytical procedure for the hydrolisate after the catalytic hydrolysis with SO_2.

2.2 Pressure study

Material and equipments

The pressure study was performed on a single 220 mL reactor vessel (bomb) placed in a 5 liters oil bath that is temperature controlled through an Isotemp 2150 controller (Fisher Scientific). Pressure was recorded by using a wireless device placed on

the top of the small reactor (PressureSensorOne™ Wireless Pressure Sensor, pressure range 0-500 psi, and radio type IEEE 802.15.4, from IntelliSensing) (Figure A.4).

Experimental

Two simulated hemicellulose extracts were tested: a simulated hot water extract (HWE) and a near neutral extract (NNE). Both HWE and NNE extract use commercial birch xylan (SIGMA) as model compound. The pressure study was carried on at a range of temperatures between 130-160C and SO_2 concentrations of 2.0, 5.0, and 10.0%. The pressure of pure water at 100°C, in addition to the temperature rage of the SO_2 study, was investigated for calibration and comparison purposes.

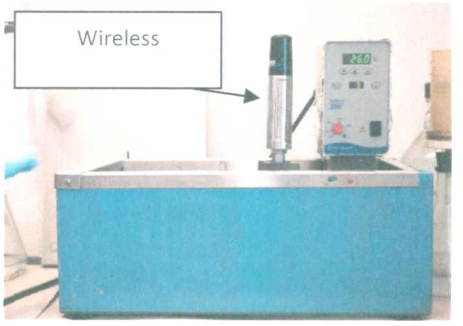

Figure A.4. Pressure study set up showing the wireless pressure sensor.

III. RESULTS AND DISCUSSION

3.1 Hydrolysis kinetic study

The effect of SO2 concentration and temperature on xylose yield

Figures A.5 and A.6 show the effect of SO_2 concentration, temperature and time on the xylose yield for the hot water simulated extract. In general, for the lowest temperature range (130-140°C) it is possible to observe a maximum yield close to 90%. For the case of the highest range of temperature (Figure A.6) the maximum yield can be obtained for low concentrations of SO_2 (85% yield). It can also be noted that xylose yield starts decreasing with increasing SO_2 concentration and this is more evident at higher temperatures. This behavior must be due to degradation of xylose. The determination of furfural on samples hydrolysates from hydrolysis condition at 140°C, 30 minutes, and 10% SO_2 showed a concentration lower than 0.3% based on the original xylan (data no presented). Besides, the HPLC chromatogram showed a high sharp peak at the formic acid position; however it was concluded after performing a mass balance analysis, through calibration and quantification, that this peak do not correspond to acetic acid. From the theory for the sulfite chemical pulping process the concentrations of the sulfur species in the aqueous cooking liquor are defined through the following equilibria (Sixta, 2006):

$$SO_2 + H_2O \rightleftharpoons H_2SO_3(SO_2 \cdot H_2O) \rightleftharpoons H^+ + HSO_3^- \qquad \text{Equation A.1}$$

It is known that sulfur dioxide in an aqueous solution is not found as sulfurous acid. Then hydrogen sulfite and a hydrated SO_2 form are found in equilibrium in the solution. Hydrogen sulfite in aqueous solutions normally acts as reducing agent and is consumed by the reducing end groups of sugar monomers under formation of α-hydroxysulfonates and subsequent oxidation of the reducing end to the corresponding aldonic acid (xylonic acid). This mechanism can explain the lower xylan yield with increasing SO_2 concentration at high temperatures (150°C and 160°C).

Figure A.7 shows the pH for the different experiments with a range between 1.5 and 1.2 for the simulated hot water extract conditions and 2.4 and 1.4 for the simulated near neutral extract conditions. Looking at Figure A.8 it is clear that there is an important concentration of hydrogen sulfite ions in this range of pH. It can be noted that this concentration increases with increasing pH.

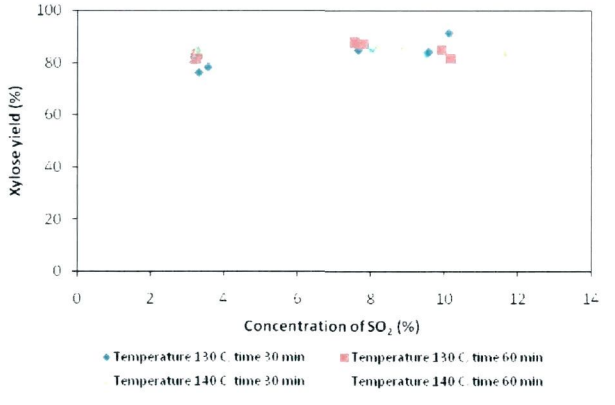

Figure A.5. Effect of SO_2 concentration, temperature and time on xylose yield for the simulated hot water hemicellulose extract. Low range of temperatures.

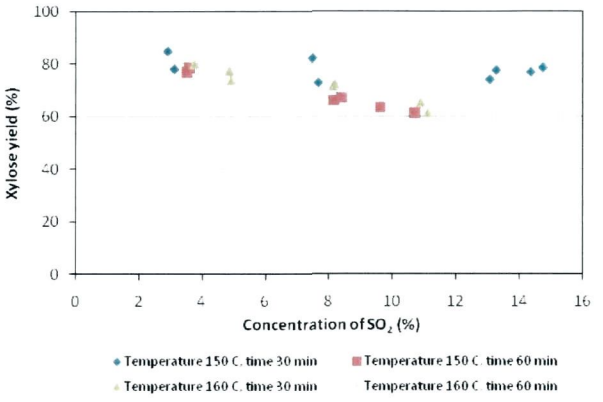

Figure A.6. Effect of SO_2 concentration, temperature and time on the xylose yield for the simulated hot water hemicellulose extract. High range of temperatures.

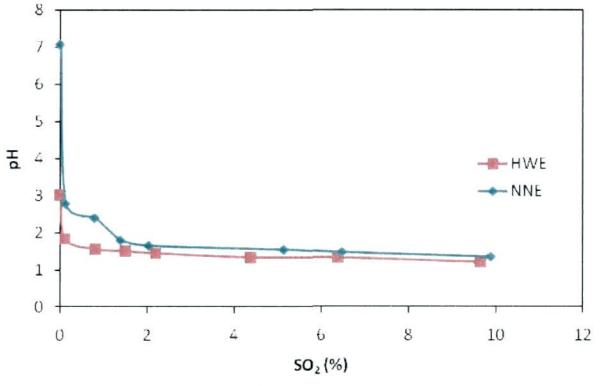

Figure A.7. Effect of SO_2 concentration of pH at 25°C.

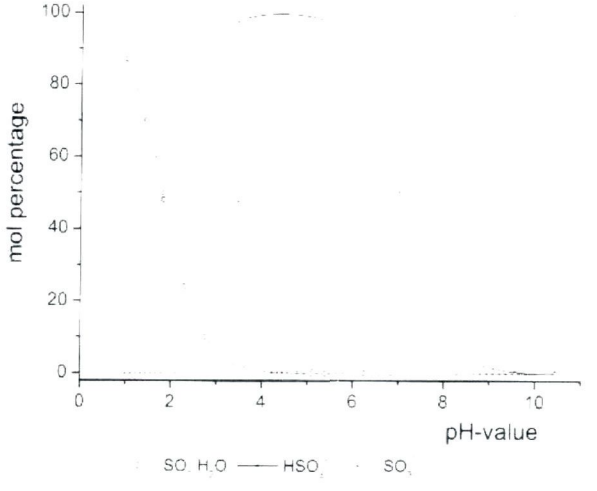

Figure A.8. Relative molar percentage of $SO_2 \cdot H2O$, hydrogen sulfite, and sulfite ions as a function of pH at 25°C.

Figures A.9 and A.10 depict the xylose yield versus the SO_2 concentration at various temperatures for the simulated near neutral hemicellulose extract. It can be immediately noted that the yield values are rather lower than those for the simulated hot water extract reaching a maximum xylose yield of 72% at 140°C, 60 minutes, and 10% of SO_2 which is 10% less than the xylose yield for the simulated hot water extract at the same conditions and 20% lower than the maximum yield reached for this extract. In the simulated near neutral hemicellulose extract 2% of sodium acetate is added resulting in a higher pH and higher hydrogen sulfite concentration (Figures A.7 and A.8 respectively). The higher pH can explain the lower yield values at low SO_2 concentrations observed in Figures A.9 and A.10. The higher hydrogen sulfite concentration can result in higher xylose degradation to xylonic acid.

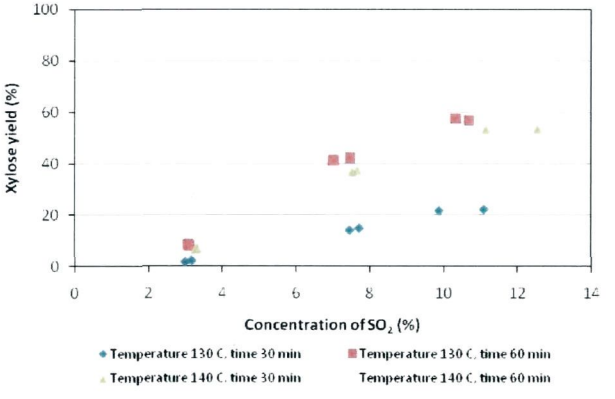

Figure A.9. Effect of SO_2 concentration, temperature and time on the xylose yield for the simulated near neutral hemicellulose extract. Low range of temperatures

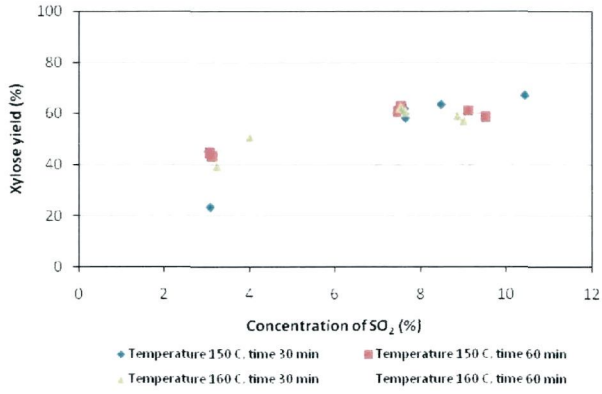

Figure A.10. Effect of SO_2 concentration, temperature and time on the xylose yield for the simulated near neutral hemicellulose extract. High range of temperatures

Modeling the xylose yield with a modified P-factor

The severity parameter has been used to study the kinetic of acid hydrolysis of hemicelluloses (Abatzoglou et al., 1992; Garrote et al., 2002). Lloyd and Wyman (2003) developed a modified severity factor to study the acid hydrolysis of lignocellulosics (Equation A.2).

$$Mo = t \cdot nA \cdot exp\left[\frac{(T_H - T_R)}{14.75}\right] \qquad \text{Equation A.2}$$

where,

t : time (minutes)

n : proportionality constant (10)

A :acid concentration in weight percent (%)

T_H : hydrolysis temperature (°C)

T_R : reference temperature (100°C)

A similar approach to the modified severity factor proposed by Lloyd is possible to make for the P-factor, based on the work of Tunc and van Heiningen (2009). The modified P-factor thus proposed has the following expression:

$$MP = t \cdot nA \cdot exp\left[40.48 - \frac{15{,}106}{T_H}\right] \qquad \text{Equation A.3}$$

n: assuming a value of 1

t : time (hours)

A :acid concentration in weight percent (%)

T_H : hydrolysis temperature (K)

T_R : reference temperature (373.15 K)

Figure A.11 depicts the xylose yield as a function of the Mo factor. It can be noted that this factor works fairly almost for all range of temperatures and SO_2 concentrations. At the most severe condition (160°C and 60 min.) points do not fit on the general pattern most probably due to the presence of side reactions other than xylose oxidation, i.e. dehydration to furfural (Sixta, 2006).

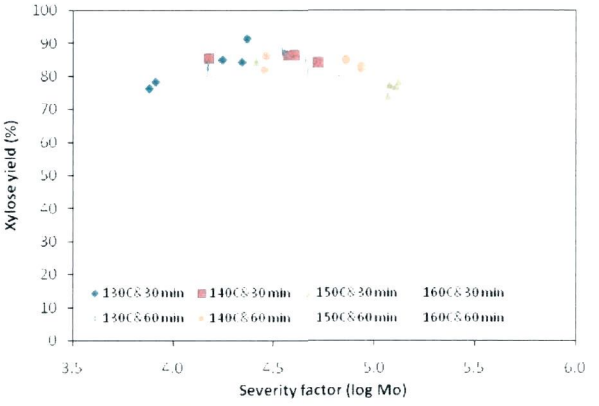

Figure A.11. Effect of severity (log Mo) on the xylose yield for the hydrolysis of the simulated hot water extract.

Figure A.12 depicts the xylose yield versus the modified MP factor. It can be noted that both parameters show a similar behavior, which means MP could be used as a kinetic model for the xylose yield in the hydrolysis of hot water extracts.

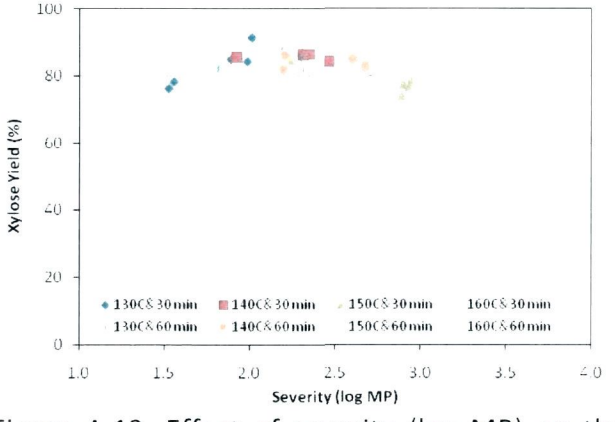

Figure A.12. Effect of severity (log MP) on the xylose yield for the hydrolysis of the simulated hot water extract.

However, the MP factor did not work to model the xylose yield in the hydrolysis of the simulated near-neutral extract (Figure A.13). It can be observed that the data does not fit on all range of severities and it is observed a shifting with temperature.

Looking at the equation for the equilibrium for the sulfur species (Equation A.1) in pure aqueous solutions it can be noted that for each mole of SO_2 one mol of proton is produced, which is the situation for the hydrolysis of the simulated hot water extract. So then, in this case, SO_2 concentration is proportional to the hydrogen concentration. On the other hand, in the simulated near neutral extract the addition of sodium acetate changes the equilibrium (pH) and then the SO_2 concentration is not proportional to the proton concentration. Also, this new equilibrium condition seems to be temperature dependant, which explains the shifting with temperature on Figure A.13. Figure A.14 depicts the effect of SO_2 concentration on the hydrogen ion concentration at 25°C. It can be observed that the concentration of hydrogen ions is lower for the simulated near-neutral extract.

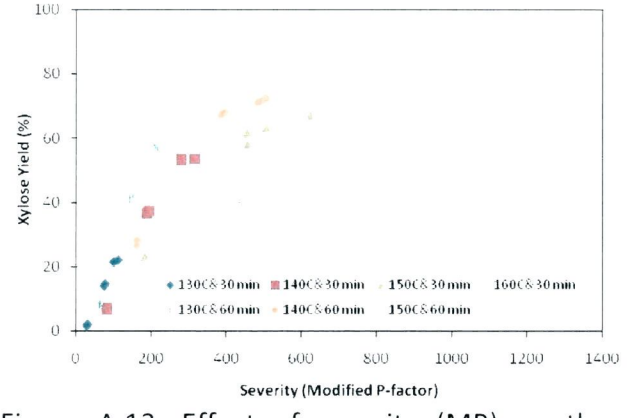

Figure A.13. Effect of severity (MP) on the xylose yield for the hydrolysis of the simulated near-neutral extract.

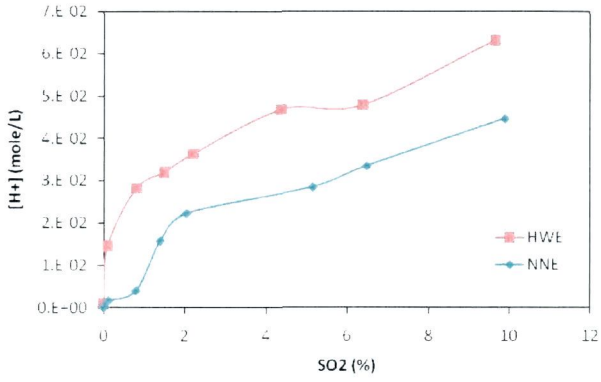

Figure A.14. Effect of SO_2 concentration on the hydrogen ion concentration at 25°C.

Quantification of SO_2 recovery

Three experiments were performed to release and quantify SO_2 from the hidrolisate after a hydrolysis process of the simulated hot water extract at 140°C for 30 min. The procedures are summarized in Table A.2. The hydrolisate was bubbled with helium gas (nitrogen can also be used). Then, SO_2 is released and bubbled in a solution containing hydrogen peroxide N molar where SO_2 is converted to sulfuric acid. A sample of know volume is taken, diluted, and run on the ion chromatographer (IC) for SO_4^{2-} quantification (Figure A.16).

Table A.2. Experiment description for SO_2 releasing.

Experiment number	Description: bubbling step with inert gas.
1	Vessel was cooled down after hydrolysis to room temperature with ice bath. 11.2% SO_2
2	Vessel was kept at 140°C until steam appeared. Then it was cooled down with ice bath. 10.8% SO_2
3	Vessel was kept at 90 C. 11.6% SO_2

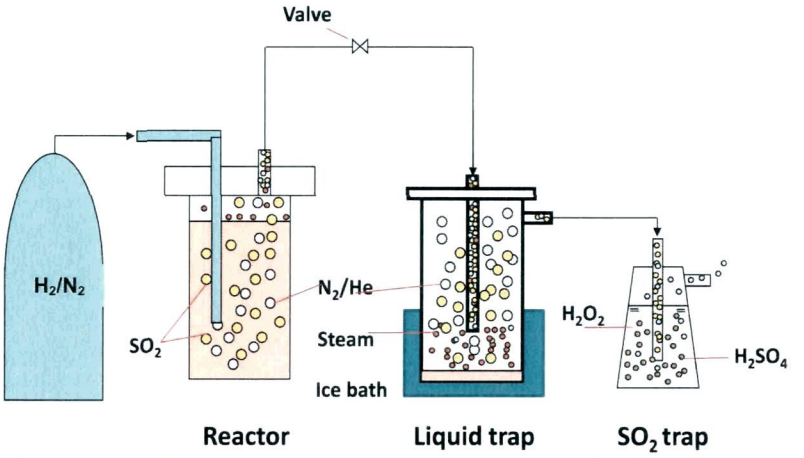

Figure A.15. Set up scheme for the recovery of SO_2 from the hidrolisate.

For all experiments the inert gas was bubbled for about one hour. The best result was for the experiment number 3 where the SO_2 recovery was about 99%. This means, at least for this set the experiments, SO_2 did not react during the hydrolysis so it can be concluded SO_2 can be used to catalyze the hydrolysis of xylan.

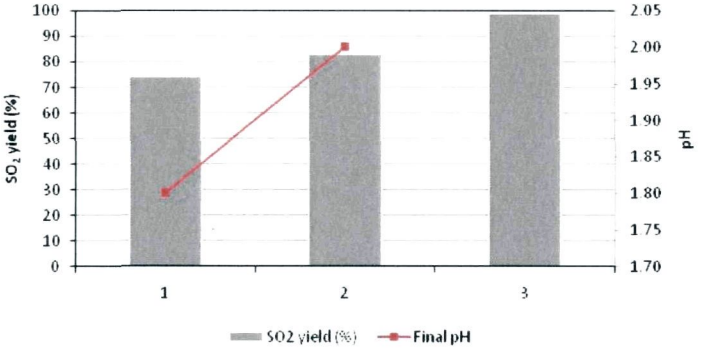

Figure A.16. Recovery of SO_2 from simulated hot water hydrolisate.

3.2 Pressure study

Data reproducibility

In order to investigate the experiment data reproducibility a set of three experiments were preformed. 2% of SO_2 was dissolved in pure water. Figure A.17 depicts the results showing that there is fair data reproducibility at all temperature conditions.

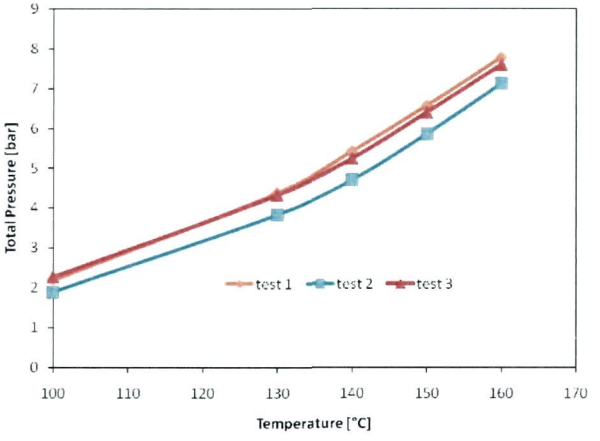

Figure A.17. Reproducibility of pressure measurements.

Pressure calibration

Figure A.18 depicts the pressure data for an experiment carried out on pure water. For comparison purposes literature data for water vapor pressure is also depicted in the graph. It is clear that the total pressure increases when air is not removed from the reactor. It also clear that this difference of about 1.5 bar is almost constant with increasing temperature. This difference will be subtracted to the total

pressure for all other experiments with SO_2 in order to correct for the over pressure of air.

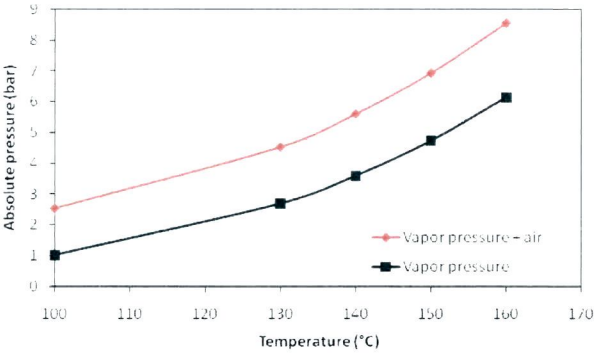

Figure A.18. Absolute vapor pressure for pure water and effect of air at different temperatures.

Effect of temperature and SO_2 concentration on total pressure

Figure A.19 depicts the effect of SO_2 concentration on the total pressure of three different solutions: pure water, simulated hot water extract (HWE), and simulated near neutral extract (NNE). From the figure it is clear that the pressure increases with increasing the SO_2 concentration for all three different solutions as expected. It is also clear that the pressure increases with increasing temperature. With 0% SO_2 the three solvents show exactly the same pattern with increasing temperature with the maximum pressure of 6 bar at 160°C. With increasing the SO_2 concentration the extracts start showing a difference in their behavior, however this is not very significant. The maximum pressure of 17 bar is reached at 160°C with 10% SO_2.

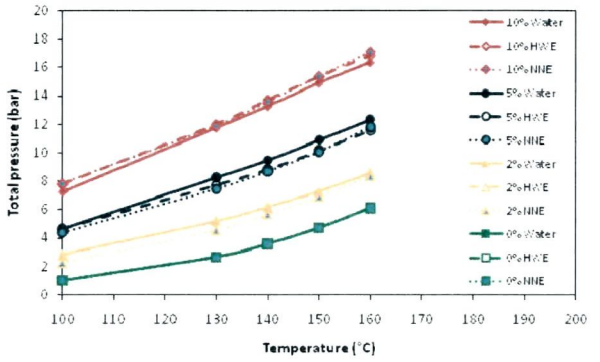

Figure A.19. Effect of SO_2 concentration and temperature on the total pressure.

Figure A.20 depicts the effect of SO_2 concentration and temperature on the partial pressure of SO_2. All three extracts show almost the same behavior. The partial pressure of SO_2 increases with SO_2 concentration with a maximum of 11 bar at the most severe condition (160°C and 10% SO_2). It is also noted that temperature does not have an important effect on the partial pressure of SO_2 which does not agree with literature (Sixta, 2006). The only reasonable explanation is that there was a systematic error during the experimental procedure.

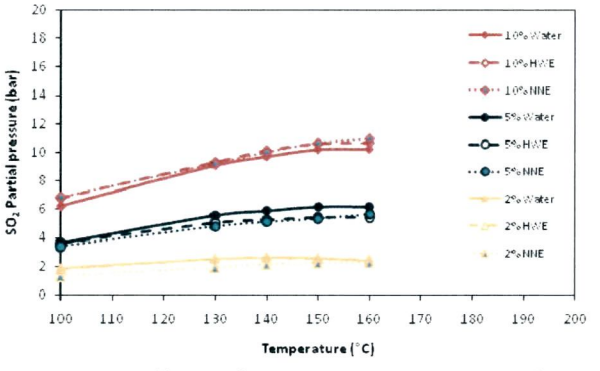

Figure A.20. Effect of SO_2 concentration and temperature on the partial pressure of SO_2.

REFERENCES

Abatzoglou, N; Chornet, E; Belcacemi, K. (1992). Phenomenological kinetics of complex systems: the development of a generalized severity parameter and its aplication to lignocellulosics fractionation. *Chem. Eng. Sci. , 47* (5), 1109-1122.

Forss, K. (1961). *The composition of a spent spruce sulfite liquor.* Helsingfors, Finland: The Finnish pulp and Paper Research Institute.

Garrote, G., Domínguez, H., & Parajó, J. C. (2002). Interpretation of deacetylation and hemicelluloses hydrolysis during hydrothermal treatments on the basis of the severity factor. *Process Biochem. , 37*, 1067-1073.

Lloyd, T., & Wyman, C. E. (2003). Application of a depolymerization model for predicting thermomechanical hydrolysis of hemicellulose. *Appl. Biochem. Biotechnol. , 105/108*, 53-67.

Sixta, H. (2006). Sulfite chemical pulping. In H. Sixta, *Handbook of pulp* (pp. 392-482). Weinheim: WILEY-vch.

Tunc, M. S., & van Heiningen, A. R. (2009). Autohydrolysis of mixed southern hardwoods: effect of P-factor. *Nordic Pulp an Paper Journal* , (accepted for publishing).

BIOGRAPHY OF THE AUTHOR

Rory Jara was born in Concepción, Chile on Dec. 21, 1971. He received his Bachelor in Chemical Engineering from the Universidad de Concepción in 1998.

Upon graduation he was hired by the Unidad de Desarrollo Tecnológico of the Universidad de Concepción as a Project Engineer. In summer of 2006 Rory was offered an assistantship to continue his studies as a graduate student in the Chemical and Biological Engineering Department of the University of Maine where he attended with the hope of obtaining a Ph.D. degree.

Rory Jara is a candidate for the Doctorate of Philosophy degree in Chemical Engineering from The University of Maine in December, 2010.